MECHANICAL STIMULATION AND MORPHOGENESIS OF THE EMBRYONIC CHICK KNEE JOINT

By

VIKESH VIJAY CHANDARIA

Imperial College London

IMPERIAL COLLEGE LONDON

DEPARTMENT OF BIOENGINEERING

This thesis is submitted in partial fulfilment of the requirements for the degree of Doctor of Philosophy

"Our real teacher has been and still is the embryo, who is, incidentally, the only teacher who is always right"

Viktor Hamburger

(1900-2001)

Vikesh Vijay Chandaria

Mechanical stimulation and morphogenesis of the embryonic chick knee joint, © May 2017

Supervised by Dr. Niamh C. Nowlan

Imperial College London, United Kingdom

DECLARATION OF ORIGINALITY

I hereby declare that this thesis, and the research presented within, is the product of my own work. Any ideas or quotations from the work of other people, published or otherwise, or from my own previous work are fully acknowledged in accordance with the standard referencing practices of the discipline.

This thesis was carried out between October 2013 and May 2017 under the supervision of Dr. Niamh C. Nowlan in the Department of Bioengineering at Imperial College London UK.

COPYRIGHT DECLARATION

The copyright of this thesis rests with the author and is made available under a Creative Commons Attribution Non-Commercial No Derivatives licence. Researchers are free to copy, distribute or transmit the thesis on the condition that they attribute it, that they do not use it for commercial purposes and that they do not alter, transform or build upon it. For any reuse or redistribution, researchers must make clear to others the licence terms of this work.

ABSTRACT

Evolution has led to specialised shapes for each individual joint which are created during prenatal development through joint morphogenesis. Alterations or abnormalities in joint shape development can severely compromise joint function and have long-term health implications. Mechanical stimulation, due to fetal movements, plays an important role in the creation of joint shapes and a reduction in fetal movements has been highlighted as a risk factor for bone and joint shape malformation, which can lead to physical disability.

This doctorate explored the relationship between mechanical stimulation and joint morphogenesis. A novel culture system was created in which embryonic chick hindlimb explants were subjected to controlled and quantified magnitudes of movements. The morphology of the knee joint from explants cultured under different mechanical conditions were compared to reveal how the magnitude of applied movement affects key aspects of the developing joint. A complex relationship was found between the magnitude of movement and the progression of joint shape development. This study provided evidence, for the first time, that the amount of movement experienced during development is a significant variable that impacts of the fate of prenatal joint development. Whilst dynamic movements were applied to developing joints, potential mechanotransduction pathways were tested for their involvement in modulating joint morphogenesis. Blocking the action of both stretch activated ion channels and voltage gated calcium channels produced joints shapes similar to those that had experienced no movement, suggesting the stimulating effects of dynamic movement were not acted upon.

This research has provided a novel insight into how mechanical stimulation influences joint morphogenesis which is extremely valuable for understanding of the etiology of congenital joint conditions. Knowledge of how joints are first created is also valuable to the field of tissue engineering for developing treatments to regenerate degenerated joints.

ACKNOWLEDGMENTS

First and foremost, I would like to thank Dr. Niamh C. Nowlan for her guidance and supervision. I would also like to thank Niamh for being a great mentor to me outside of the PhD. I am truly grateful for all the advice and encouragement she has given me throughout my studies. She always believed in me and pushed me to reach my full potential. I will forever be grateful for all she has taught me.

I would like to thank the whole of the Developmental Biomechanics group, Dr. Mario Giorgi, Dr. Stefaan Verbruggen, Dr. Rebecca Rolfe, Lisa Abela, Devi Bridglal, Vivien Sotiriou and Samantha Martin. You have always been on hand for those dramatic discussions, much needed coffee breaks and created a great environment to be a part of. A very special thank you goes to Dr. Mario Giorgi, who was an amazing colleague and friend. It was an honour to work alongside you. Thank you all.

I would also like to thank all those who helped me with the practical skills I developed during this PhD. Samantha Martin for sharing your expertise in histology and IHC with me and supporting me during those long hours spent in the lab. Dr. Mariea Brady for introducing me to tissue culture and teaching me the necessary techniques needed to conduct my experiments. Dr. James McGinty for building the OPT system and advice for imaging techniques. Dr. James Henstock for sharing his technique for stripping explants of their soft tissues and advice for conducting bioreactor experiments.

Finally, I would like to thank my family, who have undoubtedly supported me in my endeavour to complete this PhD and encouraged me to pursue my passion for research. Most importantly, I would like to thank you for all your teachings and guidance to become the man I am today. A special thank you goes to Parita, who has always been by my side and even agreed to spend the rest of her life by mine. Thank you for your patience, understanding and love.

This research was funded by the European Research Council under the European Union's Seventh Framework Programme (ERC Grant agreement no. [336306]), and in part by the Medical

Engineering Solutions in Osteoarthritis Centre of Excellence (reference number: 088844/Z/09/Z), which is funded by the Wellcome Trust and the EPSRC.

PUBLICATIONS AND PRESENTATIONS RESULTING FROM THIS WORK

Chandaria, V.V., Nowlan, N.C., *"The Power of Prenatal Movements: Shaping of the Knee Joint",* STEM for Britain, 2017, Westminster, UK (Poster).

Chandaria, V.V., McGinty, J., Nowlan, N.C., 2016. *"Characterising the effects of in vitro mechanical stimulation on morphogenesis of developing limb explants"*, Journal of Biomechanics, 49, 3625-2642

Chandaria, V., Nowlan, N.C., "*The Effect of Dynamic Stimulation on Joint Morphogenesis of the Embryonic Chick Knee Joint"*, SB3C, 2016, Maryland, USA (Podium).

Chandaria, V., Nowlan, N.C., *"Optimisation of Embryonic Chick Knee Joint Explant Culture"*, MEIbioeng, 2015, Leeds, UK (Poster).

- Winner of Student Poster Competition

Chandaria, V., Nowlan, N.C., "*A Novel in Vitro Culture System to Study the Influence of Biomechanical Stimulation on Joint Morphogenesis"*, Medical Engineering Centres, 2014, London, UK (Poster).

Chandaria, V., Nowlan, N.C., *"A Novel in Vitro Culture System to Study the Influence of Biomechanical Stimulation On Joint Shape Morphogenesis"*, 7th World Congress of Biomechanics, 2014, Boston, USA (Podium).

ACRONYMS

2D – 2 Dimensional

3D – 3 Dimensional

AER – Apical Ectodermal Ridge

BABB – Benzyl Alcohol and Benzyl Benzoate

DAPI - 4',6-Diamidino-2-Phenylindole

DDH – Developmental Dysplasia of The Hip

DMSO – Dimethyl Sulfoxide

ECM – Extracellular Matrix

FADS – Fetal Akinesia Deformation Sequence

FE – Finite Element

Gd - Gadolinium

Gdcl3 – Gadolinium Chloride

Hcl – Hydrochloric Acid

HH – Hamburger Hamilton Stage

IFD – Indentation Force Deflection

LMPA – Low Melting Point Agarose

MSC – Mesenchymal Stem Cells

Nf - Nifedipine

OA – Osteoarthritis

OPT – Optical Projection Tomography

PBS – Phosphate Buffered Solution

PBTD – Phosphate Buffered Solution + Tween + Dmso

PFA – Paraformaldehyde

Ppi – Pore Per Inch

TUNEL - Terminal Deoxynucleotidyl Transferase (TdT) dUTP Nick-End Labelling

TABLE OF CONTENTS

Declaration of Originality 3

Copyright Declaration 5

Abstract 7

Acknowledgments 9

Publications and Presentations Resulting From This Work 11

Acronyms 13

Table of Contents 15

List of Figures 21

List of Tables 31

1. Introduction 33

1.1 Embryonic Joint Morphogenesis and Mechanical Stimuli 33

1.2 Objectives and Hypotheses 35

1.3 Thesis Structure 37

2. Background 39

2.1 The Role of the Skeleton and Synovial Joints 39

2.1.1 The Knee Joint 40

2.2 Appendicular Skeletogenesis 42

2.2.1 Synovial Joint Formation 44

2.3 Cartilage Mechanobiology 46

2.4 The Role of Mechanical Stimuli During Synovial Joint Development 47

2.4.1 Culture Models 48

2.4.2 Animal Models 49

2.4.3 Computational Studies 53

2.5 Summary 56

3. Materials and Methods 57
3.1 Harvest and Dissection of Embryos 57
3.2 3D Imaging of Explants 59
3.2.1 Staining of Explants 59
3.2.2 Embedding Explants for Imaging 61
3.2.3 Optical Projection Tomography Scanning 62
3.3 3D Shape and Size Analysis 63
3.4 Histology and Immunohistochemistry 65
3.4.1 Histology Staining 66
3.4.2 Proliferation Assay 66
3.4.3 Live Dead Assay 67
4. Physiological Chick Knee Joint Development 69
4.1 Introduction 69
4.2 Methods 70
4.3 Results 71
4.3.1 The Distal Femur 71
4.3.2 The Proximal Tibia 72
4.3.3 The Proximal Fibula 73
4.4 Discussion 74
5 Explant Culture Methodology 77
5.1 Introduction 77
5.2 Design of Culture System 78
5.2.1 The Bioreactor 78

5.2.2 Foam Support System 79
5.3 Validation and Calibration of Mechanical Stimulation 84
5.4 Optimisation of Explant Culture 86
5.4.1 Nutrient Delivery 88
5.4.2 Presence of Soft Tissues 90
5.4.3 Culture Duration 91
5.4.4 Summary 92
5.5 Discussion 94
6 The Effect of Dynamic Movement 97
6.1 Introduction 97
6.2 Methods 98
6.2.1 Explant Culture 98
6.2.2 Dynamic Stimulation Regime 98
6.2.3 Joint Shape Analysis 99
6.2.4 Specimen Numbers 99
6.2.5 Statistical Analysis 99
6.3 Results 100
6.4 Discussion 103
7 The Effects of Movement Magnitude 105
7.1 Introduction 105
7.2 Methods 106
7.2.1 Explant Culture 106
7.2.2 Dynamic Movement Regimes 107

7.2.3 Specimen Numbers 107
7.2.4 3D Joint Shape and Size Analysis 108
7.2.5 Immunohistochemistry Analysis 108
7.2.6 Statistical Analysis 108
7.3 Results 109
7.3.1 3D Joint Region Shapes and Sizes 109
7.3.2 Cell Viability and Proliferation 113
7.4 Discussion 114
8 The Role of Mechanosensitive Ion Channels 117
8.1 Introduction 117
8.2 Methods 119
8.2.1 Explant Culture 119
8.2.2 Dynamic Movement Regime 119
8.2.3 Administration of Ion Channel Inhibitors 120
8.2.4 Specimen Numbers 120
8.2.5 3D Joint Shape and Size Analysis 121
8.2.6 Statistical Analysis 121
8.3 Results 122
8.3.1 Effects of Blocking Stretch Activated Ion Channels 122
8.3.2 Effect of Blocking Calcium Ion Channels 125
8.3.3 Comparison of Blocked Ion Channels 129
8.4 Discussion 132
9 General Discussion 135

9.1 Introduction 135

9.2 Outcomes and Contributions 136

9.3 Limitations and Further Work 144

9.4 Conclusions 146

Bibliography 147

Appendix I – Experimental Protocols 155

Appendix II – Copyright Permissions 165

Appendix III – Published Work 169

LIST OF FIGURES

Figure 1.1: The relationship between mechanical stimuli and joint morphogenesis remains a mystery. No quantified data exists to determine if there is a linear, convergent or binary contribution of mechanical stimulation to promote joint shape development. 35

Figure 2.1: The motion of the knee joint can be simplified into two degrees of freedom. A) Anterior-posterior flexion and extension about the sagittal axis which causes the lower limb to bend and straighten. B) medial-lateral rotation of the tibia/fibula about the transverse axis which occurs during large flexion turning the foot in and outwards. 41

Figure 2.2: Cartoon drawings showing the bony anatomy of the human and chick knee joint. The femur articulates with both the tibia (tibiotarsus) and fibula in the chick whereas in humans the femur only articulates with the tibia. Fe – femur; Pa – patella; Fib – Fibula; Tib – Tibia; FT – femoro-tibial joint; FF – femoro-fibular joint. 41

Figure 2.3: Early joint development has four stages: joint site determination, interzone formation, cavitation and morphogenesis. A) MSCs condense within a continuous anlage of skeletal elements at the location of the future joint. B) Here they commit to an articular fate to form a dense interzone of joint progenitor cells. C) The two ends either side of the joint location start to take shape through morphogenesis. D) Eventually the two ends physically separate to create individual skeletal elements and a joint cavity. 45

Figure 2.4: A clear difference in joint formation was observed in seven day old chick knee joints cultured for six days *in vitro*. A) Under static conditions the knee joint became fused (filled arrow) and lost its recognised articular shape. B) Manual manipulation of the joints during culture allowed for formation of a joint cavity and a defined articular shape. Adapted from Lelkes (1958). 49

Figure 2.5: Joint development was compromised in immobilised chick embryos. Joint cavitation (red arrows) was seen in control embryos (A), but did not occur in embryos following pharmacological (B) or surgical paralysis (C). The shape of the articular ends of the femur (fem)

and tibia (tib) were also abnormal following immobilisation. Adapted from Drachman and Sokoloff (1966)..... 50

Figure 2.6: Rigid paralysis in the chick embryo caused the shape of the distal femur to become simplified. Arrow heads indicate regions of reduced outgrowth in the immobilised animals. Arrows indicate flattening of rudiment surfaces. (A-D) after 4 days of immobilisation; (E,F) after 5 days immobilisation. Adapted from Roddy et al. (2011b)..... 52

Figure 2.7: The shape of the jaw from zebrafish was found to be abnormal under altered mechanical environments. Outlines show the frontal shape of the A) Meckel's cartilage (MC) element, B) palatoquadrate (PQ) element and C) the two elements aligned together. The medial side of the MC was elongated under altered conditions included hyper-activity. The biggest effect was found in the alignment of the two elements which overlapped under altered mechanical conditions. Adapted from Brunt et al. (2016)..... 52

Figure 2.8: Joint cavitation was missing in mutant muscle-less mice at the elbow joint along with the development of articular joint shapes. Adapted from Nowlan et al. (2010a). 53

Figure 2.9: Joint morphogenesis can be predicted using mechanobiology theory for cartilage growth. Applying A) single plane motion from 45^{o} to 120^{o} and B) multi plane motion from 40^{o} to -40^{o} to basic geometries of two skeletal elements, joint shapes can be predicted that resemble the C) knee joint and D) hip joint. Convex (arrowhead) and concave (arrow) profiles can be seen in both examples. Adapted from Giorgi et al. (2014)..... 54

Figure 2.10: Abnormal fetal movements in the hip joint leads to progressive opening of the acetabulum whilst the femoral head loses sphericity. The predicted hip joint shape is similar to a hip joint from an infant affected by DDH. Adapted from Giorgi et al. (2015). 55

Figure 2.11: Predicted patterns of biophysical stimuli in matched areas of localised growth seen in normal development of the distal femur in chick embryos. Adapted from Roddy et al. (2011b). 56

Figure 3.1: (A) Fertilised eggs were incubated at 37.5^{o}C in humidified incubators. Each egg was (B) windowed to gain access to the embryo. (C) Membrane attachments (arrow) were removed

from the embryos to give clear visualisation of the hindlimbs. (D) Incisions were made either side of the spine to dissect the hindlimbs from the embryo body. 58

Figure 3.2: Image of OPT system used to create projections of explants. Explants were mounted to the rotating stage and imaged using the sCMOS camera during a 360 degree rotation. 59

Figure 3.3: Tissue shrinkage was not significant following dehydration and staining of explants. A) overlays of unstained and stained explants before and after staining. No significant differences were found between the B) length of thigh and C) length of the shank in stained and unstained explants for 7 day (n = 12), 8 day (n = 20) and 9 day (n = 14) old embryos. Bars represent mean length. Error bars represent standard deviation. 61

Figure 3.4: Explants were embedded in molten agarose for OPT scanning. A) hindlimbs were paired and placed adjacent to each other in 6cm dishes. B) hindlimbs were submerged and suspended at mid-depth parallel to the top and bottom surface of the agarose. C) the solid agarose was trimmed to center the knee joint onto the axis of rotation (dotted line) used during imaging. Scale bars = 1cm. 62

Figure 3.5: Illustration showing the concept of acquiring projections of the hindlimb explants. Explants embedded in agarose were mounted to the electric motor and rotated to capture 400 images at 9 degree increments. 63

Figure 3.6: 3D models of the distal femur, proximal tibia and fibula were aligned following the same guidelines to ensure shape analysis was consistent. Rudiments were aligned in the frontal and lateral views using their longitudinal axis and axis of the lateral condyle for the distal femur. Joint were positioned into a neutral resting flexed position. 64

Figure 3.7: 3D rendered model of the chick knee joint in a neutral flexed position. Medial, frontal and lateral views of the joint were used to produce joint shape profiles and measure joint region sizes. Adapted and reproduced from Chandaria et al. (2016) 65

Figure 3.8: Cultured explants were embedded in a medium of OCT and 30% sucrose and frozen over dry ice. Explants were orientated to face upwards with the knee joint (circled) just below the surface of medium ready for cryosectioning. Scale bar = 1cm. 66

Figure 4.1: 3D models of the embryonic chick knee joint at 7, 8 and 9 days. 71

Figure 4.2: Normal shape changes occurring in the chick knee joint during development. Shape profiles of 7, 8 and 9 day old chick embryo knee joints were outlined and overlaid (n=6). Hollow arrows: posterior curl of condyles; * dorsal groove between the two femoral condyles; single edged bars: intercondylar fossa; + concave curve of the tibial plateau; filled arrows: anterior tibial crest. Adapted and reproduced from Chandaria et al. (2016). 73

Figure 4.3: The increase in joint region size is most dramatic between days 8 and 9. Columns represent mean size of joint regions (n=6). Error bars represent standard deviation. *p-values < 0.05; **p-values < 0.01. 74

Figure 5.1: (A) Ebers TC-3 Bioreactor System. (B) Compression Culture Chambers. (Ebers Med Tech SL, 2016) 79

Figure 5.2: Cyclic loading improved the support factor for all foam types. 10ppi and 45ppi had the highest support factors before and after loading. Support factors were calculated as the ratio of 65% IFD/25% IFD before and after 30mins of cyclic loading to 30% compression. Error bars represent the standard deviation. 81

Figure 5.3: After 30mins of cyclic loading 45ppi foam showed the least amount of dynamic fatigue. Fatigue was calculated as the percentage change in 25% IFD before and after 30mins of cyclic loading to 30% compression. Error bars represent the standard deviation. 82

Figure 5.4: Schematic of the explant culture setup. A) Rectangular polyurethane foam supports were cut to create a step along the horizontal axis. Measurements are in mm. B) Explants were positioned onto the lower level of the foam and pinned into place. Explants were orientated medial side down with the hip joint furthest away from the step. C) The culture setup could be compressed in both the vertical or horizontal orientations. Adapted from Chandaria et al. (2016). 83

Figure 5.5: Increasing compression of the foam support resulted in a bending motion at the knee joint as indicated by the decrease in internal knee flexion angle. 85

Figure 5.6: Flexion angle increased linearly (trend line) with compressive magnitude. Flexion angles of developing knee joints in explants experiencing 1 – 4mm of uniaxial compression. Error bars represent standard deviation..... 85

Figure 5.7: Explants would start to deteriorate after 3 days of culture under submerged conditions during initial experiments. Arrows indicate areas of reduced Alcian Blue staining of the femur and proximal tibia. Images not to scale..... 86

Figure 5.8: Submerged and air-liquid interface culture setups. In submerged culture the explant is fully surrounded by culture media with the hindlimb in the vertical position. At an air-liquid interface the explant lies above the level media exposed to the culture atmosphere with the hindlimb in the horizontal position. 89

Figure 5.9: Removal of the soft tissues exposed the cartilaginous rudiments on the skeleton. Left hindlimb (left hand side) left intact after dissection. Right hindlimb (right hand side) with the soft tissues stripped after dissection. Both hindlimbs are from the same embryo. Digits of the foot were also removed during the removal of soft tissue. 91

Figure 5.10: Progression of joint shape development increased following the optimisation of culture conditions (n=6). An air-liquid interface, removal of soft tissues and 6 days of culture were considered as optimal culture conditions. Hollow arrows: posterior curl of condyles; single edged bars: intercondylar fossa; + concave curve of the tibial plateau; filled arrows: anterior tibial crest. 93

Figure 5.11: Joint region sizes were seen to increase as culture conditions were optimised. An air-liquid interface, removal of soft tissues and 6 days of culture produced the largest joints on average. Group 1: uncultured day 7; group 2: submerged, intact, 3 days; group 3: air-liquid, intact, 3 days; group 4: air-liquid, stripped, 3 days; group 5: air-liquid, stripped, 6 days. Columns represent mean size of joint regions (n=6). Error bars represent standard deviation. *p-values < 0.05, **p-values < 0.01..... 94

Figure 6.1: Shape profiles of uncultured (n=6), static (n=6) and dynamic (n=8) knee joints reveal differences in joint shape. Both cultured groups show signs of shape development compared to

uncultured joints. Squares: dominance of the lateral condyle over the medial condyle; Hollow arrows: posterior curl of condyles; single edged bars: intercondylar fossa; + concave curve of the tibial plateau; filled arrows: anterior tibial crest. 101

Figure 6.2: Dynamically stimulated joints were significantly larger in size compared to joints in the static group. Columns represent mean size of joint regions measured for uncultured (n=6), static (n=6) and dynamic (n=8) groups. Error bars represent standard deviation. *p-values < 0.05; **p-values < 0.01 102

Figure 6.3: Both statically cultured and dynamically cultured showed potential joint cavities. Images are frontal sections of the knee joint. Arrows indicate areas of reduced staining which are present around the rudiments and between rudiments. f – femur; fi – fibula, t – tibia. 102

Figure 7.1: The average-flexion movement regime led to more normal progression of morphogenesis than other movement regimes or static culture. Shape profiles of the 3D reconstructed joint regions were outlined and overlaid for each cultured group. Static controls (n=26), reduced-flexion (n=7), average-flexion (n=12), over-flexion (n=11). Squares: dominance of the lateral condyle over the medial condyle; hollow arrows: posterior curl of condyles seen in moved explants; * dorsal groove between the two femoral condyles; single edged bars: intercondylar fossa; + concave curve of the tibial plateau; filled arrows: anterior tibial crest. Adapted and reproduced from Chandaria et al. (2016). 111

Figure 7.2: Significant differences in joint region measurements were most pronounced between the average-flexion regime and static culture. Mean size of joint regions measured for static (n=26), reduced-flexion (n=7), average-flexion (n=12) and over-flexion (n=11) explants. Error bars represent standard deviation. *p-values < 0.05; **p-values < 0.01. ‘a’ indicates a difference of 10-15%, ‘b’ indicates a difference of 16-20% and ‘c’ indicates a difference of 21-35%, where differences represent how much smaller the regions measured relative to the larger joint. Adapted and reproduced from Chandaria et al. (2016). 112

Figure 7.3: Average-flexion or over-flexion led to significant increases in cell proliferation, while movement regime did not affect cell viability. Stained sections are shown from the average-

flexion group for live/dead and proliferating cells. Viability staining shows dead cells in brown and live cells in green. Proliferation staining shows background cells in blue and proliferating cells in red. Scales bars = 200um. A) shows live cell count as a percentage of total number of cells for each group. B) shows the total number of proliferating cells in the distal femur for each group (n=4). Error bars represent standard deviation. *p-values < 0.05; **p-values < 0.01. Adapted and reproduced from Chandaria et al. (2016). 113

Figure 8.1: Voltage-gated channels and stretch activated ion channels open and close to regulate transmembrane ion concentrations. Voltage-gated ion channels respond to changes in the voltage difference across the membrane. Stretch activated ion channels respond to tension applied to the membrane..... 118

Figure 8.2: The shape profiles of the distal femur and tibia were most affected following the administration of gadolinium chloride. Shape profiles for each joint region were overlaid for each group and analysed for characteristics of joint shape development. Dynamic controls (n=10), gadolinium vehicle (n=6), 100uM gadolinium chloride (n=6), 1mM gadolinium chloride (n=6). Squares: dominance of the lateral condyle over the medial condyle; hollow arrows: posterior curl of condyles seen in moved explants; * dorsal groove between the two femoral condyles; single edged bars: intercondylar fossa; + concave curve of the tibial plateau; filled arrows: anterior tibial crest..... 123

Figure 8.3: Blocking of stretch activated ion channels reduced the average size of joint regions following a high dose of 1mM gadolinium chloride. Bars represent the mean joint region size. Dynamic controls (n=10), gadolinium vehicle (n=6), 100uM gadolinium chloride (n=6), 1mM gadolinium chloride (n=6). Error bars represent the standard deviation. *p-values < 0.05, **p-values < 0.01..... 124

Figure 8.4: The shape profiles of the distal femur, medial condyle and tibia were most affected following the administration of nifedipine. Shape profiles for each joint region were overlaid for each group and analysed for characteristics of joint shape development. Dynamic controls (n=10), nifedipine vehicle (n=6), 100uM nifedipine (n=5), 1mM nifedipine (n=5). Squares: dominance of

the lateral condyle over the medial condyle; hollow arrows: posterior curl of condyles seen in moved explants; * dorsal groove between the two femoral condyles; single edged bars: intercondylar fossa; + concave curve of the tibial plateau; filled arrows: anterior tibial crest. . 127

Figure 8.5: Blocking of L-type calcium ion channels reduced the average size of joint regions following a high dose of 1mM Nifedipine. Bars represent the mean joint region size. Dynamic controls (n=10), nifedipine vehicle (n=6), 100uM nifedipine (n=5), 1mM nifedipine (n=5). Error bars represent the standard deviation. *p-values < 0.05, **p-values < 0.01. 128

Figure 8.6: Joint shapes were equally affected when cultured with a high dose of nifedipine and a high dose of gadolinium chloride compared to dynamic controls. Shape profiles for each joint region were overlaid for each group and analysed for characteristics of joint shape development. Dynamic controls (n=10), 1mM gadolinium chloride (n=6), 1mM nifedipine (n=5). Squares: dominance of the lateral condyle over the medial condyle; hollow arrows: posterior curl of condyles seen in moved explants; * dorsal groove between the two femoral condyles; single edged bars: intercondylar fossa; + concave curve of the tibial plateau; filled arrows: anterior tibial crest. 130

Figure 8.7: Joint region sizes were equally affected by a high dose of either gadolinium chloride (Gd) or nifedipine (Nf). Bars represent the mean joint region size. Dynamic controls (n=10), 1mM gadolinium chloride (n=6), 1mM nifedipine (n=5). Error bars represent the standard deviation. *p-values < 0.05, **p-values < 0.01. 131

Figure 9.1: Following the studies of this thesis, a new theorised relationship between the magnitude of movement and joint morphogenesis during development is hypothesised. This includes a non-linear dose dependent bell-shaped curved which sits above a threshold, 't', and is skewed around an optimal magnitude of movement, 'M_o'. 139

Figure 9.2: Several morphological events were affected during embryonic chick knee joint development when the mechanical conditions were altered except under average-flexion for which all events were unaffected. Morphological events that were unaffected are highlighted in blue and those that were affected are highlighted in red. 143

LIST OF TABLES

Table 5.1: Groups of knee joints compared to optimise culture conditions. Group 1 included knee joints from uncultured day 7 chick embryos. Comparisons of groups 2 and 3 were made to assess the method of nutrient delivery. Comparisons of groups 3 and 4 were made to assess the effect of soft tissue presence. Comparisons of groups 4 and 5 were made to assess the effect of culture duration. 88

Table 8.1: Number of cultures performed, explants cultured and explants used for analysis. ... 121

CHAPTER 1

1. INTRODUCTION

1.1 EMBRYONIC JOINT MORPHOGENESIS AND MECHANICAL STIMULI

Morphogenesis is defined as the development of form and structure, or shape, during growth. Joint morphogenesis therefore refers to the development of joint shape, which involves the moulding of cartilage and bone into mature, functional and distinctive joint structures. The complex shapes of the different types of synovial joints are formed from basic mesenchymal materials during embryonic development. Correct formation at this stage is therefore critical for joint function including smooth articulation during movement and tolerable transmission of biomechanical loads through the joint structure. Every year 2-3% of newborns are affected by some sort of congenital malformation worldwide (Corsello and Giuffrè, 2012). The most commonly occurring joint condition, developmental dysplasia of the hip (DDH), has an incidence of 0.15-2.5% worldwide depending on the criteria used for diagnosis (Schwend, 2014). Abnormal joint shapes can severely impact a patient's life, limiting their range of motion and increasing the chance of dislocation due to reduced joint stability. For those suffering from joint malformations, such as DDH, there is also an increased risk of developing degenerative joint diseases such as osteoarthritis (OA) due to abnormal articulation and load transmission (Sandell, 2012). With an increasing life expectancy and an ageing population, joint diseases such as OA are becoming more and more prevalent. Understanding prenatal joint formation is therefore significantly important

for the creation of diagnostic and treatment tools to try and reduce the incidence of joint abnormalities and consequently reduce the number at risk of developing degenerative joint diseases in later life.

Mechanical stimulation has been identified as a crucial variable during embryonic development to promote and direct normal joint formation. Clinical conditions of abnormal skeletal development have been linked to situations where fetal movements were restricted *in utero,* providing evidence for the importance of mechanical stimuli during development (Rodríguez et al., 1988a, Rodríguez et al., 1988b). Furthermore, animal model based investigations have continued to show detrimental effects on skeletal and synovial joint formation when the mechanical environment was altered (as reviewed in Nowlan et al., 2007, Nowlan et al., 2010b). The majority of studies performed to date have removed or inhibited movements during embryonic development and found synovial joints are under developed and lack fully defined interlocking shapes. Despite the growing evidence supporting the theory that mechanical stimuli are necessary for joint morphogenesis to occur correctly, its contribution is under researched. It remains unclear how variations in mode, magnitude and frequency of mechanical stimuli alters joint shape development.

This doctorate targeted this gap in scientific knowledge which has remained open for the last 80 years. The relationship between mechanical stimulation and joint morphogenesis has not yet been characterised and it is unknown whether the contribution of mechanical stimulation to promote joint shape development is linear, convergent or binary (Figure 1.1). Knowledge about the relationship between mechanical stimuli and joint morphogenesis is valuable for a variety of research areas. How different levels of movement affects normal joint shape development could potentially be used clinically to identify patients at risk of developing congenital joint malformations. How mechanical stimuli controls growth and development of joint structures can also aid in creating OA treatments and help with cartilage tissue engineering, where the aim is to

recapitulate developmental conditions *in vitro* to produce functional tissues in the lab for a variety of uses.

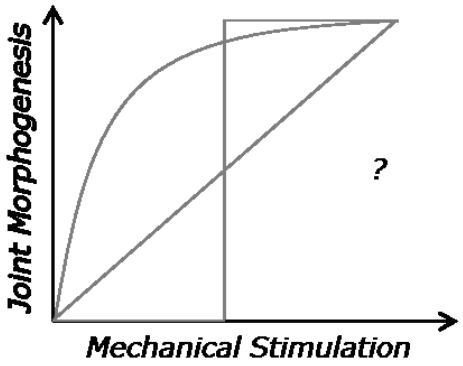


Figure 1.1: The relationship between mechanical stimuli and joint morphogenesis remains a mystery. No quantified data exists to determine if there is a linear, convergent or binary contribution of mechanical stimulation to promote joint shape development.

1.2 Objectives and Hypotheses

The aims of this doctorate were to experimentally characterise the effect of quantified mechanical stimuli on prenatal joint morphogenesis and identify mechanotransduction mechanisms involved in directing this process. In order to achieve these aims the following series of objectives were determined:

- Create a novel methodology to develop synovial joints in a controlled mechanical environment.
- Select and optimise methodology to analyse joint shape development.
- Characterise the morphological events involved in normal joint shape development.
- Apply a variety of quantified movements to developing joints without inducing trauma.
- Compare and evaluate the progression of joint shape development following different levels of mechanical stimulation to characterise the contribution of movement to joint morphogenesis.
- Block mechanotransduction pathways in developing joints to assess their involvement in joint morphogenesis.

Through the course of this doctorate a novel culture system was designed and optimised which allowed the embryonic chick hindlimb to be grown under a controlled environment with the option to apply physiological movements to the developing knee joint. Protocols for three-dimensional (3D) joint shape analyses were created for the chick knee joint to give qualitative and quantitative evaluations of joint morphology. These protocols were used to analyse physiological shape development of the embryonic chick knee joint to use as a reference to assess the progression of joint morphogenesis in cultured explants. Different magnitudes of movement were then systematically applied to developing knee joints to test the following hypotheses:

- Dynamic stimulation leads to a more developed joint shape than static conditions.
- Joint shape development is affected by movement magnitude in a dose dependent manner.
- The most physiological movement regime leads to a joint with the most normal progression of shape morphogenesis.

Finally, the additions of mechanosensitive ion channel blockers in culture were used to impede the regulation of ion concentrations during development to test the hypothesis:

- Mechanical stimuli that direct localised joint shape development are transduced through the function of mechanosensitive ion channels.

This thesis presents the work carried out to complete these objectives and the results of the experiments performed to test the proposed hypotheses.

1.3 THESIS STRUCTURE

Chapter 2 - This chapter includes a thorough review of the current literature regarding synovial joint formation and the role of mechanical stimuli during joint morphogenesis to place the research carried out in this thesis in the appropriate context.

Chapter 3 - Methods used to prepare embryos for culture, image and analyse joint morphology are described here. The exact step by step protocols used in the laboratory are attached in Appendix 1.

Chapter 4 - This chapter describes the normal sequence of knee joint morphogenesis for the chick embryo. This includes current knowledge along with new findings made during this doctorate to characterise the emergence and shape development of key landmarks of the knee joint.

Chapter 5 - The new culture system developed as part of this doctorate is presented in this Chapter. This includes the design of the culture system, calibration of knee joint movement and the optimisation of culture conditions. Creation of this system formed a major part of this doctorate.

Chapter 6, 7 & 8 - These three chapters present the different studies conducted to test the hypotheses set out above. Chapter 6 compared joint shapes produced following dynamic and static movement regimes. Chapter 7 explored the effect of varying movement magnitudes of the knee joint during development. Chapter 8 tested the involvement of ion channels in transducing mechanical stimuli for joint shape development.

Chapter 9 - In this chapter, the work carried out during the course of this doctorate is summarised and put into the context of current scientific knowledge. Future studies that directly follow the work of this doctorate are also proposed here.

CHAPTER 2

2. BACKGROUND

2.1 THE ROLE OF THE SKELETON AND SYNOVIAL JOINTS

The skeleton is defined as *"the bones or bony framework of an animal body considered as a whole" (Oxford English Dictionary)*. In vertebrates, the skeleton is divided into two parts: the axial skeleton and the appendicular skeleton. The axial skeleton is composed of the vertebral column, the rib cage and the skull. The appendicular skeleton attaches onto the axial skeleton and forms the framework for the limbs including the shoulder and pelvic girdles. The main functions of the skeleton are to provide support for the body, allow for movement, provide protection of vital organs, for storage of minerals and produce blood cells. Synovial joints are found between skeletal elements and allow the skeleton to move. There are six types of synovial joint, each shaped to allow for different patterns of motion. These are planar, hinge, pivot, condyloid, saddle, and ball and socket joints (Faller et al., 2004). A synovial joint consists of two or more bony skeletal elements, articular cartilage, ligaments, synovium and a joint capsule (Faller et al., 2004). The mammalian and avian skeletons contain many homologous elements but are each adapted and shaped for different functions (Dumont, 2010). Correct formation of the skeletal elements during embryonic development (skeletogenesis) is ultimately responsible for functional success postnatally, with alterations in joint architecture being identified as a risk factor for joint degenerative diseases such as osteoarthritis (OA) (Sandell, 2012).

2.1.1 THE KNEE JOINT

To explore embryonic joint morphogenesis, it was necessary to choose a suitable developing joint model and a method of applying mechanical stimulation. It was aimed to recreate a physiological joint movement *in vitro* as opposed to applying a deformation or hydrostatic pressure to a developing joint, since a biomechanical movement would be more comparable to physiological conditions. The knee joint, is an accessible joint that can be manipulated along a single plane to capture the majority of its biomechanical range of motion compared to other joints where the biomechanics are more complex such as the hip.

The knee joint is a complicated anatomical structure, which is composed of many bony interactions. There are four skeletal elements within the knee joint: the femur, tibia, fibula and patella. In human anatomy, three joints exist between these four elements: the femoro-tibial joint, the patella-femoral joint and the fibula-tibial joint (Blackburn and Craig, 1980). The knee joint is classified as a condyloid joint which has two main degrees of freedom. The primary movement allows for flexion and extension of the femur relative to the tibia/fibula about the sagittal axis (Figure 2.1A). The secondary movement is medial-lateral rotational of the tibia/fibula relative to the femur about the transverse axis and only occurs during large flexion of the joint (Figure 2.1B). The knee joint also allows for some translational movement of the femur over the tibia/fibula however these movements are small and often neglected to simplify the biomechanical description of the knee.

The femoro-tibial joint connects the distal femur with the proximal tibia and the fibula-tibial joint connects the supportive fibula to the tibia in humans (Figure 2.2A). In the chick skeleton, the femur articulates with both the tibia (or tibiotarsus due to the fusion of tarsal bones to the distal tibia) and fibula creating a femoro-tibial and femoro-fibular joint (Haines, 1942) (Figure 2.2B). For the purpose of this doctorate the formation of these two joints were considered together as the stifle and are referred to as the knee joint from here onwards.

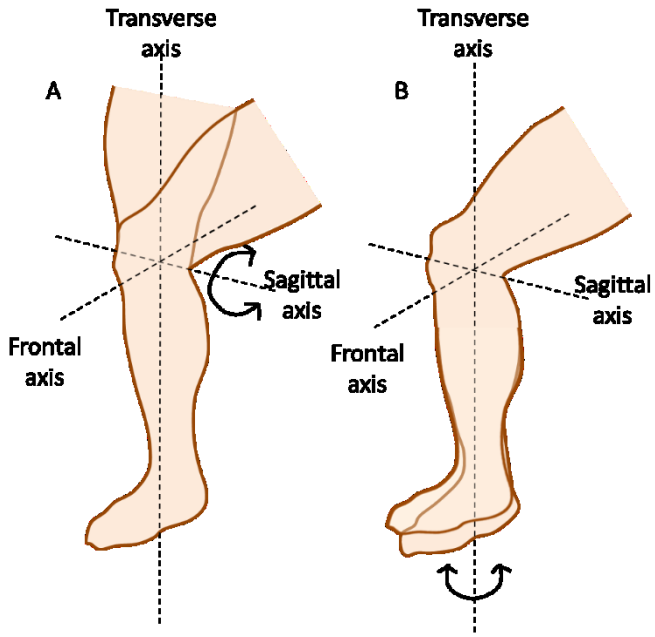


Figure 2.1: The motion of the knee joint can be simplified into two degrees of freedom. A) Anterior-posterior flexion and extension about the sagittal axis which causes the lower limb to bend and straighten. B) medial-lateral rotation of the tibia/fibula about the transverse axis which occurs during large flexion turning the foot in and outwards.

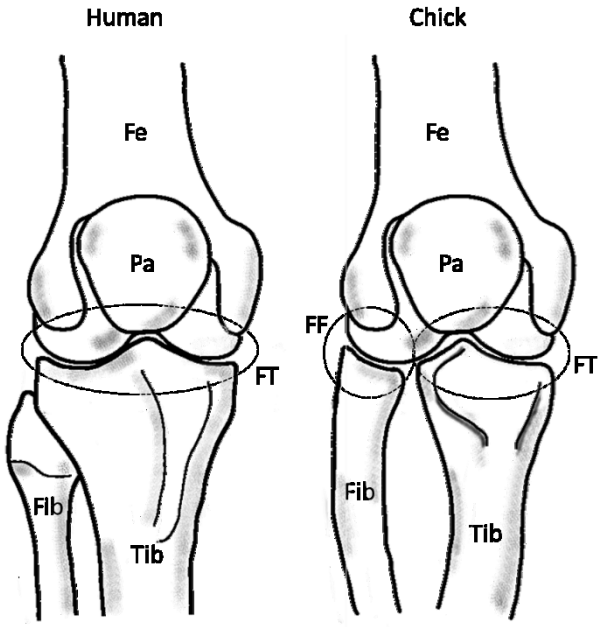


Figure 2.2: Cartoon drawings showing the bony anatomy of the human and chick knee joint. The femur articulates with both the tibia (tibiotarsus) and fibula in the chick whereas in humans the femur only articulates with the tibia. Fe – femur; Pa – patella; Fib – Fibula; Tib – Tibia; FT – femoro-tibial joint; FF – femoro-fibular joint.

The shape of the knee joint is described as bicondylar due to the presence of two convex condyles located on the distal femur. The medial and lateral femoral condyles articulate with the tibia and the fibula respectively in the chick which both have slight concave profiles to create an interlocking joint. Not a lot is known about the formation of the patella during development. A recent study found that the patella initially forms as part of the femur which then separates due to mechanical loading of the knee joint in the mouse (Eyal et al., 2015). In humans, it is believed the patella forms as a cartilaginous structure within the quadriceps tendon and does not ossify until after birth. Assessment of the development of the patella-femoral joint was not included in this project.

2.2 Appendicular Skeletogenesis

Bones are produced by the transformation of mesenchymal stem cells (MSCs) into cartilaginous tissues and bone via the process of intramembranous ossification or endochondral ossification (Gilbert, 2000). Intramembranous ossification involves the direct conversion of MSCs into bone and occurs primarily for flat or short bones. Most of the long bones of the skeleton are created first through the conversion of MSCs into cartilage which is then later replaced by bone, through a process called endochondral ossification.

Skeletal positional identity is determined early during embryonic development through skeletal patterning mechanisms (Yang, 2013). Skeletal patterning begins with migration of MSCs to sites of the future skeleton (Lefebvre and Bhattaram, 2010). Skeletal progenitor cells are known to arise from three locations in the developing embryo. The neural crest hosts a population of cells which establish the craniofacial skeletal elements, the paraxial mesoderm gives rise to the somites which produce the axial skeleton and the lateral plate mesoderm gives rise to the limb elements or appendicular skeleton (Lefebvre and Bhattaram, 2010, Yang, 2013). Condensations of skeletal progenitor cells form an outline of the skeleton termed the membranous skeleton where they undergo a series of progressive cellular processes, including migration, adhesion, proliferation, differentiation and growth (Hall and Miyake, 2000). In the case of the long bones,

the MSCs undergo chondrogenesis and differentiate into chondrocytes leading to the formation of a continuous cartilaginous skeleton (or primary skeleton) which eventually becomes the osseous (bony) skeleton.

The appendicular skeleton develops proximal to distal, anterior to posterior and dorsal to ventral (Yang, 2013). Proximal-distal outgrowth of the limbs initiates with the formation of a limb bud headed by the apical ectodermal ridge (AER) which directs 3-dimensional (3D) development of the limb segments. In each limb, the membranous skeleton forms a continuous 'Y' shaped condensation corresponding to the humerus and forked radius and ulna in the forelimb and the femur and forked tibia and fibula elements in the hindlimb (Storm and Kingsley, 1996, Pacifici et al., 2005, Decker et al., 2014). Chondrogenesis, the process by which skeletal progenitor cells construct the cartilage limb anlagen, initiates when MSCs stop proliferating and condense into compact nodules (Gilbert, 2000). The mesenchymal tissue undergoes early differentiation into chondroblasts which resume proliferation and start to produce cartilage extracellular matrix (ECM) containing proteoglycans and glycosaminoglycans (Lefebvre and Bhattaram, 2010). As chondroblasts mature, they differentiate further into chondrocytes and shape the cartilaginous rudiments to give rise to a diaphysis (shaft) and two epiphyses (rounded end). Eventually, chondrocytes undergo hypertrophy and stop dividing. Hypertrophic chondrocytes start to alter the composition of the ECM they produce, adding collagen X, which enables it to become mineralised by calcium carbonate (Gilbert, 2000). Eventually these terminal chondrocytes die and their space is invaded by osteoblasts which lay down bone matrix in their place during ossification (Lefebvre and Bhattaram, 2010). The primary ossification centre is found in the middle of the diaphysis of long bones, followed by secondary ossification centres in the epiphyses.

The initial stages of formation of the appendicular skeleton in mammals and avian species are similar during which a cartilaginous template of the skeleton is first laid out. It has to be acknowledged however, that differences do exist in the process of ossification (Nowlan et al., 2007). In mammals, the cartilage templates are turned into bone through endochondral

ossification as described above, whereas in avian species the mature cartilage in the centre of the long bones is resorbed to create hollow structures (Nowlan et al., 2010b). In both genera, the periosteum is formed directly from MSCs by intramembranous ossification.

2.2.1 Synovial Joint Formation

Synovial joints develop between the ends of long bone elements. MSCs that will form the future joint follow an articular fate at the epiphyses of the long bones, where they differentiate into the various joints structures through the process of joint formation (Lefebvre and Bhattaram, 2010). The formation of the bony ends has four main stages: joint site determination, interzone formation, cavitation and morphogenesis (Pacifici et al., 2005). Skeletal progenitor cells assigned for joint formation migrate and condense at future joint locations which are believed to be genetically predetermined (Figure 2.3A). The condensed area of progenitor cells forms a thicker and more compact structure of cells orientated perpendicular to the long bone anlagen called the interzone (Figure 2.3B). The formation of the interzone divides the continuous cartilaginous template of the primary skeleton and is known to act as the signalling centre to control further joint development and host the materials needed for the formation of all joint structures (Khan et al., 2007, Decker et al., 2014). Cells in the interzone are closely packed together and structured into three interconnected layers (Archer et al., 2003). The centre of the interzone differentiates into articular chondrocytes to eventually become articular cartilage, whilst the outer layers differentiate into normal chondrocytes and merge with the epiphyses of the long bones (Pacifici et al., 2005). The process of joint formation up to this point is believed to be preprogramed and internally controlled.

Joint morphogenesis and cavitation (Figure 2.3C & D) are responsible for the creation of joint shape and the individual skeletal elements. The articular shape of the joint starts to form before cavitation has occurred and continues well after to create the joint shapes we recognise in mature skeletons (Nowlan and Sharpe, 2013). Cavitation is the process of physical separation of the joint and creation of individual skeletal elements (Figure 2.3D). Separation is induced by local

production and accumulation of hyaluronan which causes a loss of tissue integrity in the interzone leading to physical separation of the joint sides through programmed cell death (Pacifici et al., 2005). Hyaluronan synthesis within the interzone has been associated with movement of the joint during development (Archer et al., 2003). Separation of the skeletal elements leads to the formation of a fluid filled joint cavity. Joint morphogenesis is the least researched and least understood stage in early skeletal formation.

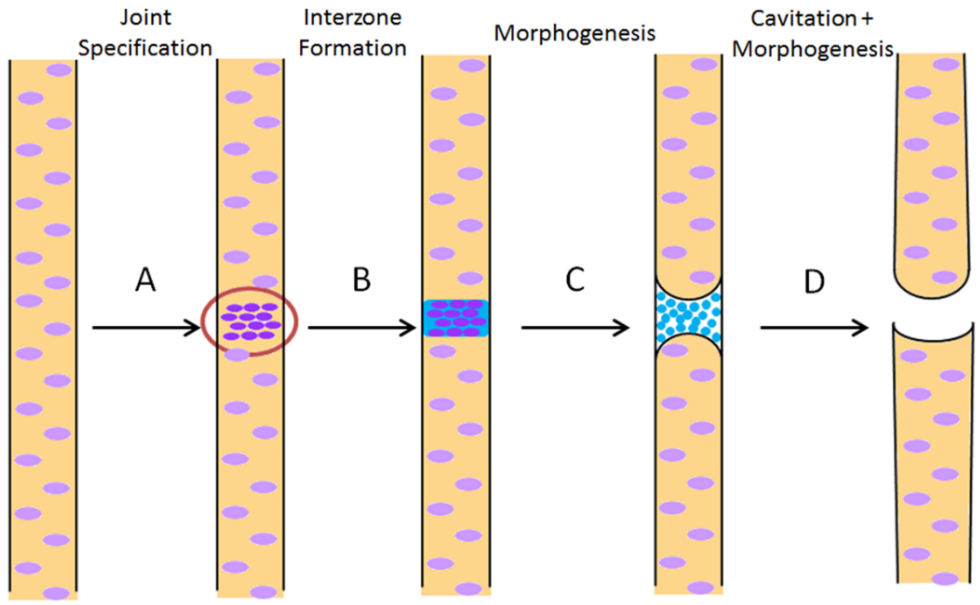


Figure 2.3: Early joint development has four stages: joint site determination, interzone formation, cavitation and morphogenesis. A) MSCs condense within a continuous anlage of skeletal elements at the location of the future joint. B) Here they commit to an articular fate to form a dense interzone of joint progenitor cells. C) The two ends either side of the joint location start to take shape through morphogenesis. D) Eventually the two ends physically separate to create individual skeletal elements and a joint cavity.

The mechanisms behind how specialised joint shapes are created are a mystery currently being investigated. Pacifici et al. (2005) proposed 3 simple theories for how the two sides of a synovial joint acquire their distinctive shapes: "*1) the distal side would preferentially grow and protrude into the proximal side; 2) the lateral portions of proximal side would preferentially grow and "wrap" themselves around the distal side; 3) both events would occur simultaneously".* These theories though, assume that cavitation has taken place before the joints are shaped, however, we know

that joint morphogenesis initiates before cavitation (Nowlan and Sharpe, 2013). Recently, it was suggested that a change in rates of differentiation, proliferation, or migration could potentially all be responsible for changes to joint shape (Brunt et al., 2015). The cellular mechanisms involved in creating these complex shapes remains ambiguous to this day, but, it is strongly believed that mechanical stimulation directly influences these cellular behaviours and joint morphogenesis.

2.3 CARTILAGE MECHANOBIOLOGY

Cartilage is composed of chondrocytes embedded in an ECM of collagen, proteoglycans and water. There are three types of cartilage: hyaline cartilage, fibrocartilage and elastic cartilage. Hyaline cartilage is produced during bone formation during endochondral ossification and makes up the primary skeleton (Scheuer and Black, 2004). Hyaline cartilage is therefore involved in joint formation and the type of cartilage of interest for this research. Fibrocartilage is a more fibrous type of cartilage and appears in structures subjected to high impact forces such as the intervertebral disk and meniscus (Fisher et al., 2007). Elastic cartilage, as the name suggests, gives rise to structures able to deform and return to their original shape such as the external ear and epiglottis (Fisher et al., 2007).

There is significant evidence that the development of the skeleton is regulated by mechanical stimuli (stresses and strains) within pre-cartilaginous and cartilaginous tissues (Carter and Wong, 2003, Nowlan et al., 2007, Kelly and Jacobs, 2010, Rolfe et al., 2013). Cartilage is mechanically sensitive and responds to cell to cell and cell to matrix interactions within the local environment (Kelly and Jacobs, 2010). Mechano-sensors such as stretch activated ion channels, primary cilia and transmembrane proteins provide the means to transduce mechanical stimuli into cellular responses which can regulate growth and maintenance of cartilage.

A vast number of studies have repeatedly shown that both MSCs and chondrocytes respond to mechanical stimuli such as deformation, fluid flow, streaming potentials, hydrostatic pressure and osmotic pressure (reviewed in O'Conor et al., 2013). Experimental evidence suggests that mechanical stimulation can direct the fate of undifferentiated MSCs and is needed to trigger

processes such as chondrogenesis and endochondral ossification (reviewed in Kelly and Jacobs, 2010, O'Conor et al., 2013). Remodelling of mature healthy joints shows that cartilage continues to respond to mechanical stimuli throughout its entire life (Bader et al., 2011). Experimental studies have repeatedly shown that dynamic loading of cartilage can enhance matrix production and constant static loading can inhibit growth (reviewed in O'Conor et al., 2013). Insufficiently loaded or high impact loading has also been shown to cause catabolic chondrocyte activity causing cartilage degeneration (Bader et al., 2011). Whilst experimental studies provide evidence for the different tissue responses to mechanical stimuli, computational mechanobiology theories have tried to quantify the biological laws that govern responses such as differentiation, proliferation and remodelling (Nowlan et al., 2007). In computational mechanobiological models, it is generally agreed that loading of cartilage by hydrostatic stress (compression) inhibits growth and intermittent tensile strains accelerate growth and ossification (Carter and Wong, 2003). Computational models of cartilage growth have been made based upon such rules to quantify the mechanical stimuli (stresses and strains) involved during the development of synovial joints (Giorgi et al., 2014).

Although strong experimental evidence exists for the mechano-sensitivity of cartilage at the cellular scale in isolated circumstances, the exact role of mechanical stimuli during synovial joint formation and morphogenesis at the tissue scale is under researched. The literature provides a strong case for the importance of cartilage mechanobiology for correct joint formation, however, no quantified data exists to map the relationship between mechanical stimulation and joint morphogenesis.

2.4 The Role of Mechanical Stimuli During Synovial Joint Development

Clinical case studies highlighted the negative effect of abnormal fetal movements on skeletal and synovial joint formation. Lowered mineral density (osteopenia) and physical defects in long bones were reported in newborns whose fetal movements were restricted due to neuromuscular diseases (Rodríguez et al., 1988a, Rodríguez et al., 1988b). Commonly occurring musculoskeletal

abnormalities include developmental dysplasia of the hip (DDH), arthrogryposis and fetal akinesia deformation sequence (FADS) (reviewed in Nowlan, 2015). Since clinical reports do not allow for the assessment of the developmental mechanics involved, researchers have turned to culture and animal models to experimentally explore the role of mechanics during skeletogenesis. Computational models have also been used to quantify the contribution of different biophysical stimuli during synovial joint formation. It is understood that only the later stages of synovial joint formation (cavitation and morphogenesis) are affected by mechanical stimuli; synovial joint site determination and interzone formation have both been shown to proceed even in the absence of prenatal movements (Archer et al., 2003, Pacifici et al., 2005, Kahn et al., 2009). Researchers initially concentrated on joint cavitation as a biomarker of normal and abnormal joint formation as it could easily be identified using traditional histology methods. Interest in joint shape though, has increased recently and newer studies have been able to comment on normal and abnormal joint shapes using higher resolution imaging modalities. Below is a review of published literature focused on the role of mechanical stimuli on joint morphogenesis.

2.4.1 Culture Models

Classic culture models involved isolating embryonic limb fragments and culturing them as explants, or grafts on other embryos. This allowed researchers to study the consequences of removing muscular activity during development (e.g. Fell, 1925, Murray and Selby, 1930). The majority of these models were used to evaluate skeletal development of the long bones with only a few studies focusing on synovial joint development. Hindlimb explants from four day old chick embryos cultured for up to 17 days *in vitro* showed the location of the knee joint could be clearly made out after four days of culture showing that the early stages of joint formation continued in the absence of muscular activity (Fell and Canti, 1934). After six days of culture, fusion across the joint site caused cartilaginous continuity between the three rudiments in the chick hindlimb (Fell and Canti, 1934). This result exposed the consequence of removing movement during development, which was corroborated with similar findings for seven day old embryonic chick knee joints also cultured under static conditions for six days (Figure 2.4A) (Lelkes, 1958). The

effects of static culture on joint development were confirmed to be due to the mechanical environment when manual manipulation of the explants during culture led to cavitation and the development of articular surfaces between the femur and tibia after six days (Figure 2.4B) (Lelkes, 1958).

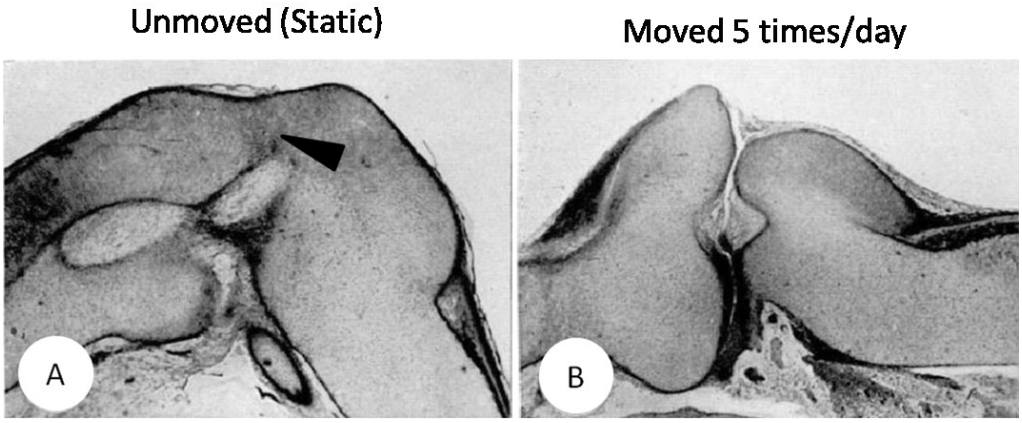


Figure 2.4: A clear difference in joint formation was observed in seven day old chick knee joints cultured for six days *in vitro*. A) Under static conditions the knee joint became fused (filled arrow) and lost its recognised articular shape. B) Manual manipulation of the joints during culture allowed for formation of a joint cavity and a defined articular shape. Adapted from Lelkes (1958).

This result confirmed that external passive mechanical stimulation promotes normal joint development processes whereas explants experiencing no mechanical stimulation developed abnormal joint features. More recently, a feasibility study was published which showed the whole chick hindlimb could be cultured whilst mounted to a plastic hinge to apply flexion and extension movements to the knee joint (Rodriguez and Munasinghe, 2016). The study however was not able to comment on joint development due to methodological limitations.

2.4.2 Animal Models

In vivo animal models have the advantage of keeping the developing joint in its native environment. Controlling the mechanical stimulation of the developing joints, however, becomes more challenging. In most cases this is achieved by reducing muscle activity through paralysis or using specific genetic mutations where muscle contraction is affected. Embryonic synovial joint

formation has mainly been studied using both the developing chick and mouse model, although more recent studies have included the use of the zebra fish.

The chick embryo is a valuable animal model for developmental studies as paralysis can be induced by dropping pharmacological agents into the egg or via surgical techniques such as spinal cord destruction. Decamethonium bromide has been commonly used to induce rigid paralysis in chick embryos during development causing the chick to go into a state of tetanus (all muscles contracted) applying an unchanging static environment. Similar to *in vitro* discoveries, authors described articular joints such as the knee, as becoming fused across the joint site and report a loss of normal interlocking joint shapes following rigid paralysis (Figure 2.5) (Drachman and Sokoloff, 1966, Hall and Herring, 1990, Hosseini and Hogg, 1991, Osborne et al., 2002).

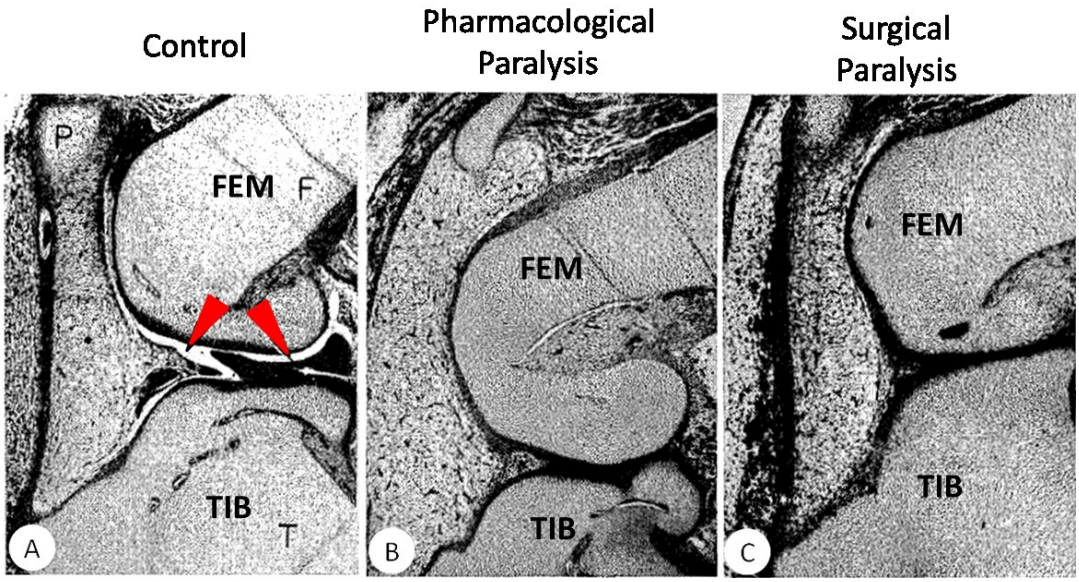


Figure 2.5: Joint development was compromised in immobilised chick embryos. Joint cavitation (red arrows) was seen in control embryos (A), but did not occur in embryos following pharmacological (B) or surgical paralysis (C). The shape of the articular ends of the femur (fem) and tibia (tib) were also abnormal following immobilisation. Adapted from Drachman and Sokoloff (1966).

Looking closer at joint shape, Roddy et al. (2011b) found a consistent difference between the shape of the distal femur in the chick knee joint after five days of paralysis. The resulting shape of the paralysed knee was observed to be flattened and much smaller compared to controls

(Figure 2.6). The largest difference was found to be the width of the intercondylar fossa which separates the two femoral condyles on the ventral side of the femur (Roddy et al., 2011b). Rigid paralysis of the chick embryo was recently shown to be a suitable model of DDH by affecting morphogenesis of the hip joint (Nowlan et al., 2014). Compared to age-matched controls, the indentation of the femoral neck was missing in immobilised embryos obscuring definition of the femoral head (Nowlan et al., 2014). Abnormal shapes of the proximal femur and acetabulum in immobilised embryos were identified as markers of DDH and joint instability, further supporting the consensus that prenatal movements are important for correct joint morphogenesis. The consequences of removing spontaneous movements were also noted to be more severe after the timepoint that cavitation should have occurred, suggesting that the process of joint separation contributes to normal joint morphogenesis.

Similar effects of altered mechanical stimuli during joint morphogenesis have been observed in the zebra fish jaw (Brunt et al., 2015). Reduced muscle mutants, flaccid paralysis (all muscles relaxed) and rigid paralysis altered the alignment of the two skeletal elements in the jaw by affecting the gap size on the medial and lateral sides of the joint (Figure 2.7). Differences in the shape outlines also revealed a medial-lateral effect on joint morphogenesis where the Meckel's cartilage became very asymmetrical under altered mechanical conditions (Figure 2.7A) (Brunt et al., 2016). Interestingly, these shape abnormalities were also present in jaws from hyper-active mutant fish experiencing excessive joint movements during development (Brunt et al., 2016).

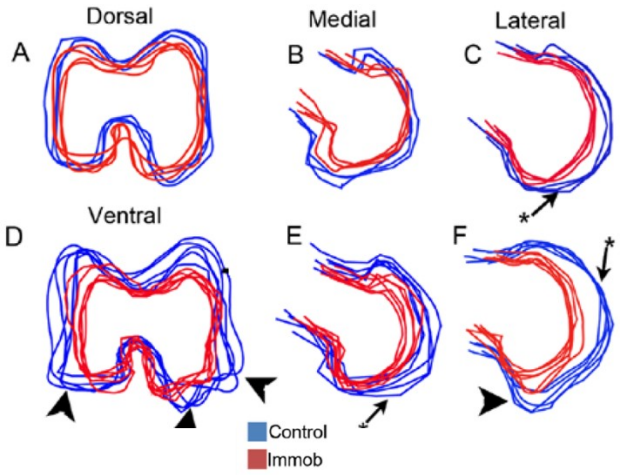


Figure 2.6: Rigid paralysis in the chick embryo caused the shape of the distal femur to become simplified. Arrow heads indicate regions of reduced outgrowth in the immobilised animals. Arrows indicate flattening of rudiment surfaces. (A-D) after 4 days of immobilisation; (E,F) after 5 days immobilisation. Adapted from Roddy et al. (2011b).

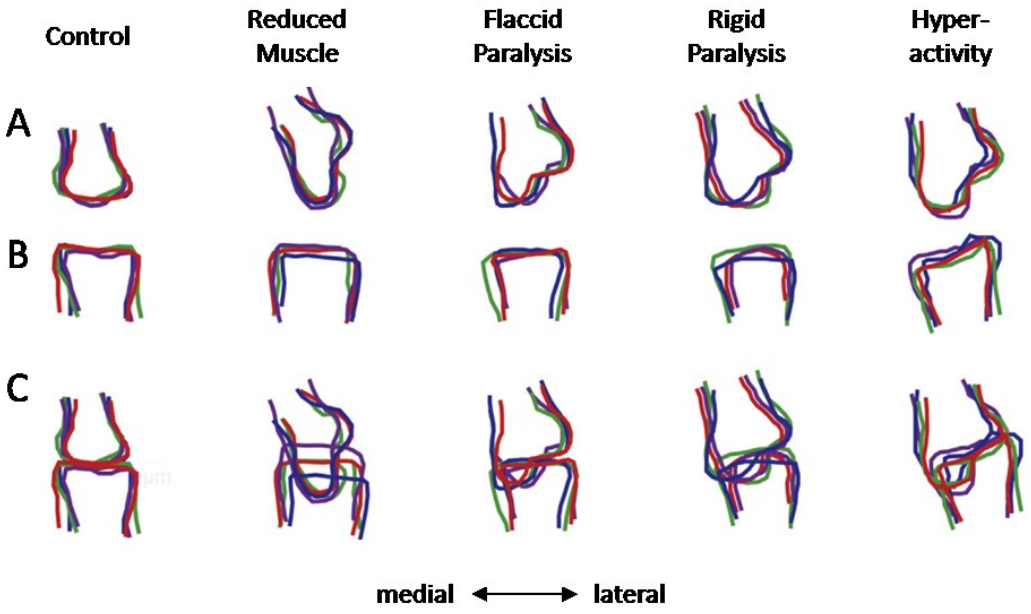


Figure 2.7: The shape of the jaw from zebrafish was found to be abnormal under altered mechanical environments. Outlines show the frontal shape of the A) Meckel's cartilage (MC) element, B) palatoquadrate (PQ) element and C) the two elements aligned together. The medial side of the MC was elongated under altered conditions included hyper-activity. The biggest effect was found in the alignment of the two elements which overlapped under altered mechanical conditions. Adapted from Brunt et al. (2016).

Mutant murine models allowed to develop in an undisturbed environment provide further evidence for the importance of spontaneous movements during joint formation. Failure in the separation of joint sides has been seen in muscle-less limb mouse embryos, particularly at the elbow joint (Figure 2.8) (Nowlan et al., 2010a). The process of joint morphogenesis was also reported as missing in mice with reduced limb muscle and muscle-less limb phenotypes Kahn et al. (2009). Interzone specification was seen in mutant embryos but as development proceeded, chondrogenic markers were increasing expressed, leading to joint fusion and the cease of normal joint development (Kahn et al., 2009).

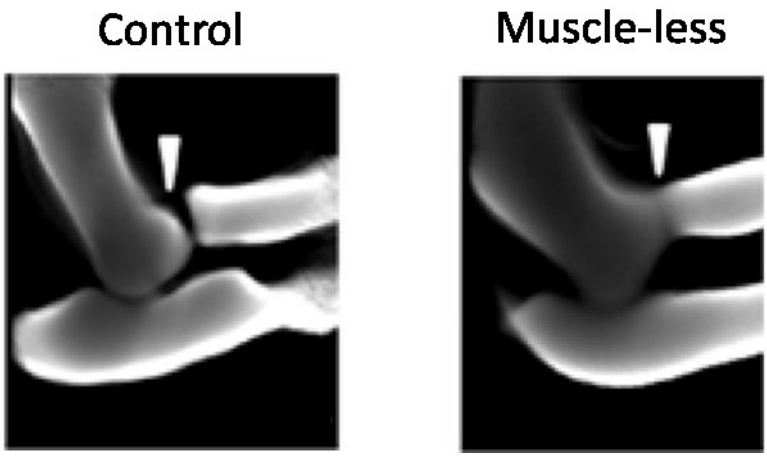


Figure 2.8: Joint cavitation was missing in mutant muscle-less mice at the elbow joint along with the development of articular joint shapes. Adapted from Nowlan et al. (2010a).

2.4.3 Computational Studies

Computational models using cartilage growth laws have tried to predict how mechanical stimuli affect joint shape development. The first simulation of joint morphogenesis was carried out by Heegaard et al. (1999) to predict the surface shape of the finger joint. This study showed that biological growth of the joint alone was not sufficient to produce an interlocking joint shape. However, with the inclusion of hydrostatic stress due to joint motion the model was able to produced one convex and one concave surface (Heegaard et al., 1999). Further research has

shown that the inclusion of stresses generated during simple joint movements to simulated cartilage growth laws can predict anatomically recognisable joint shapes from simple starting configurations (Giorgi et al., 2014) (Figure 2.9). Simulation of normal and abnormal movement on more advanced joint shapes, such as the hip joint, also revealed that symmetric movements maintained a stable joint shape, whereas abnormal movements lead to a deformed asymmetric acetabulum and femoral head (Giorgi et al., 2015) (Figure 2.10).

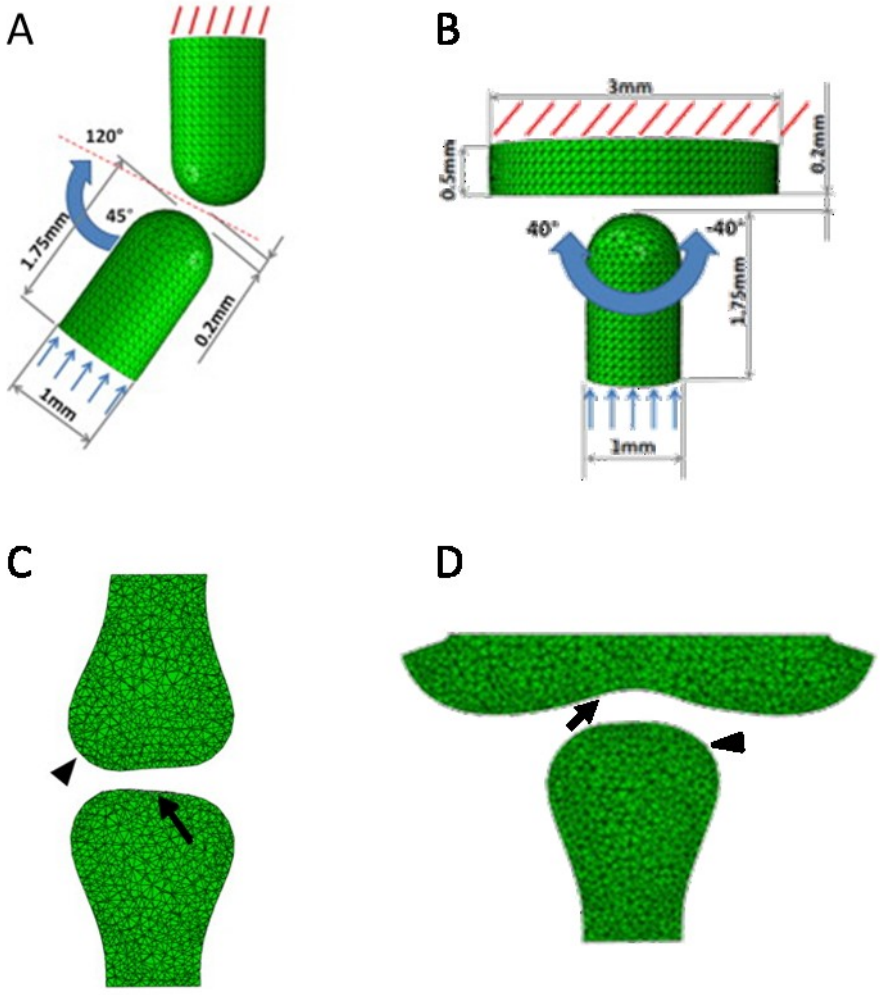


Figure 2.9: Joint morphogenesis can be predicted using mechanobiology theory for cartilage growth. Applying A) single plane motion from 45° to 120° and B) multi plane motion from 40° to -40° to basic geometries of two skeletal elements, joint shapes can be predicted that resemble the C) knee joint and D) hip joint. Convex (arrowhead) and concave (arrow) profiles can be seen in both examples. Adapted from Giorgi et al. (2014).



Figure 2.10: Abnormal fetal movements in the hip joint leads to progressive opening of the acetabulum whilst the femoral head loses sphericity. The predicted hip joint shape is similar to a hip joint from an infant affected by DDH. Adapted from Giorgi et al. (2015).

Researchers have also applied finite element (FE) models to developing joints based on 3D joint morphology to assess the distribution of biophysical stimuli across the joint region. When applied to the chick knee joint, areas of increased biophysical stimuli matched localised areas of growth measured experimentally during a simulated knee flexion and extension movement (Roddy et al., 2011a). A consistent increase in biophysical stimuli over the medial condyle was observed which matches its increased growth seen experimentally during the same stages of development (Figure 2.11) (Roddy et al., 2011a). Using the same FE model, a comparison to rigid paralysis was also made which revealed that under these conditions the levels of biophysical stimuli were reduced and more evenly spread (Figure 2.11) (Roddy et al., 2011b). Comparing the experimental results with the FE models, it was proposed that a decrease in biophysical stimuli causes flattening of the femoral condyles and simplification of shape in the developing chick knee (Roddy et al., 2011b).

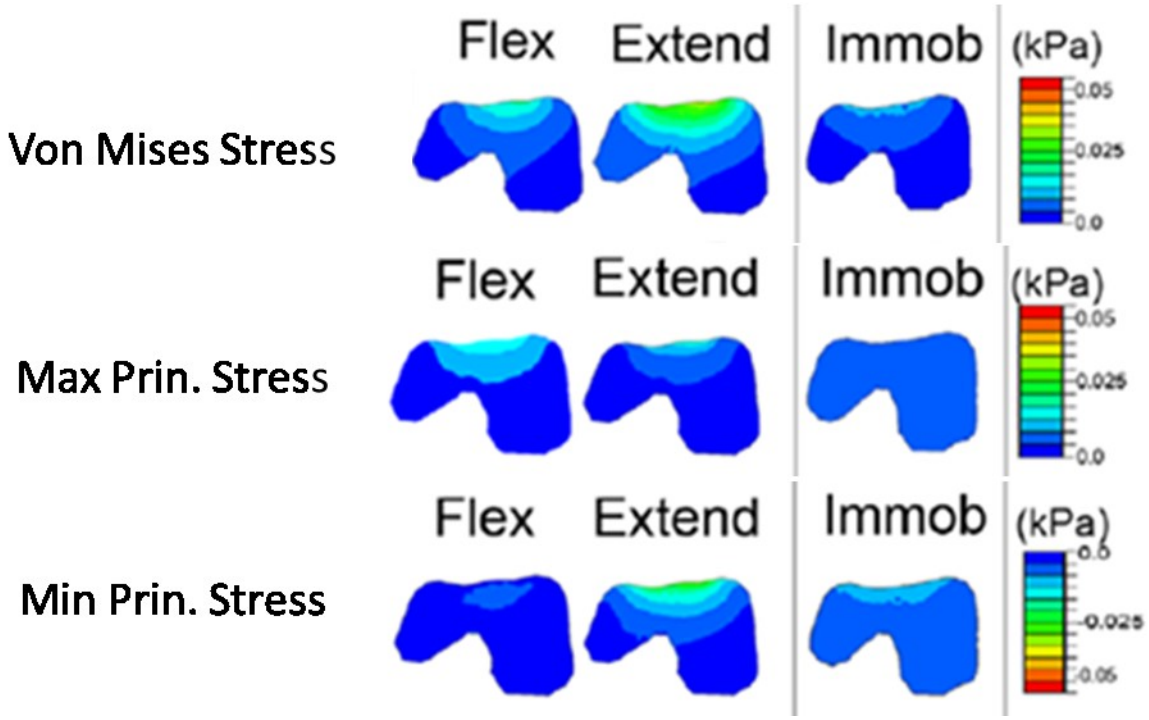


Figure 2.11: Predicted patterns of biophysical stimuli in matched areas of localised growth seen in normal development of the distal femur in chick embryos. Adapted from Roddy et al. (2011b).

2.5 SUMMARY

This chapter has presented a review of skeletogenesis, synovial joint formation and the role of mechanical stimuli on joint morphogenesis from published literature. Cartilage is mechanically sensitive and can adapt to changes in its environment to direct localised growth, resorption and remodelling. The process of joint shape development is also clearly mechanically sensitive, with multiple examples of abnormal joint formation under altered mechanical conditions found in literature. In this thesis, research is presented that builds on existing knowledge of joint morphogenesis using a novel culture model. Specifically, this research focused on investigating the unknown influence of quantified movements on joint shape development to characterise the relationship between mechanical stimulation and joint morphogenesis.

CHAPTER 3

3. MATERIALS AND METHODS

Generic methods used throughout this thesis are explained in detail within this chapter. Additional methods specific to individual parts of the thesis are explained within their relevant chapters. The explant culture methodology developed and optimised during the course of this doctorate is presented separately in Chapter 5. Step-wise protocols for the methods described here can be found in Appendix I.

3.1 HARVEST AND DISSECTION OF EMBRYOS

Fertilised DeKalb White eggs were used throughout the doctorate (Henry Stewart & Co Ltd, UK). During shipment and upon arrival, eggs were stored at 13^{o}C to pause the initiation of embryo development. To begin each experiment, eggs were transferred into Corti Semi-Automatic incubators (The Incubator Shop, UK) and kept at 37.5^{o}C (Figure 3.1A). Humidified conditions were constantly maintained by keeping distilled water inside the incubators underneath the eggs. During incubation, the eggs were turned once a day to mimic the natural behaviour of the mother hen until the day of harvest. On the day of harvest, eggs were removed from the incubator and a window was cut into the egg shell using curved scissors (Figure 3.1B). The embryo was lifted out of the shell carefully using a perforated spoon. Vasculature membranes were severed at this point using straight scissors to free the embryo from the contents of the egg. Each embryo was placed in a 9cm plate containing sterilised phosphate buffered solution (PBS). Embryos were cleaned to

remove any pieces of egg shell and remaining membranes using curved and straight forceps (Figure 3.1C). Embryos were euthanized by decapitation using curved forceps and a scalpel. Embryos were then transferred into the lid of the 9cm plate with fresh PBS for dissection under a microscope (Leica EZ4HD). To dissect the hindlimbs, the embryo was positioned onto its front to spread the limbs from the vertebral column. An incision was then made each side of the spine on the medial side of the pelvis using a scalpel (Figure 3.1D).

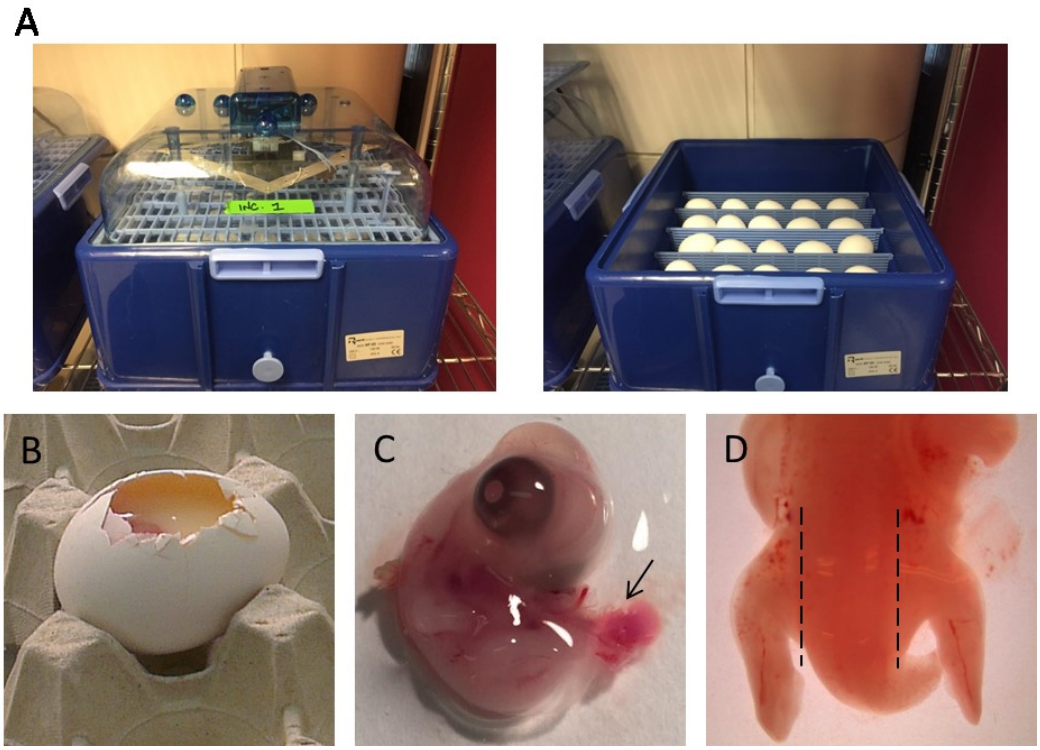


Figure 3.1: (A) Fertilised eggs were incubated at 37.5°C in humidified incubators. Each egg was (B) windowed to gain access to the embryo. (C) Membrane attachments (arrow) were removed from the embryos to give clear visualisation of the hindlimbs. (D) Incisions were made either side of the spine to dissect the hindlimbs from the embryo body.

Using curved forceps, the hindlimbs were then pulled away from the embryo body. All dissections were carried out at room temperature. Immediately after dissection, hindlimb explants were kept in warmed basal media (alpha - minimum essential media (GlutaMAX, Gibco) supplemented with 1% antibiotic antimycotic solution and 100uM Ascorbic Acid (Sigma, UK)) in preparation for

culture, or serially dehydrated in ethanol for 3D shape analysis. All experiments were performed in accordance with European Legislation (Directive 86/609/EEC), under which no license is necessary when working with embryos younger than two thirds through gestation.

3.2 3D Imaging of Explants

Optical projection tomography (OPT) can be used to acquire 3D information of large biological tissues (>2-3mm) in a non-destructive way (Sharpe et al., 2002). The advantage of using an optical imaging system meant a higher resolution could be achieved compared to other imaging modalities such as microscopic magnetic resonance imaging. Producing a 3D reconstruction of the developing joints was crucial for further analysis to be carried out since specimens could be virtually orientated, segmented and manipulated. A custom OPT system was used throughout this doctorate (Figure 3.2). A 3D tomographic reconstruction was made using a collecting of projections (images) acquired during a 360 degree rotation of a specimen. Explants needed to be stained, embedded and scanned using the OPT machine to produce these projections.

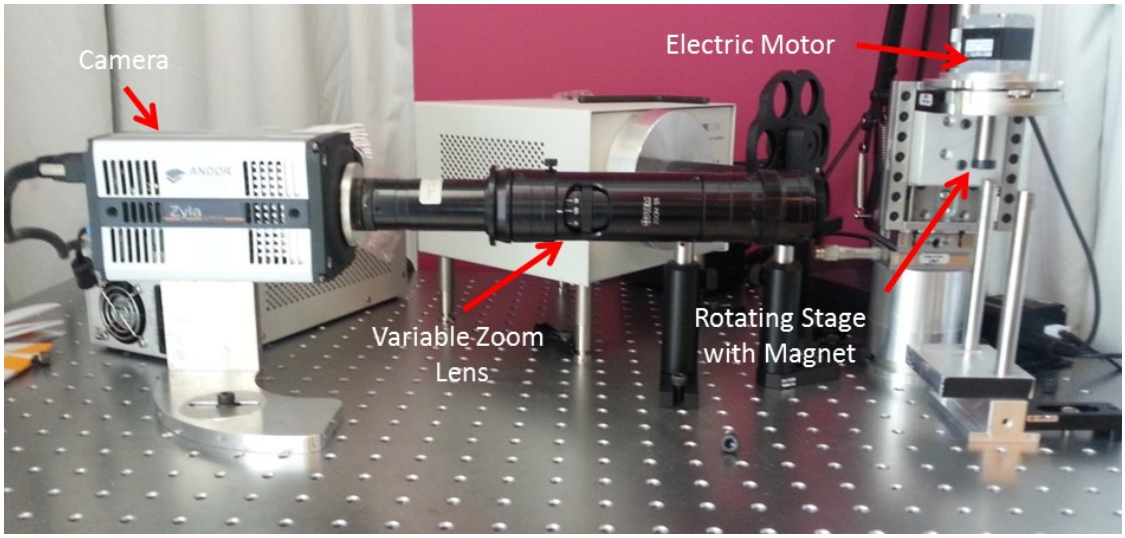


Figure 3.2: Image of OPT system used to create projections of explants. Explants were mounted to the rotating stage and imaged using the sCMOS camera during a 360 degree rotation.

3.2.1 Staining of Explants

Explants were stained to identify cartilage tissue and improve the contrast of the skeletal rudiments. Alcian Blue and Alizarin Red dyes can be used to stain embryos as young as five days for cartilage and bone respectively (Bronner-Fraser, 2008). In preparation for staining, it was necessary to dehydrate the specimens. Immediately after harvest or culture, hindlimbs were gradually dehydrated in 25%, 50%, 75% and 95% ethanol for 10 minutes each. To visualise the cartilaginous skeletal rudiments each explant was then stained with 0.055% Alcian Blue (0.005% Alcian Blue 8GX (Sigma-Aldrich, UK), 95% Ethanol and 20% Acetic Acid) for 5 hours and cleared in 1% KOH for 2 hours at room temperature to remove any non-specific background staining. Once cleared, specimens were then fixed in 4% paraformaldehyde (PFA) made in 1x PBS for 2 hours at room temperature. Specimens were not stained for bone since the joint region had not yet mineralised due to the young age of the explants used. Once fixed, samples were stored in PBS at 4^{o}C. Due to cartilage's high water content, the process of dehydration is often thought to induce artefacts and deformations due to tissue shrinkage. To test this, a comparison of thigh and shank segment lengths before and after staining for each day was performed. Measured lengths were tested for normality using the Anderson-Darling test. The results revealed that measurements made after staining were not normally distributed, hence a Wilcoxon rank-sum test was performed to test if segments lengths were statistically significantly different before and after staining. No statistical differences existed before and after staining (p-value > 0.05) (Figure 3.3). All tests were performed using MATLAB (The MathWorks Inc., USA).

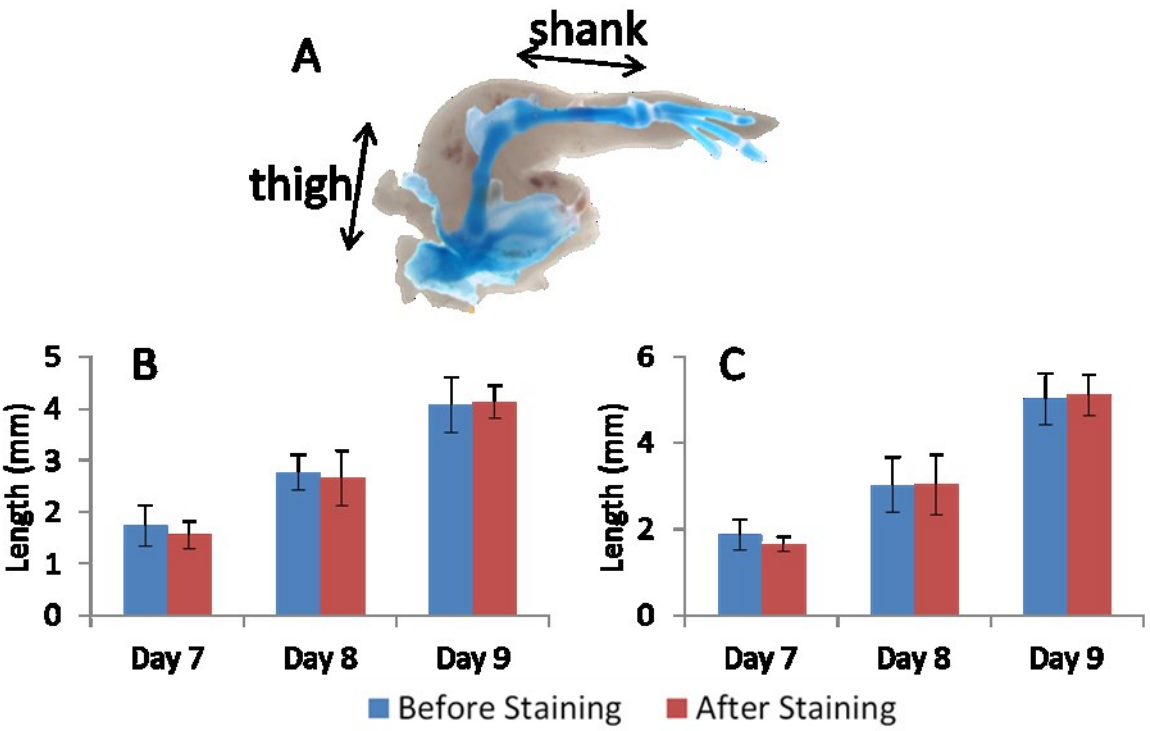


Figure 3.3: Tissue shrinkage was not significant following dehydration and staining of explants. A) overlays of unstained and stained explants before and after staining. No significant differences were found between the B) length of thigh and C) length of the shank in stained and unstained explants for 7 day (n = 12), 8 day (n = 20) and 9 day (n = 14) old embryos. Bars represent mean length. Error bars represent standard deviation.

3.2.2 Embedding Explants for Imaging

Samples were prepared for OPT imaging following protocols outlined in Quintana and Sharpe (2011). Each explant was embedded in low melting point agarose (LMPA). A 1% solution of LMPA was made using sterilised distilled water on a heated magnetic stirring plate at 100°C. The molten agarose was filtered through 0.4µm pore filter paper before use to remove any lumps and dirt from the mixture. The filtered agarose was poured into 6cm dishes and two hindlimbs washed in dH_2O were placed adjacent to each other and submerged into the agarose (Figure 3.4A). As the agarose cooled and solidified, the hindlimbs were suspended at a medium depth parallel to the top and bottom surface of the agarose (Figure 3.4B). Once solid, each dish was transferred to cold storage (4°C) for 2 hours. A scalpel blade was used to cut around each hindlimb to remove them

from the 6cm dishes. Blocks were transferred into 9cm dishes for trimming. Hindlimb explants were aligned so that the axis of rotation for imaging would run through the centre of the knee joint. The agarose blocks were then cut parallel either side of the axis (Figure 3.4C). The top and bottom of the agarose was squared off leaving a gap of at least 5mm below the specimen for mounting to the OPT. Once trimmed each specimen block was dehydrated in 100% methanol for 24 hours and cleared in benzyl alcohol and benzyl benzoate (BABB) solution for a further 24 hours.

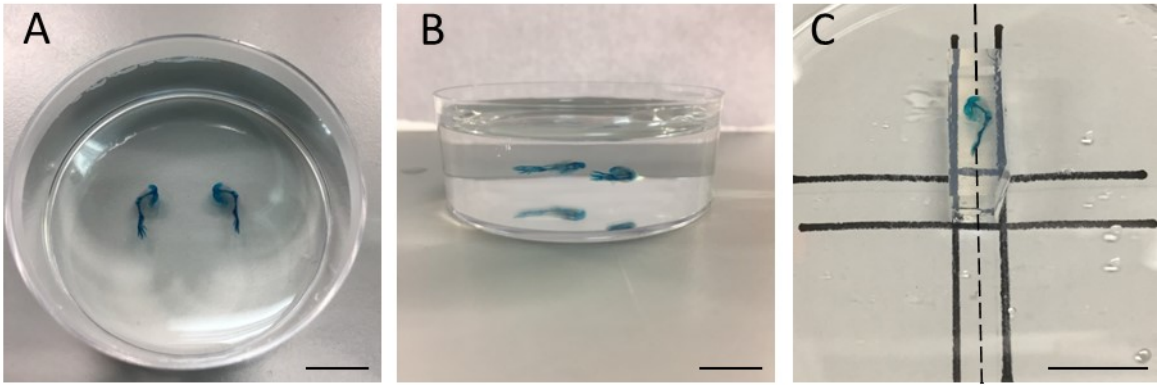


Figure 3.4: Explants were embedded in molten agarose for OPT scanning. A) hindlimbs were paired and placed adjacent to each other in 6cm dishes. B) hindlimbs were submerged and suspended at mid-depth parallel to the top and bottom surface of the agarose. C) the solid agarose was trimmed to center the knee joint onto the axis of rotation (dotted line) used during imaging. Scale bars = 1cm.

3.2.3 Optical Projection Tomography Scanning

Each specimen block was glued onto a steel chuck and mounted into the OPT scanner. The steel chuck was positioned onto a permanent magnet stuck to the electric motor. The lens was adjusted to bring the explants into focus and centred on the axis of rotation. Specimens were imaged in a cuvette of BABB solution 400 times at 9 degree increments during a 360 degree rotation (Figure 3.5). Imaging in BABB solution meant the agarose blocks became optically transparent improving the contrast and resolution of the stained rudiments.

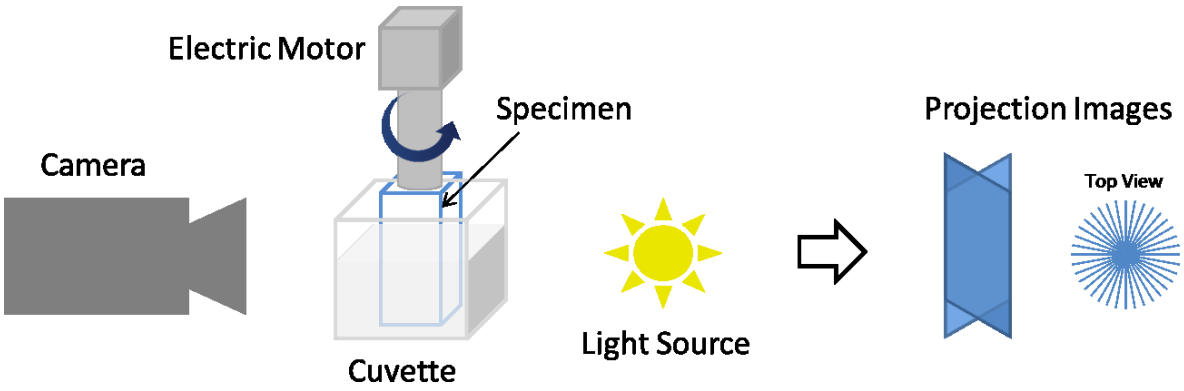


Figure 3.5: Illustration showing the concept of acquiring projections of the hindlimb explants. Explants embedded in agarose were mounted to the electric motor and rotated to capture 400 images at 9 degree increments.

3.3 3D Shape and Size Analysis

The 400 projections for each explant were reconstructed into a stack of 2D tomographic slices using a backscatter algorithm in a dedicated program called NRecon by SkyScan (Brucker microCT, 2011). Projection images had a resolution of 18µm/pix which was maintained during reconstruction. Tomographic reconstructions were imported into Mimics (Mimics, v17.0, Materialise NV, Belgium) and a mask was created to select the knee joint region. The mask was then rendered into a 3D object (.stl). The distal femur, proximal tibia and fibula were virtually segmented into separate 3D models and analysed independently. Once 3D models of the femur, tibia and fibula for each explant were created they were aligned into a neutral flexed position. The femur of each explant was orientated using the longitudinal axis and the axis of the lateral condyle as a reference. First the femur was independently rotated into the frontal view until the longitudinal axis was parallel with the y-axis (Figure 3.6A). In the lateral view, the femur was then rotated about the x-axis so that axis of the lateral condyle was also parallel with the y-axis (Figure 3.6B). The tibia and fibula were also aligned in the frontal view by aligning their longitudinal axes with the y-axis (Figure 3.6C) and then adjusted again in the lateral view so that the longitudinal axis was still aligned with the y-axis (Figure 3.6D). Orientated 3D models were then presented in

the frontal, lateral and medial views. To analyse and compare joint shapes, 2D joint shape profiles were traced of the frontal femur, medial and lateral condyle, medial tibia and lateral fibula (Figure 3.7).

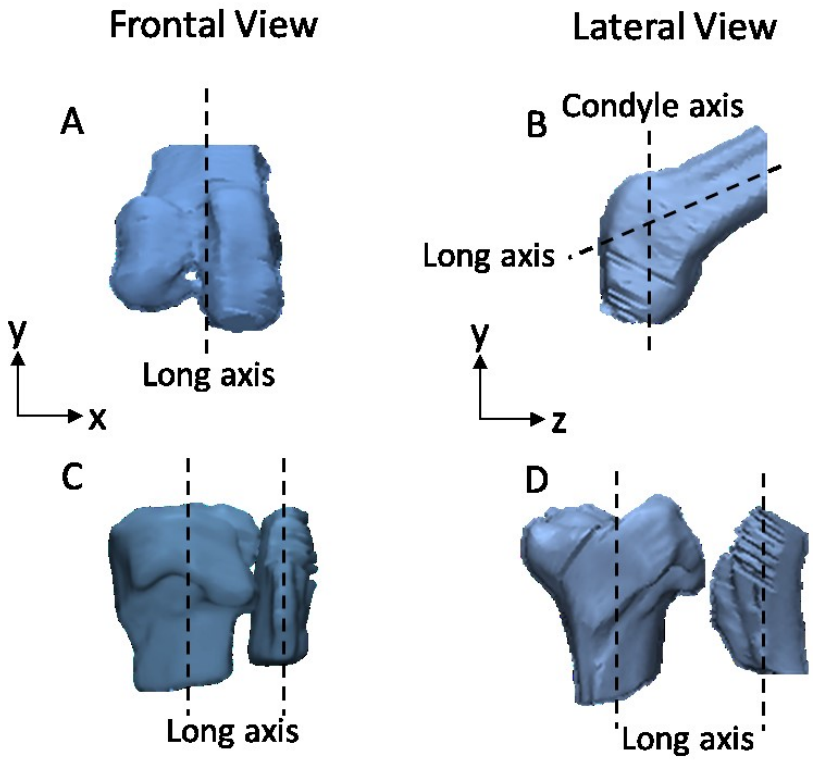
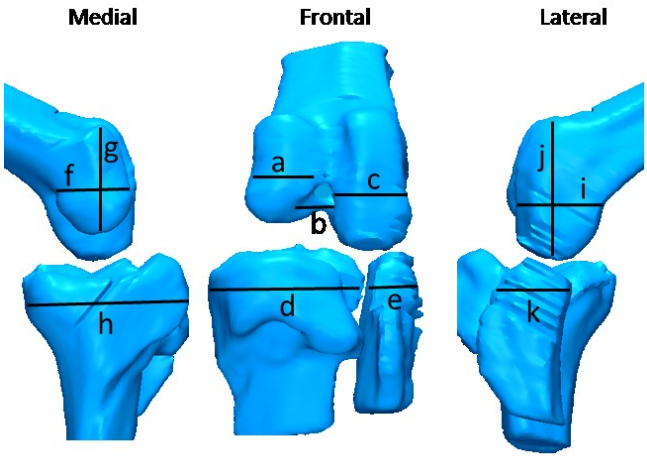


Figure 3.6: 3D models of the distal femur, proximal tibia and fibula were aligned following the same guidelines to ensure shape analysis was consistent. Rudiments were aligned in the frontal and lateral views using their longitudinal axis and axis of the lateral condyle for the distal femur. Joint were positioned into a neutral resting flexed position.

Joint shape profiles for each rudiment belonging to the same experimental group were pooled together and overlaid. Each joint region was analysed independently across groups. The size of the knee joint was analysed using the 3D models in ParaView (Ahrens et al., 2005). Eleven measurements were made of the distal femur, proximal tibia and fibula in the frontal, medial and lateral planes (Figure 3.7).



Measurement	Region
a	Medial Condyle Width
b	Intercondylar Fossa Width
c	Lateral Condyle Width
d	Tibia Width
e	Fibula Width
f	Medial Condyle Depth
g	Medial Condyle Height
h	Tibia Depth
i	Lateral Condyle Depth
j	Lateral Condyle Height
k	Fibula Depth

Figure 3.7: 3D rendered model of the chick knee joint in a neutral flexed position. Medial, frontal and lateral views of the joint were used to produce joint shape profiles and measure joint region sizes. Adapted and reproduced from Chandaria et al. (2016)

3.4 HISTOLOGY AND IMMUNOHISTOCHEMISTRY

Hindlimbs for 2D morphology and cellular activity analysis were fixed in 4% PFA immediately after culture for 2 hours at room temperature inside a fume cabinet. Explants were prepared for cryopreservation by incubating in 15% sucrose in PBS overnight at 4°C followed by 30% sucrose in PBS overnight at 4°C again. A final incubation at room temperature in an OCT-30% sucrose (50:50) medium for 2 hours was performed before embedding the explants into OCT-30% sucrose blocks. The hindlimbs were submerged into the embedding medium with the knee joint facing upwards (Figure 3.7) so frontal section could be cut during cryosectioning. The blocks were then flash frozen in dry ice and kept at 20°C for storage. Embedded explants were sectioned using a cryostat at -18°C in the frontal plane. Cut sections were serially mounted to Superfrost™ Plus slides (ThermoFisher Scientific, UK) for each specimen.

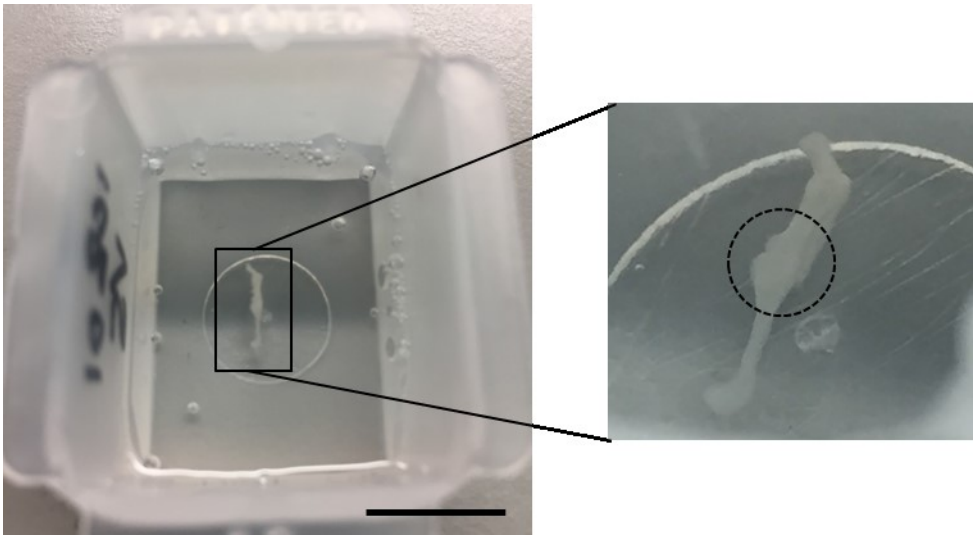


Figure 3.8: Cultured explants were embedded in a medium of OCT and 30% sucrose and frozen over dry ice. Explants were orientated to face upwards with the knee joint (circled) just below the surface of medium ready for cryosectioning. Scale bar = 1cm.

3.4.1 Histology Staining

Histology staining was performed using Alcian Blue (Alcian Blue 8GX, Sigma-Aldrich, UK) and Picro Sirius Red (Direct Red 80, Sigma-Aldrich, UK) to visualise the cartilaginous rudiments and surrounding tissues respectively. Slides for histology were washed in PBS for 5 minutes twice before being stained with Alcian Blue (0.025% Alcian Blue, 3% acetic acid in dH_2O) for 30 minutes at room temperature. Slides were then washed in tap water for 10 minutes before being counterstained with Picro Sirius Red (1% Direct Red in picric acid) for 10 minutes. Finally, slides were washed in 0.5% acidified water for 10 minutes followed by PBS for 5 minutes before being mounted using DPX mounting media (Sigma-Aldrich, UK). The cartilaginous rudiments were stained blue and muscle fibres and connective tissues were stained pink.

3.4.2 Proliferation Assay

Proliferating cells were identified using the mitosis marker phospho-Histone H3 (pHH3), as used by Roddy et al. (2011a). Slides were washed in PBTD (PBS, 1% Tween (Sigma-Aldrich, UK), 1% DMSO (Sigma-Aldrich, UK)) for 5 minutes at room temperature. Sections were then blocked (5%

normal goat serum, 1% DMSO in PBS) for 2 hours at room temperature before being incubated with anti-phospho-Histone H3 from rabbit ser10 (Merck Millipore, Germany) diluted 1:50 in blocking solution overnight at 4°C. During incubation slides were kept in a humidified chamber. Sections were then washed in PBTD for 30 minutes before a second incubation with goat anti-rabbit secondary antibody, Cy3 conjugate (Invitrogen, USA) diluted 1:200 in blocking solution at room temperature for 1 hour. A final wash in PBTD for 25 minutes was performed before mounting slides using a DAPI fluoroshield medium (Sigma-Aldrich, UK). Under ultraviolet excitation (~365nm) the DAPI mounting medium shows all cells in blue (~450nm), whilst under green excitation (~560nm) the proliferating cells show up in red (~645nm).

3.4.3 LIVE DEAD ASSAY

Cell viability was assessed to identify cells undergoing apoptosis or necrosis. A terminal deoxynucleotidyl transferase (TdT) dUTP nick-end labelling (TUNEL) detection kit for cryosections (APO-BRDU-IHC, Bio-Rad Laboratories, USA) was used following the recommended protocols (AbD Serotec, 2016). Slides were first washed in PBS for 15 minutes, and then incubated with proteinase K for 10 minutes to permeabilise cellular membranes for antibody binding. To reduce non-specific background staining, slides were incubated with a hydrogen peroxide solution (30% H_2O_2 diluted 1:10 in methanol) for 5 minutes. Slides were then incubated with reaction buffer for 30 minutes at room temperature. A labelling solution was then applied to each slide for 1.5 hours at 37°C. Slides were then rinsed in PBS and covered in blocking buffer for 10 minutes after which they were incubated with antibody solution (Biotin anti BrdU) for 1.5 hours at room temperature. Slides were rinsed in PBS and covered in blocking buffer and conjugate for 30 minutes. Dead cells were then stained using a mix of DAB (3,3′-Diaminobenzidine) and urea for 15 minutes at room temperature. This coloured dead cells brown. Methyl Green was used to counterstain viable cells green for 3 minutes.

CHAPTER 4

4. PHYSIOLOGICAL CHICK KNEE JOINT DEVELOPMENT

Parts of this chapter have been published in the Journal of Biomechanics (Appendix III) (Chandaria et al., 2016).

4.1 INTRODUCTION

In order to evaluate the progression of joint morphogenesis in joint explants cultivated *in vitro*, it was important to first understand the physiological sequence of morphological events that occur in the embryonic chick knee joint. The emergence of anatomical structures, such as femoral condyles and soft tissue attachment points, has previously been reported for the chick knee joint during development (O'Rahilly and Gardner, 1956, Roddy et al., 2009) along with the shape and structure of the adult chick knee joint (Haines, 1942). However, the incremental shape changes involved in the creation of these joint features were yet to be documented.

It has already been reported that the location of the chick knee joint and formation of the interzone is evident by day 5.5 (HH28) as shown by a decrease in Alcian Blue staining between the femur, tibia and fibula (Roddy et al., 2009). Individual movements of the hindlimbs start to occur on day 6 (HH29) (Hamburger and Hamilton, 1951) when the first indication of a femoral condyle emerges on the lateral side of the joint above the fibula (Roddy et al., 2009). This is followed by the clear visualisation of the three segments of the hindlimb: the thigh, shank and

foot. At 6.5 days (HH30) the knee joint becomes flexed giving external identification of the location of the knee joint with a bend between the thigh and the shank segments (Hamburger and Hamilton, 1951). On day 7 (HH31), the medial condyle emerges alongside the developing lateral condyle on the distal femur above the tibia (Roddy et al., 2009). Cavitation of the knee joint occurs on day 8 (HH34) (Roddy et al., 2009).

Further detailed analysis of physiological knee joint morphogenesis was essential to evaluate the finer differences in joint shapes of *in vitro* cultured explants and assess the progression of development and comment on their normality. This chapter took a deeper look at shape development of the distal femur and proximal tibia and fibula elements of the chick knee joint.

4.2 METHODS

Since the major morphology of the chick knee joint is created between day 7 and day 9 of incubation, this was the period of development of interest for this chapter. Six embryos were harvested after 7, 8 and 9 days of incubation under humidified conditions at 37^{o}C following the methodology described in Chapter 3.1. The hindlimbs were dissected from each embryo and dehydrated serially in ethanol, stained for cartilage and prepared for 3D imaging following protocols described in Chapter 3.2. A single hindlimb was chosen from each embryo to give a total of six specimens for each age group. The chosen hindlimbs were reconstructed and analysed for joint shape and size as described in Chapter 3.3. Joint region measurements were tested for normality using the Anderson-Darling test. For joint region measurements that followed a normal distribution, 1-way ANOVA was used to test for significant differences between each day. Where significant differences existed, the Tukey-Kramer pairwise comparison was made to identify which groups were significantly different from each other.For joint region measurements that were deemed to not follow a normal distribution, the non-parametric Kruskal Wallis ANOVA was used to test for significant differences between each day and a pairwise rank-sum post hoc test was performed to identify which groups were significantly different. p-values less than 0.05 were

considered significantly different. Statistical tests were performed in MATLAB (The MathWorks Inc., USA).

4.3 RESULTS

All three skeletal rudiments were clearly identifiable in all samples as illustrated in Figure 4.1. Morphological changes were observed from the 3D reconstructions over the three days of interest and presented below for each rudiment.

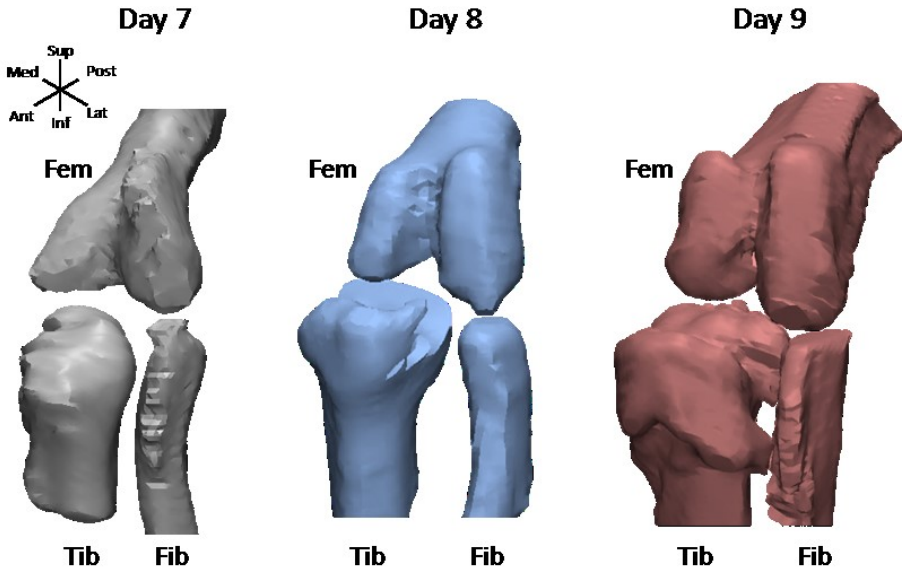


Figure 4.1: 3D models of the embryonic chick knee joint at 7, 8 and 9 days.

4.3.1 THE DISTAL FEMUR

At 7 days, both femoral condyles can be identified as simple outgrowths from the distal femur giving it a forked appearance in the frontal view (Figure 4.2A). The lateral condyle is the dominant feature exceeding the size of the medial condyle by 38%, 45% and 39% on average in width, height and depth respectively (Figure 4.3A & B). At 7 days, both condyles have a simple rounded shape as shown by the shape profiles in the medial and lateral views (Figure 4.2B & D). At 8 days, the lateral condyle still holds a slight dominance over the medial condyle (Figure 4.2F). The width, height and depth of each femoral condyle remain similar to those measured at 7 days (Figure 4.3A

& B). At 8 days, the shapes of the condyles have developed to create a slight posterior curl which can be seen in the sagittal plane (Figure 4.2G & I). This curl of the condyle is more defined in the lateral condyle than the medial condyle. The curling of the condyles leads to the creation of an intercondylar fossa between the two protruding ends of each femoral condyle on the posterior side of the joint (Figure 4.2F). At 9 days, the medial condyle has considerably enlarged and appears similar to the lateral condyle giving the frontal femur a nearly symmetric appearance. The difference in lateral to medial condyle size is now reduced to 20%, 20% and 12% in width, height and depth respectively (Figure 4.3A & B). At 9 days, the posterior curls of the femoral condyles are now more apparent and have increased the width of the intercondylar fossa (Figure 4.2L & N). The femoral condyles were significantly larger in all measurements at 9 days compared to day 7 and 8 joints except for medical condyle width. (Figure 4.3A & B). The increase in size of each femoral condyle leaves behind a channel like groove on the superior surface of the distal femur between the two condyles to give the femur its recognisable condylar shape (Figure 4.2K).

4.3.2 The Proximal Tibia

At 7 days, the shape of the tibia does not resemble anatomical images of a mature tibia. The proximal end of the tibia appears to protrude posteriorly from the main shaft of the tibia giving it a sloped articular surface (Figure 4.2C). At 8 days, the shape of the tibia has completely changed with a rapid outgrowth on the anterior side of the rudiment (Figure 4.2H). It was assumed this emergence forms the anterior tibial crest. At 9 days, the anterior tibial crest has further protruded and lengthened the anterior-posterior depth by 20% and 55% compared to at 8 days and 7 days respectively. The width and depth of the proximal tibial are significantly larger at 9 days compared to 7 days (Figure 4.3C). The extension of the anterior tibial crest is accompanied by the formation of a concave tibial plateau which can be made out in the medial shape profile of the rudiment (Figure 4.2M).

4.3.3 The Proximal Fibula

The shape of the fibula is very simple and does not dramatically change throughout the three days studied. At 7 days, the fibula appears rod-like with the proximal end rounded off in a convex dome shape (Figure 4.2E). At 8 days, the top surface of the fibula appears to have flattened compared to the previous day which can be noticed in the lateral view (Figure 4.2J). The anterior-posterior depth of the epiphysis is significantly larger at 8 days compared to 7 days. The average depth measures 22% larger at 8 days compared to the previous day (Figure 4.3D). This expansion of the proximal end is even more pronounced at 9 days measuring on average 14% deeper than at 8 days. The average width and depth of the fibula become significantly larger at 9 days compared to at 7 days (Figure 4.3D). At 9 days the shape of the proximal end of the fibula is similar to that of day 8 resembling a flattening rod. It was also noticed the proximal end becomes slightly curled in the posterior direction (Figure 4.2O).

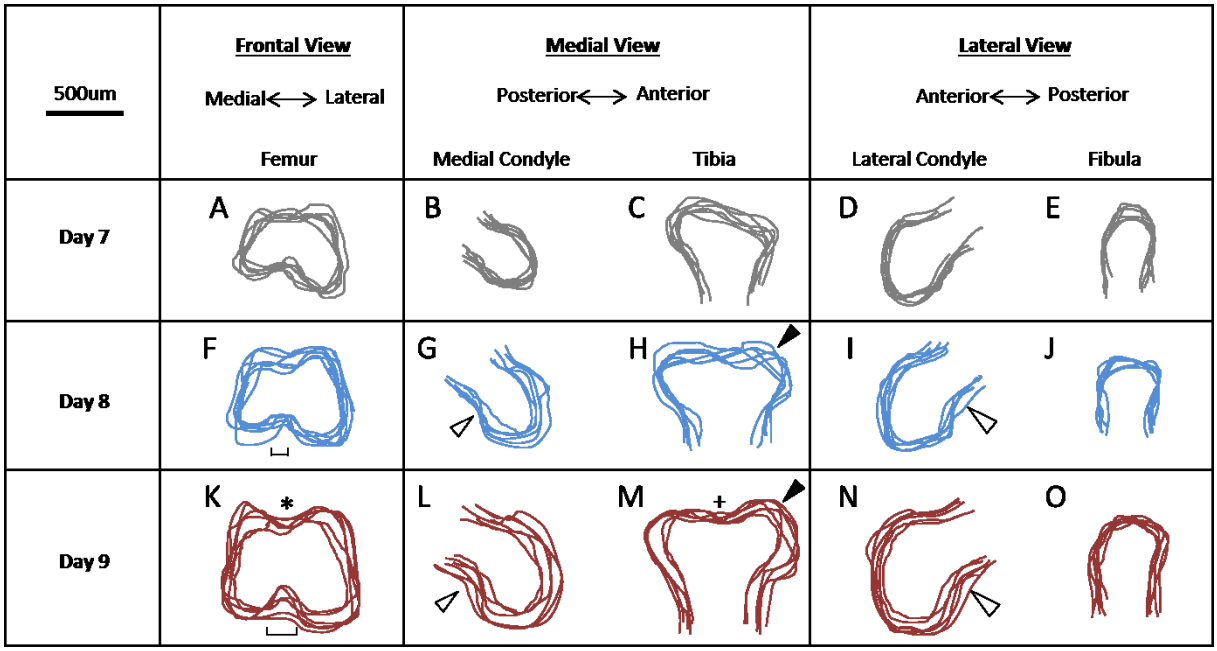


Figure 4.2: Normal shape changes occurring in the chick knee joint during development. Shape profiles of 7, 8 and 9 day old chick embryo knee joints were outlined and overlaid (n=6). Hollow arrows: posterior curl of condyles; * dorsal groove between the two femoral condyles; single edged bars: intercondylar fossa; + concave curve of the tibial plateau; filled arrows: anterior tibial crest. Adapted and reproduced from Chandaria et al. (2016).

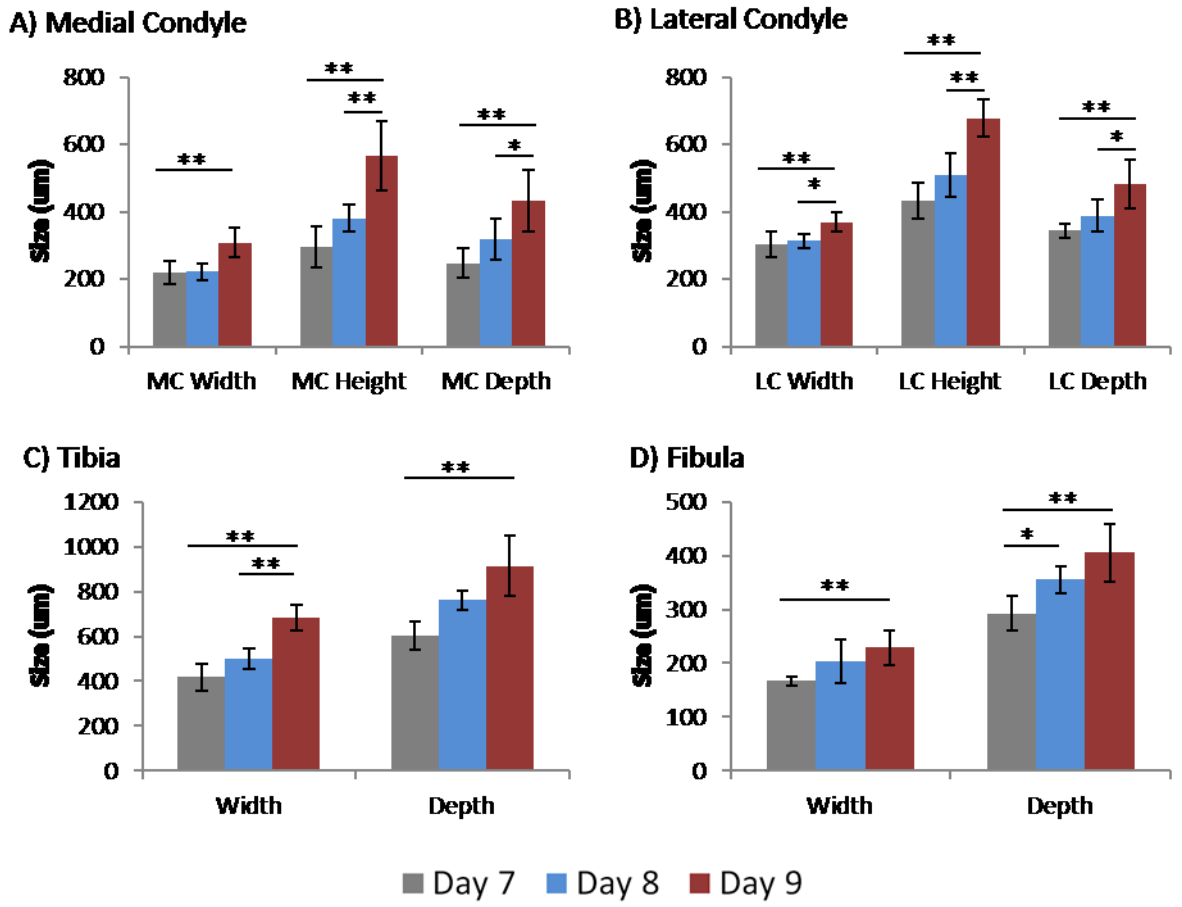


Figure 4.3: The increase in joint region size is most dramatic between days 8 and 9. Columns represent mean size of joint regions (n=6). Error bars represent standard deviation. *p-values < 0.05; **p-values < 0.01.

4.4 Discussion

Shape development of the chick knee joint can be divided into several morphological events which occur between day 7 and day 9 of incubation. The distal femur forks to create a lateral protrusion followed by a medial protrusion, which eventually form the femoral condyles. Individual enlargement of the condyles and posterior curl separates the two condyles on the dorsal and ventral sides leading to the maturation of the femoral shape. The proximal tibia undergoes a considerable shape change during the three days. Growth of the anterior tibial crest, anterior-posterior elongation of the superior surface and creating of the tibial plateau are

characteristics of tibial shape development. The fibula undergoes the least amount of shape change. The dome shape of the proximal fibula becomes flatter as it matures and curls slightly in the posterior direction.

The developing morphology of the chick knee joint has previously been described by Roddy et al. (2009) for the cartilaginous rudiments and the soft connective tissues. While this gave an insight into some of the morphological events included in knee joint morphogenesis, the description of shape changes for the skeletal elements was not as detailed as this study. Their results showed that morphogenesis proceeded with the appearance of rounded prominences of the articulating surfaces on the distal femur (condyles) at day 6 and day 7 and the protrusion of the future cnemial crest on the anterior surface of the tibia visible at 8 days (Roddy et al., 2009). In this chapter, a closer investigation was applied to the shape of all three rudiments between day 7 and day 9 of incubation and revealed finer shape changes not previously reported, such as the posterior curling of the femoral condyles, the appearance of the intercondylar fossa and dorsal groove, the emergence of the anterior tibial crest and the flattening of the fibula. From the data collected in this study, the cnemial crest described by Roddy et al. (2009) was considered to actually be part of the newly formed anterior tibial crest. The cnemial crest is a feature that exists in some avian and reptile species and can be related to the tibial tuberosity in mammals (Hall, 2008, Shojaei et al., 2015). This structure protrudes from the anterior tibial surface in the anterior-superior direction and is considered as a separate structure that fuses to the tibia (Hall, 2008) for the patella tendon to attach.

This chapter extended the current understanding of knee joint morphogenesis for chick embryo over its developmental period. The sequence of morphological events for the distal femur and proximal tibia and fibula was used as a reference to stage the progression of joint shape development for explants cultured *in vitro* in further chapters of this thesis.

CHAPTER 5

5 EXPLANT CULTURE METHODOLOGY

The method of soft tissue removal was performed following help and advice from Dr. James Henstock.

5.1 INTRODUCTION

Fragments of embryonic skeletal tissues were first cultivated in the 1920's when it was shown that some of the biological processes, such as differentiation and cell division, operating *in vivo* also operated *in vitro* (Strangeways and Fell, 1926). This ultimately led to the pioneering 'watch-glass' technique of culturing whole embryonic chick limb buds in the concave surface of a glass watch face (Fell and Robison, 1929). Limb bud explants from four day old embryos were maintained in culture for up to six days (Fell and Canti, 1934). Explant cultures allow for the preservation of natural tissue patterning and cell to matrix interactions which can be more informative than traditional cell culture methods, which provide little information about the morphological development of complete tissue structures (Zaman et al., 1992, Henstock et al., 2013). Since these pioneering explant culture methods were published, *in vitro* culture techniques have improved dramatically. Modern bioreactors enable repeatable cultivation of skeletal tissue and application of controlled mechanical stimulation in ways that are not possible *in vivo* (Cohen et al., 2005, Pörtner et al., 2005). *In vitro* culture of embryonic chick hindlimb elements has been shown to be a versatile model for studying skeletal development (Smith et al.,

2013), including the study of growth and resorption of cartilage and bone tissue, mineralisation and the effects of chondrogenic and osteogenic media components (Roach, 1990, Kanczler et al., 2012, Henstock et al., 2013).

This chapter details the design and optimisation of the culture system used to study embryonic joint morphogenesis. A specialised culture setup was needed to apply mechanical stimulation to the embryonic chick knee joint. This included the design of a support system that would hold the hindlimb during culture and throughout stimulation regimes. The support system was designed to work with a uniaxial compression bioreactor that would stimulate the knee joint in a physiological manor. Calibration of the culture system under increasing compressive displacement was also performed. Along with designing a support system, the culture conditions needed to be considered and tested for optimal joint development *in vitro*. These included the method of nutrient delivery, the effect of soft tissue presence and culture duration.

5.2 Design of Culture System

5.2.1 The Bioreactor

Bioreactors allow explant cultures to be contained within controlled environments with the optional application of quantified mechanical stimuli. The Ebers TC-3 bioreactor (Don Whitley Scientific, UK) was used throughout this doctorate. The TC-3 bioreactor could apply a uniaxial compressive regime into three individual chambers simultaneously through a single driving piston which attaches to each culture chamber (Figure 5.1). A total of three culture chambers could be mounted to the bioreactor at any one time. The bioreactor could be operated in the vertical or horizontal position. Custom compressive grips which span across the culture chamber were included to distribute the compressive loads across the whole width of the chamber (Figure 5.1). The bioreactor ran in displacement control and could be programmed to run under cyclic loading profiles.

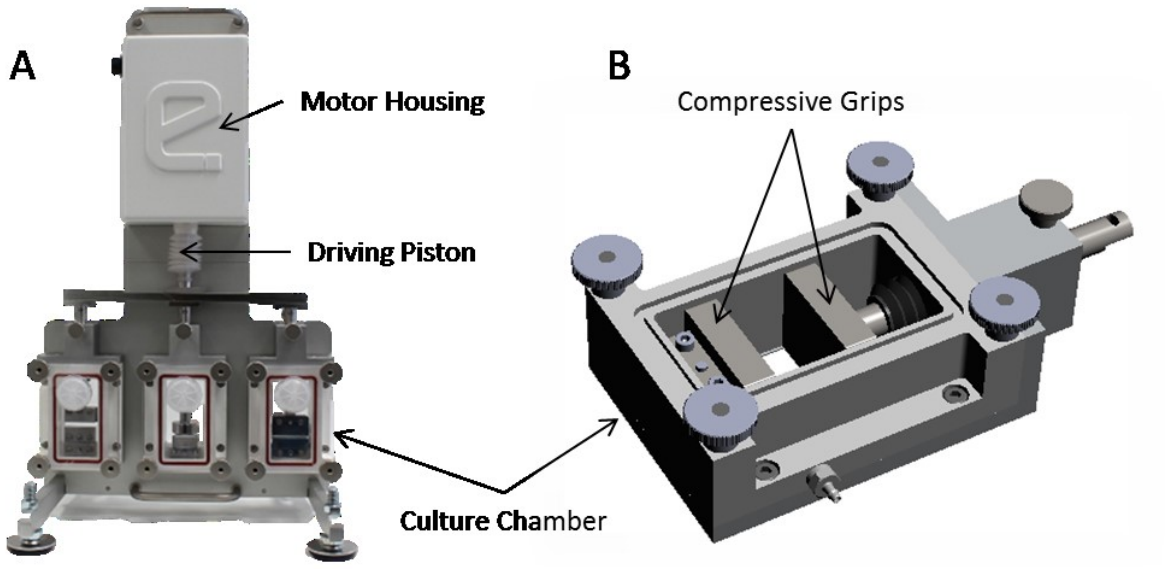


Figure 5.1: (A) Ebers TC-3 Bioreactor System. (B) Compression Culture Chambers. (Ebers Med Tech SL, 2016)

5.2.2 Foam Support System

The process of creating a culture system that could apply mechanical stimulation to the embryonic chick hindlimb was initiated during a Master of Research (MRes) program at Imperial College London (Chandaria, 2013). This included the design of a support system to hold the explants during culture and control the transfer of compressive displacements applied by the bioreactor to the developing joint region. This work was carried out for intended use with a magneto-mechano bioreactor initially, and then adapted during this doctorate for the new TC-3 bioreactor.

The support system needed to be designed to fit within the bioreactor's culture chambers and allow for the perfusion of culture media and its nutrients to the hindlimb explants. Polyurethane foam scaffolds are widely used in tissue engineering and were chosen as the support material. It can easily be sterilised using high temperature autoclaving and made to a variety of shapes. Mechanical testing of various open celled polyurethane foams was conducted to establish the

mechanical behaviour of the foam under compressive loading. Following the selection of foam material, various options were designed for the arrangement of the hindlimb explants and foam supports with an aim to induce physiological movements to the developing knee joint.

5.2.2.1 Mechanical Properties of Foam Supports

Foam supports of varying pore density were tested following guidelines from the American Society for Testing and Materials (ASTM) for flexible cellular materials including urethane foams (ASTM D3574-11, 2011). Each material was tested for "indentation force deflection (IFD)" and "dynamic fatigue by constant deflection pounding". IFD testing consists of measuring "*the force necessary to produce a designated indentation in the foam product"* resulting in IFD values for a specified strain, which are used as a measure of load bearing capacity. The ratio of IFD at 65%:25% strain is defined as the foam's "*support factor*" which determines its cushioning quality. A higher value suggests a better resistance to *"bottoming out" (compression to a point where the foam can no longer hold the load).* Dynamic fatigue was calculated as the percentage change in IFD at 25% strain before and after cyclic loading to 30% compressive strain, evaluating the material's durability by repeatedly being loaded under compression. A decrease in IFD after cyclic loading is used as a measure of how much the material has fatigued.

It was expected that an increase in pore density would increase the stiffness of the foam, increasing its resistance to deformation. Five types of foam were tested with various pore densities of 12, 20, 30, 45 and 60 pores per inch (ppi). Three specimens were tested for each foam density and the results averaged between them. Cylindrical samples (35mm dia. x 20mm) were saturated in water and tested under confined compression conditions to mimic the environment of the bioreactor chamber. Mechanical tests were performed using an Instron 5866 equipped with a 50N load cell. Strain rates were matched to those specified in ASTM D3574-11 (2011).

To measure the 25% and 65% IFD each specimen was pre-flexed to 75% compressive strain twice at 50mm/min and allowed to recover for 5 minutes. Specimens were then compressed to 25% and 65% compressive strain sequentially at 10mm/min and held for 60 seconds to stabilise the

load cell. Following the initial IFD tests, each specimen was cyclically loaded to 30% compressive strain at 250mm/min under a triangular displacement profile. After 625 cycles, the 25% and 65% IFD tests were repeated.

The support factor was calculated before and after fatigue cycling and revealed that repeatedly loading the foam increased its stiffness for all specimens. As expected, the mean support factors for the 5 samples generally increased with pore density. A pore density of 45ppi had the highest consistent support factor and showed the least amount of fatigue (Figure 5.2 & 5.3). Therefore, 45ppi foam was decided to be the optimal choice for the foam support system.

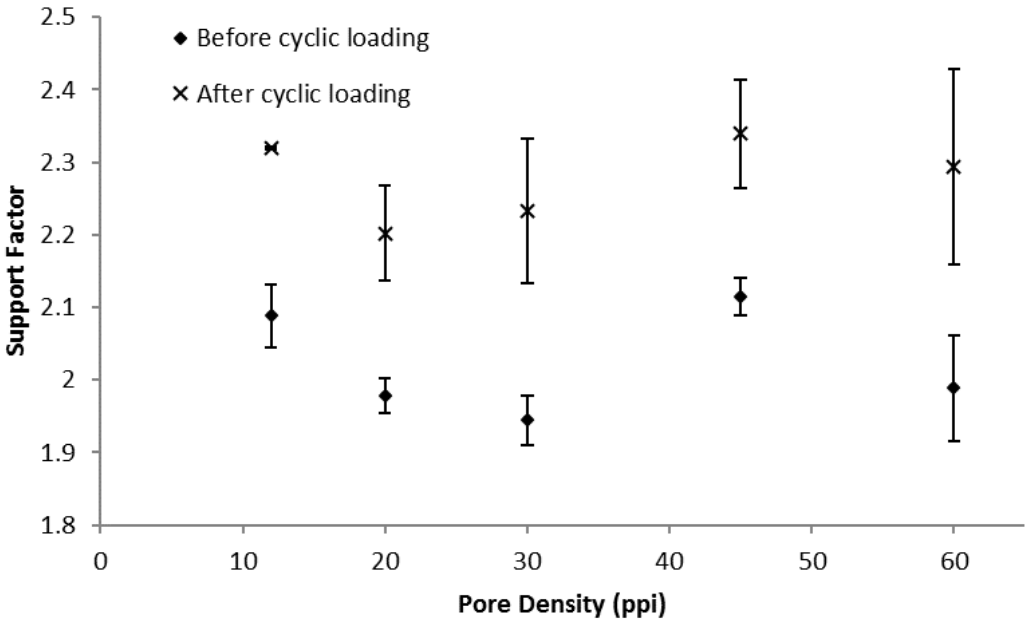


Figure 5.2: Cyclic loading improved the support factor for all foam types. 10ppi and 45ppi had the highest support factors before and after loading. Support factors were calculated as the ratio of 65% IFD/25% IFD before and after 30mins of cyclic loading to 30% compression. Error bars represent the standard deviation.

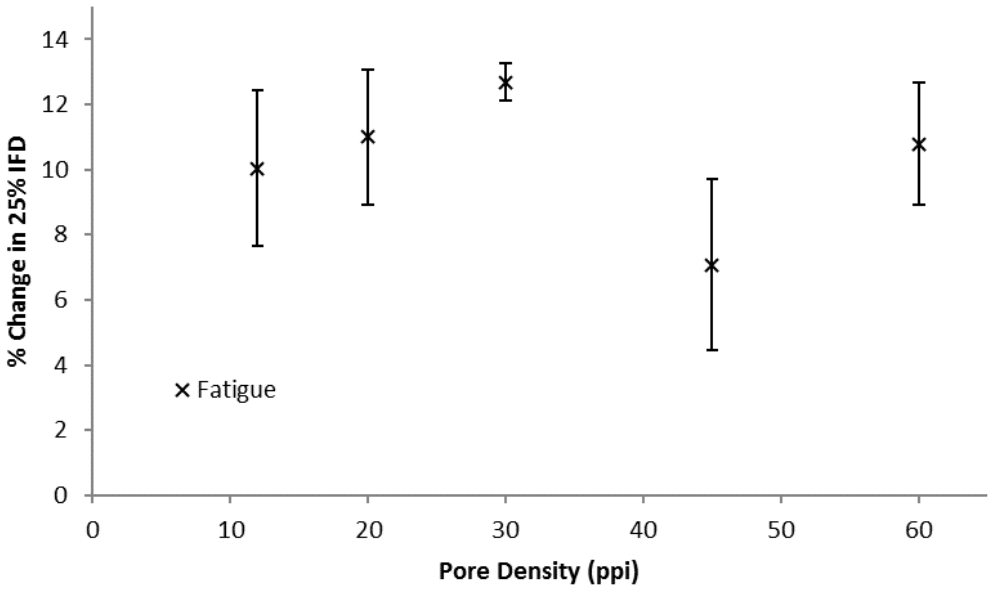


Figure 5.3: After 30mins of cyclic loading 45ppi foam showed the least amount of dynamic fatigue. Fatigue was calculated as the percentage change in 25% IFD before and after 30mins of cyclic loading to 30% compression. Error bars represent the standard deviation.

5.2.2.2 Foam and Explant Arrangement

An arrangement of the polyurethane foam and hindlimb explants was designed to hold explants in place and transfer the compressive displacements from the bioreactor. It was noticed that freshly harvested explants naturally adhered to the pore structure of the polyurethane foam pieces. Over-manipulation or excess handling of the explants led to tissue damage which meant trying to slide the hindlimbs into pre-cut holes or suspend them between pieces of foam was impractical. The simplest way, which involved the least disturbance to the hindlimb, was to rest the explant on the surface of the porous polyurethane foam. It was found that placing the hindlimb on a piece of rectangular foam with its superior-inferior axis perpendicular to the top and bottom horizontal edges of the foam would lead to the top and bottom of the hindlimb moving closer together when compression is applied vertically. Releasing the foam would then return the hindlimb to its natural resting position causing a flexion movement to occur at the knee joint. Trials of this arrangement found that after multiple movements, the hindlimbs could move or

slide along the foam surface. Therefore, to counter this, a step was cut into the foam support beneath the explant (Figure 5.4A). To stop the top of the explant sliding down towards the step, a 27G needle was pinned through the pelvis into the foam support (Figure 5.4B). Cutting rectangular pieces (35x20x15mm) of polyurethane foam (Sydney Heath & Son, UK) to the width of culture chamber meant multiple explants could be loaded in a line horizontally. For consistency, each hindlimb was positioned medial side down onto the lower level and oriented with the distal end nearest the step (Figure 5.4B). This arrangement meant explants could be loaded in vertical or horizontal orientations (Figure 5.4C).

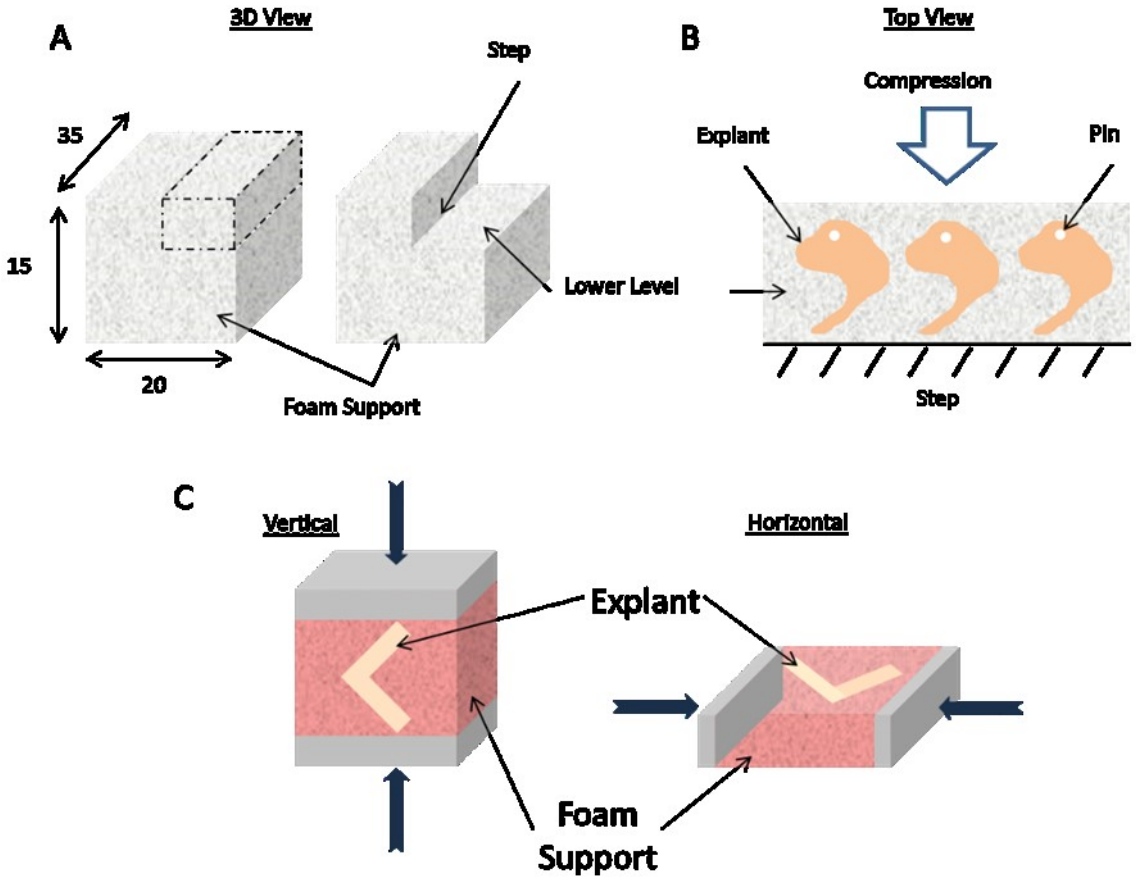


Figure 5.4: Schematic of the explant culture setup. A) Rectangular polyurethane foam supports were cut to create a step along the horizontal axis. Measurements are in mm. B) Explants were positioned onto the lower level of the foam and pinned into place. Explants were orientated medial side down with the hip joint furthest away from the step. C) The culture setup could be compressed in both the vertical or horizontal orientations. Adapted from Chandaria et al. (2016).

5.3 Validation and Calibration of Mechanical Stimulation

Movement of the explants during compression was validated and calibrated using a high-resolution camera (HV-5080, HAVIT, China). A range of displacements were applied by the bioreactor during calibration to quantify the magnitude of induced flexion movements experienced by the knee joint. Freshly harvested 7 day old chick hindlimb explants were positioned onto foam supports and loaded into a bioreactor chamber as described in the previous section. Basal culture media was added to saturate the porous foam during loading. A total of six explants were subjected to 1, 2, 3 and 4mm of cyclic compression for five minutes. A rest period of five minutes was included between each magnitude of compression to allow the foam support and hindlimbs explants to fully recover for the next test. A constant loading rate of 4mm/s was maintained for all tests to remove any effect of strain rate on the mechanical behaviour of the foam support. This was the maximum speed the bioreactor could travel at for the selected magnitudes. The internal joint angle, between the long axis of the thigh and shank, was measured using the angle tool in ImageJ (Schneider et al., 2012). Angles were measured for all six explants from a single frame of minimum and maximum compression to give the internal knee angle before and after compression respectively. Frames were randomly selected between four and five minutes of stimulation. The change in flexion was then calculated as the difference before and after compression and averaged for all explants. Analysis of the footage validated the flexion movement about the knee joint and proved this to be a simple and repeatable method to hold the limbs in the correct orientation without causing damage to the fragile tissues (Figure 5.5).

The bioreactor could induce 4±1.8 degrees (mean±SD) of flexion at 1mm of compression up to a maximum of 22±5 degrees (mean±SD) of flexion using 4mm of compression to the developing knee joint. Amongst the six explants, a range of flexion angles were measured showing some variation in response to the applied compression as shown by the standard deviation in Figure 5.6. This was thought to be due to a combination of variation during the placement of hindlimbs onto the foam and the natural variance in hindlimb size. The results show the change in knee

flexion was linearly proportional to the magnitude of compression applied by the bioreactor (Figure 5.6). Regression analysis of the raw data found a strong linear relationship between the two variables ($R^2 = 0.79$).

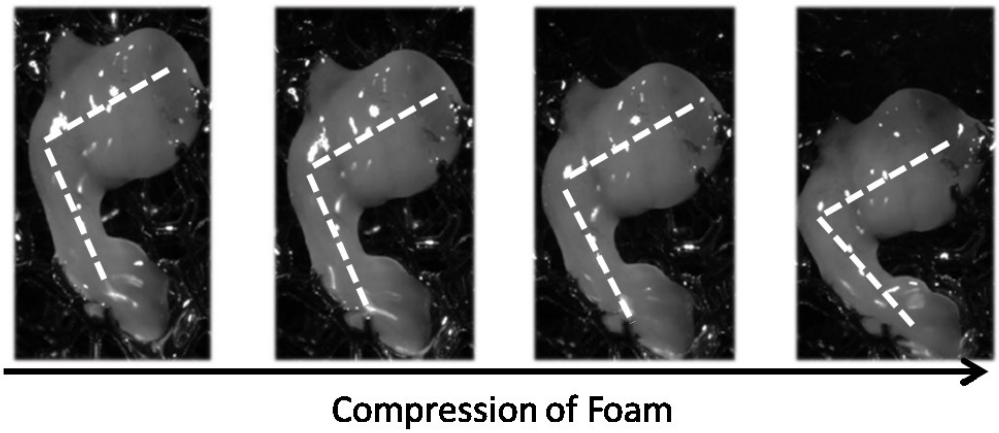


Figure 5.5: Increasing compression of the foam support resulted in a bending motion at the knee joint as indicated by the decrease in internal knee flexion angle.

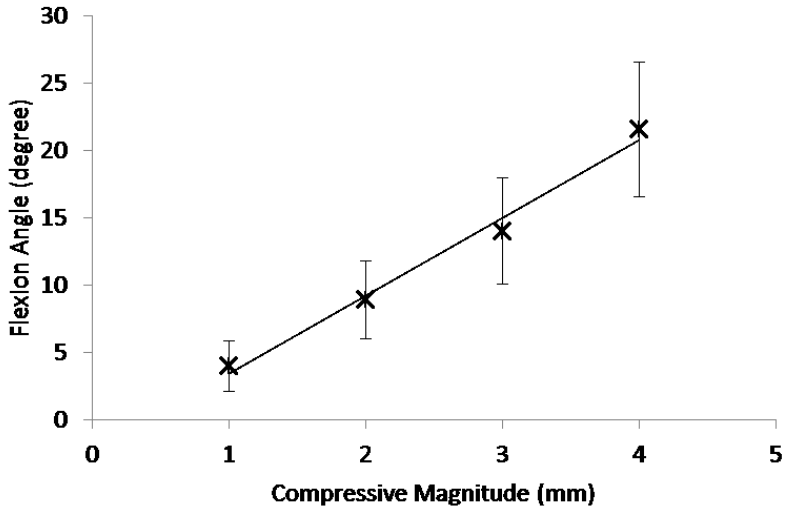


Figure 5.6: Flexion angle increased linearly (trend line) with compressive magnitude. Flexion angles of developing knee joints in explants experiencing 1 – 4mm of uniaxial compression. Error bars represent standard deviation.

5.4 Optimisation of Explant Culture

Initial cultures showed that hindlimbs explants could be cultured for up to three days when attached to the foam supports and completely submerged in basal culture media as shown by complete Alcian Blue staining of the rudiments after culture (Figure 5.9). After three days the hindlimbs explants were seen to deteriorate and fragment in culture showing signs of tissue integrity loss and reduced Alcian Blue staining (Figure 5.9). Previously, Lelkes (1958) had shown that the chick knee joint could be cultured for up to six days when excised from the hindlimb and stripped of surrounding tissues before culture. It was therefore decided to test the culture conditions used to improve future experiments. Three conditions were tested during optimisation which included the method of nutrient delivery, effect of soft tissue presence and culture duration. These conditions were tested in four individual experiments to find the optimal culture conditions to promote normal joint development *in vitro* as much as possible.

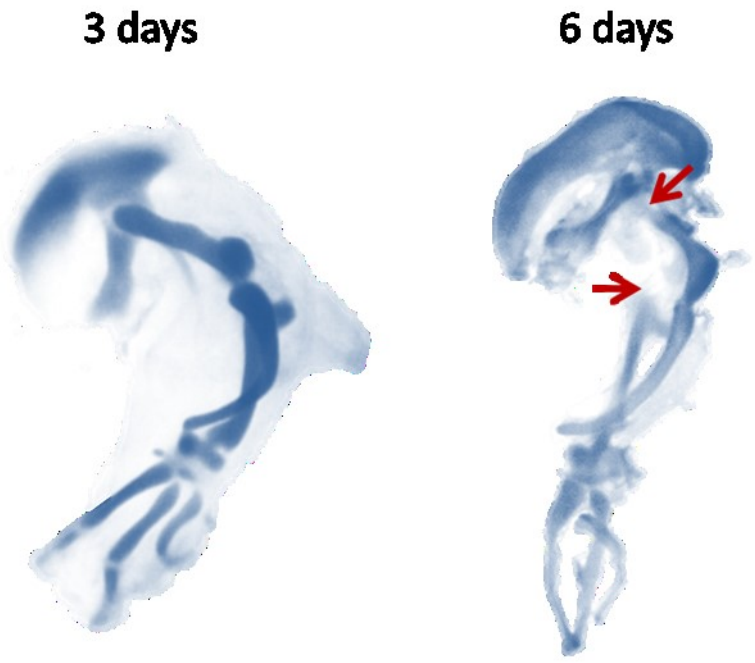


Figure 5.7: Explants would start to deteriorate after 3 days of culture under submerged conditions during initial experiments. Arrows indicate areas of reduced Alcian Blue staining of the femur and proximal tibia. Images not to scale.

All optimisation cultures were conducted under static conditions to remove any variation that may be introduced by mechanical stimulation. For all cultures the preparation of explants for culture was as described in Chapter 3.1. Embryos were harvested after seven days of incubation. After dissection, hindlimbs from each embryo were immediately incubated in 1.5ml of culture medium and kept at 37°C. Hindlimbs explants were mounted on rectangular pieces of polyurethane foam as described previously (Chapter 5.2.2.2) and cultured in well plates rather than the bioreactor since no stimulation was needed. Explants were cultured in basal media consisting of alpha-minimum essential medium (αMEM) GlutaMAX (Gibco, UK) supplemented with 1% pen/strep (Sigma-Aldrich, UK) and 100mM ascorbic acid (Sigma-Aldrich, UK) in a 5% CO_2 humidified environment. Basal media was replenished every 24 hours. Cultured explants were processed and analysed for joint shape and size using methods described in Chapter 3.2 and 3.3. Six hindlimb explants were included for analysis from each experimental group. The four cultures performed gave four experimental groups (groups 2-5) for comparison (Table 5.1). A control group (group 1), of day 7 uncultured knee joints from Chapter 4, was also included as controls to assess the change in shape during culture. The first two cultures, groups 2 and 3, assessed the method of nutrient delivery with explants cultured submerged or at an air-liquid interface. Comparisons of groups 3 and 4 assessed the effect of soft tissue presence with explants cultured with their soft tissues intact or stripped. Finally, groups 4 and 5 were used to assess the effect of culture duration with explant cultured for either three or six days. Cultures were performed sequentially based on the results from the previous experiment. The method of nutrient delivery was tested first, followed by the effect of soft tissue presence and finally, culture duration was tested. Joint region measurements were tested for normality using the Anderson-Darling test. For joint region measurements that followed a normal distribution, 1-way ANOVA was used to test for significant differences between each condition. Where significant differences existed, the Tukey-Kramer pairwise comparison was made to identify which groups were significantly different from each other. For joint region measurements that were deemed to not follow a normal distribution, the non-parametric Kruskal Wallis ANOVA was used to test for

significant differences between each condition and a pairwise rank-sum post hoc test was performed to identify which groups were significantly different. p-values less than 0.05 were considered significantly different. Statistical tests were performed in MATLAB (The MathWorks Inc., USA).

Group	Number Analysed	Nutrient Delivery	Soft Tissues	Culture Duration
1	6	Uncultured	Uncultured	Uncultured
2	6	Submerged	Intact	3 days
3	6	Air-Liquid	Intact	3 days
4	6	Air-Liquid	Stripped	3 days
5	6	Air-Liquid	Stripped	6 days

Table 5.1: Groups of knee joints compared to optimise culture conditions. Group 1 included knee joints from uncultured day 7 chick embryos. Comparisons of groups 2 and 3 were made to assess the method of nutrient delivery. Comparisons of groups 3 and 4 were made to assess the effect of soft tissue presence. Comparisons of groups 4 and 5 were made to assess the effect of culture duration.

5.4.1 Nutrient Delivery

The culture system could be used in either the vertical or horizontal orientation with the hindlimb explants fully submerged in cultured medium or left at an air-liquid interface respectively. Essentially, these configurations affect the microenvironment during culture, altering the method of nutrient delivery, waste removal and gaseous exchange, which rely on diffusion to get into and out of the developing joint region (DiMarco et al., 2014). Being fully surrounded by media means the hindlimb explants have access to nutrients in the media from all sides, but are only exposed to gases dissolved in the media (Figure 5.9). An air-liquid interface leaves half the hindlimb explants in contact with media and the other half open to the culture atmosphere (Figure 5.10). This allows for better gas exchange but reduces the capacity for nutrient delivery and waste removal. An air-liquid interface has previously been reported to increase oxygen tension within

cultured tissue and enhance viability and capacity for bone formation in a murine explant model (Smith et al., 2010) and increase bone development in embryonic chick femora (Kanczler et al., 2012).

Both submerged and air-liquid interface methods were tested over a culture period of 3 days since this was known to be a viable amount of days the explants could spend in culture. For both cases, equal amounts of culture media were used completely saturating the volume of the foam support. Both orientations were conducted with whole intact hindlimb explants.

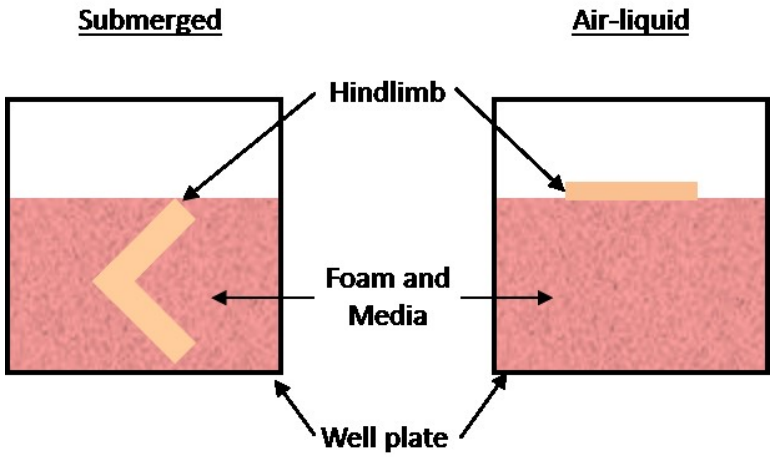


Figure 5.8: Submerged and air-liquid interface culture setups. In submerged culture the explant is fully surrounded by culture media with the hindlimb in the vertical position. At an air-liquid interface the explant lies above the level media exposed to the culture atmosphere with the hindlimb in the horizontal position.

Knee joints in the submerged group did not appear to have undergone any shape development (Figure 5.12F-J) or size change (Figure 5.13) during the 3 days of culture when compared to shape profiles from uncultured physiological day 7 joints (Figure 5.12A-E). Explants cultured at an air-liquid interface however, showed some features of normal joint shape development as reported in Chapter 4. These included the development of the anterior tibial crest and posterior curl of the lateral condyle (Figure 5.12M & N). Slight separation of the femoral condyles was also observed

in explants cultured at an air-liquid interface (Figure 5.12K). Joint shape development was therefore more advanced in knee joints cultured at an air-liquid interface compared to those cultured under submerged conditions. The size of the knee joint following 3 days of cultures under both conditions did not significantly differ from uncultured day 7 knee joints (Figure 5.13). Based on the progression of joint shape development, the air-liquid interface was deemed to be advantageous over submerged conditions.

5.4.2 Presence of Soft Tissues

During early preliminary cultures, it was observed that the surrounding soft tissue in the hindlimb explants were suffering necrosis after 3 days of static culture. The presence of surrounding soft tissues around the cartilaginous rudiments was therefore thought to be a limiting factor for development of the explant, since more tissues need to be maintained and compete for nutrients. To test, this hypothesis, hindlimbs explants were cultured with their soft tissues stripped away for 3 days at an air-liquid interface and compared to explants cultured with the soft tissues intact from the previous experiment.

Soft tissues surrounding the rudiments were removed as described by Henstock et al. (2013) immediately after dissection of the hindlimbs. Once dissected, the hindlimbs were placed on sterile filter paper and rolled laterally using curved forceps. This process removed the skin and soft tissues as they stick to the paper and are pulled away from the skeletal structure within the hindlimb (Figure 5.11). Along with the skin and soft tissues, the digits of the foot were also often removed, however, this was not considered an issue as the knee joint remained complete.

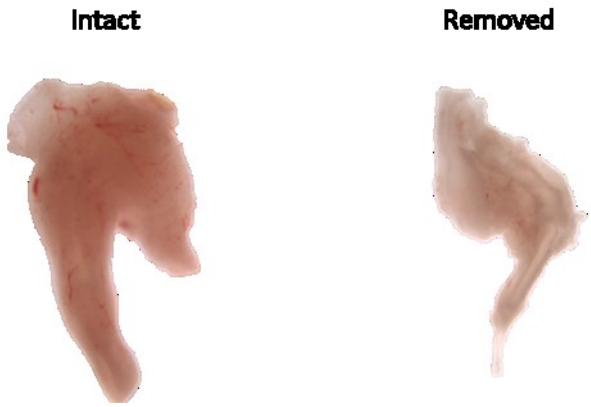


Figure 5.9: Removal of the soft tissues exposed the cartilaginous rudiments on the skeleton. Left hindlimb (left hand side) left intact after dissection. Right hindlimb (right hand side) with the soft tissues stripped after dissection. Both hindlimbs are from the same embryo. Digits of the foot were also removed during the removal of soft tissue.

Comparing explants cultured at an air-liquid interface with their soft tissues intact (group 3) and stripped away (group 4) confirmed the hypothesis that removal of tissue would promote development during culture. Stripped knee joints had an amplified emergence of the anterior tibial crest, a more defined lateral condyle and a flattened fibula (Figure 5.12R, S & T). The removal of soft tissues saw a significant increase in the average anterior-posterior depth of the lateral condyle, tibia and fibula (Figure 5.13) suggesting there was more capacity for growth in stripped explants. Removal of the soft tissues before culture was therefore considered a valuable process to advance joint development *in vitro*.

5.4.3 Culture Duration

The pioneering study by Lelkes (1958) found differences in knee joint shape between moved and unmoved chick explants only after six days of culture. It was therefore desired to extend the culture period from 3 days to 6 days to allow more time for growth and shape development to occur. Removing the soft tissues from explants had increased the development of the knee joint in the previous experiment and removed the tissue undergoing necrosis after 3 days of culture previously observed. It was therefore thought that this process would potentially extend the viability of explants in culture. To test this, explants were cultured for 6 days at an air-liquid interface with their soft tissues removed. Comparisons were made to explants cultured for 3 days

from the previous experiment to assess if extending the period affected the final joint shape and size. It was predicted that a longer period in culture would allow for more biological activity and hence advance joint development further. It could however, have a negative effect and lead to a decrease in explant survival.

Removal of soft tissues and culturing the explants at an air-liquid interface saw explants survive the complete 6 days in culture. Comparing cultures of 3 days (group 4) and 6 days (group 5) showed that doubling the time period explants spent in culture had no major effect on joint shape development under static conditions (Figure 5.12U-Y). The knee joint showed the same characteristics of shape development as explants cultured for 3 days, except for a subtle appearance of a concave tibial plateau after 6 days which was not evident previously (Figure 5.12W). Joint region sizes were also similar after the extended culture period, with only the lateral condyle significantly larger in height compared to explants cultured for 3 days under similar conditions (Figure 5.13).

5.4.4 SUMMARY

These optimisation experiments have revealed that an air-liquid interface favours normal joint shape development more than submerged conditions. At an air-liquid interface, the removal of soft tissues has also been shown to increase the size of joint features compared to when the soft tissues are left intact. Using an air-liquid interface and removing the soft tissue also increased the survival rate of explants for culture periods longer than 3 days. While, extending the culture period from 3 days to 6 days under static conditions did not dramatically change joint shape development, the longer culture period was favoured since differences between joints cultured with and without movement were previously reported after six days of culture (Lelkes, 1958). This concluded, that using an air-liquid interface, removing the soft tissues, and culturing explants for 6 days is ideal for promoting joint shape development.

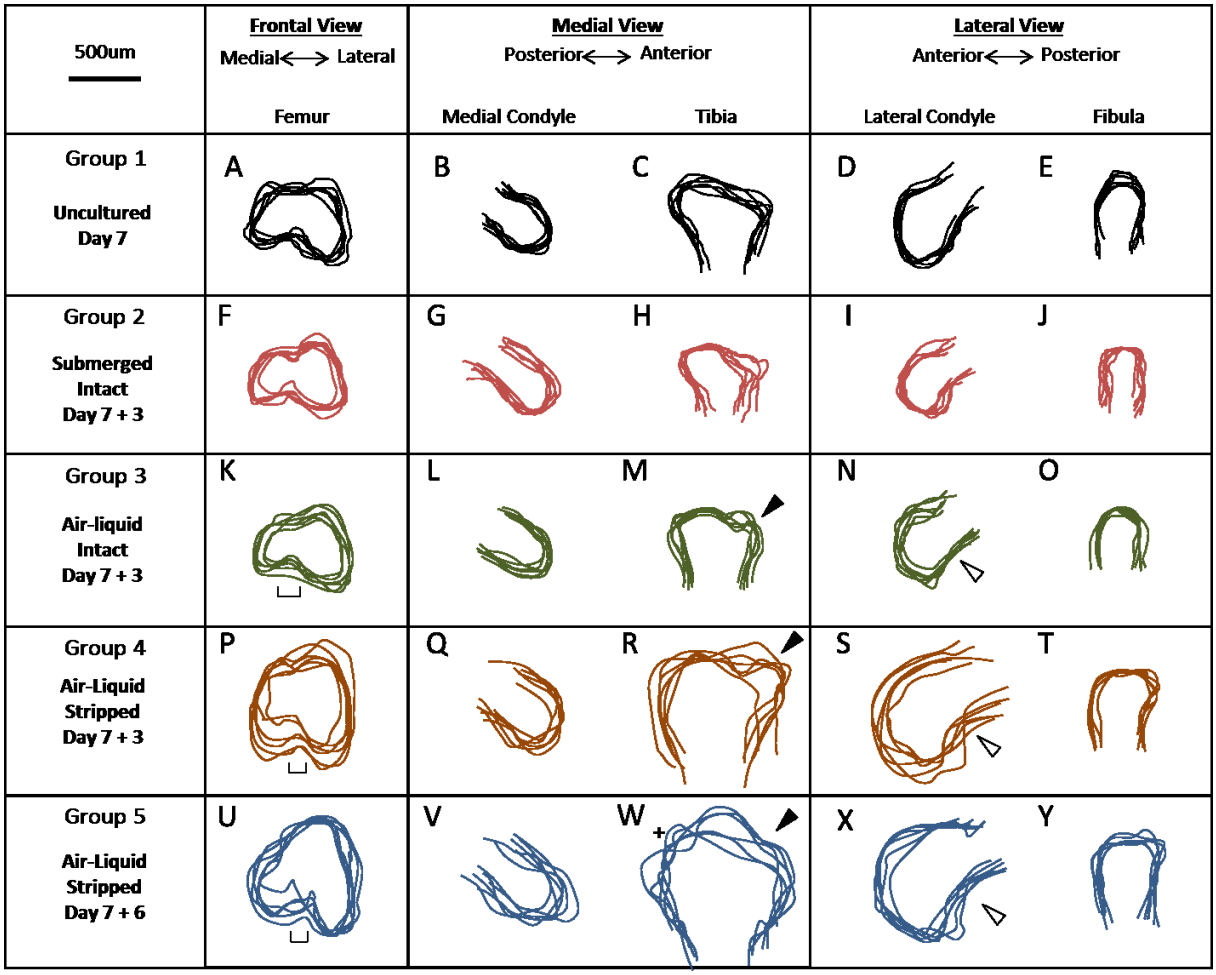


Figure 5.10: Progression of joint shape development increased following the optimisation of culture conditions (n=6). An air-liquid interface, removal of soft tissues and 6 days of culture were considered as optimal culture conditions. Hollow arrows: posterior curl of condyles; single edged bars: intercondylar fossa; + concave curve of the tibial plateau; filled arrows: anterior tibial crest.

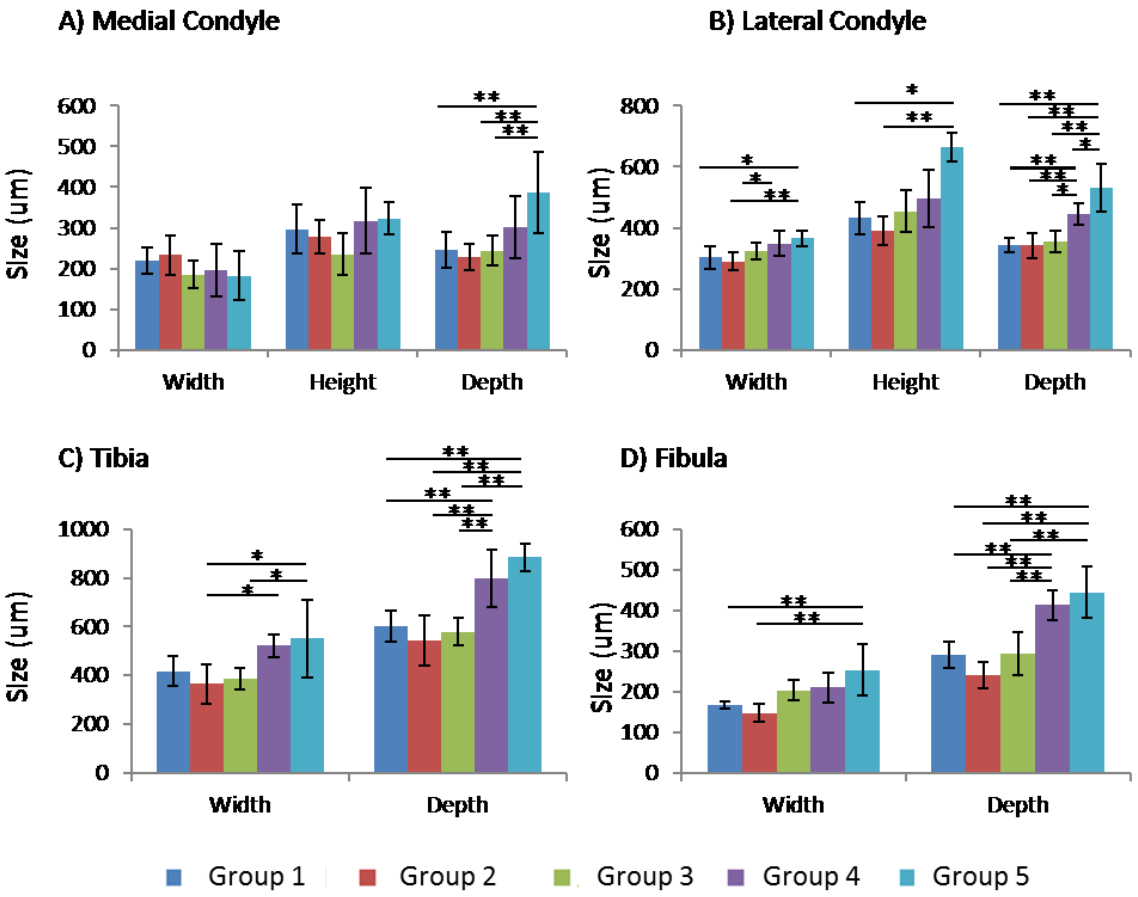


Figure 5.11: Joint region sizes were seen to increase as culture conditions were optimised. An air-liquid interface, removal of soft tissues and 6 days of culture produced the largest joints on average. Group 1: uncultured day 7; group 2: submerged, intact, 3 days; group 3: air-liquid, intact, 3 days; group 4: air-liquid, stripped, 3 days; group 5: air-liquid, stripped, 6 days. Columns represent mean size of joint regions (n=6). Error bars represent standard deviation. *p-values < 0.05, **p-values < 0.01.

5.5 Discussion

This chapter includes details of the creation of the culture system used to investigate morphogenesis in embryonic chick knee joints in further chapters of this thesis. The custom culture setup was designed to support multiple hindlimb explants during culture and allow for the application of mechanical stimulation. Combined with uniaxial compression applied by the bioreactor, the culture system could induce a flexion movement to the developing knee joints with

a range of 4 to 22 degrees from rest. Optimisation cultures, conducted under static conditions, found that growth and development of the knee joint was maximised when explants were cultured at an air-liquid interface with the soft tissues removed for a period of 6 days. Under these conditions, hindlimb explants will have the best chance to adapt to various signals during *in vitro* cultivation.

A fully functional knee joint is typically able to both flex and extend from its resting position *in ovo*, however, explants in the new culture system could only experience a flexion movement under mechanical stimulation. Even though the system did not capture the complete range of motion of the joint, the application of mechanical stimulation could still be explored and compared relatively to other joints cultivated under similar stimulation regimes. The method of attachment of the explants to the foam supports, also posed as a possible limitation since the medial side of the tissue was constantly in contact with the pore structure. The increase in explant size measured in the preliminary static cultures during optimisation however, gave confidence that growth of the explants can continue despite the adherence to the unchanging foam structure. The optimisation of culture conditions was a subjective process in which signs of normal joint shape development were used to assess the progression of joint development in culture. This could also potentially be a limitation of the culture system. Under static conditions, the optimisation experiments showed how varied the final joint shapes can be when different culture conditions are used. Therefore, when comparing joints developed, with and without stimulation, the differences noticed could stem from the culture conditions used. This however, would only make for relative changes as one would expect the culture conditions to affect both stimulated and unstimulated explants in the same way. As long as the culture conditions used are consistent with each experiment this should not impact future findings.

During the course of this doctorate another culture system was published where embryonic chick hindlimbs were mounted onto plastic hinges and cultured in glass dishes (Rodriguez and Munasinghe, 2016). Although explants were maintained in culture for up to 7 days, the method

included major manipulation of the hindlimbs in order to stitch them to each hinge, of which the effects were not documented. Since joint shape development was not assessed, the performance of this model cannot be compared to the new culture system developed during this doctorate. The culture system developed as part of this doctorate included minimal handling of the explants and has been shown to produce joints with some signs of normal joint shape development. Since the culture system was optimised under static conditions, it was not expected that explants would show all the signs of normal shape development. It is difficult to compare the results of this chapter to previous explant culture studies since most focused on joint cavitation rather than joint shape (Fell and Canti, 1934, Lelkes, 1958) and cavitation was not assessed during culture optimisation. However, similarities do exist between the joints cultured in this chapter and joints developed *in ovo* under paralysed conditions. The shape and size of the medial femoral condyle was observed to stay fairly consistent during the static cultures performed during optimisation, which agrees with a recent study of *in ovo* immobilisation in the chick embryo where the medial condyle was reported to be under-developed when dynamic muscle activity was blocked (Roddy et al., 2011b). A narrowing of the intercondylar fossa was also observed under paralysis, which matches the reduced separation of the femoral condyles in joints cultured in this study (Roddy et al., 2011b). Other studies have reported a loss of interlocking joint shapes (Drachman and Sokoloff, 1966), which match the very subtle appearance of the tibial plateau in explants cultured for 6 days. Based on these similarities, joint morphogenesis in the new culture system conforms to the literature giving confidence in its performance.

The work presented in this chapter has ultimately led to the creation of a novel explant culture model to study morphogenesis of the chick knee joint. Further chapters utilised this culture model in combination with mechanical stimulation to study changes in joint shape and the mechanobiology of the developing joint.

CHAPTER 6

6 THE EFFECT OF DYNAMIC MOVEMENT

6.1 INTRODUCTION

It has been shown in numerous animal studies that the removal of prenatal movements during development leads to joint abnormalities (reviewed in Nowlan et al., 2010b). The removal of spontaneous movements in the chick embryo has repeatedly been shown to hinder the development of the knee joint and cause cartilaginous fusion across the joint site (Drachman and Sokoloff, 1966, Osborne et al., 2002, Roddy et al., 2011b). Similar findings have also been found during *in vitro* cultivation of the knee joint (Fell and Canti, 1934, Lelkes, 1958). The study of Lelkes (1958) showed that manual manipulation of explants five times a day could counter these effects and allow the joint to cavitate and develop articular surfaces between the femur and tibia. Since this study was published, no other work has been published detailing the changes in joint morphogenesis of a developing joint experiencing applied mechanical stimulation.

This chapter compares the shape and size of joints developed under static and dynamic movement conditions. It was decided to replicate a dynamic stimulation regime that had previously been used in chondrocyte micromass cultures. It was assumed that explants would be able to tolerate higher deformations than cellular cultures, hence, a magnitude and rate of deformation that has previously been used on cells would ensure that the explants survived and

experienced no trauma or necrotic side effects. Elder et al. (2000) applied 1mm of compression at 1Hz for 2 hours, 3 times per day, to chondrocytes and found an increase in matrix synthesis compared to chondrocytes experiencing no stimulation. The same loading pattern was trialled in this chapter to test if the applied mechanical stimulation was also able to promote growth and development of the chick knee joint. It was hypothesised that dynamic stimulation would lead to a more developed joint shape than static conditions. The progression of joint shape development was assessed based on the characterised morphological changes observed in physiological joint development presented in Chapter 4.

6.2 METHODS

6.2.1 EXPLANT CULTURE

Explants for culture were prepared as described in Chapter 3.1. Right hindlimbs of each embryo were subjected to dynamic movement whist the left hindlimbs were cultured under static conditions. Explants were cultured in basal media consisting of alpha-minimum essential medium (αMEM) GlutaMAX (Gibco, UK) supplemented with 1% antibiotic antimycotic solution (Sigma-Aldrich, UK) and 100mM ascorbic acid (Sigma-Aldrich, UK) in a 5% CO2 humidified environment. Complete basal media was replenished every 24 hours. Explants were loaded into the bioreactor chambers as described in Chapter 5.2.2.2 and maintained at an air-liquid interface, with their soft tissues removed for a period of 6 days following protocols determined during culture optimisation in Chapter 5.4.

6.2.2 DYNAMIC STIMULATION REGIME

The bioreactor was programmed to apply 1mm of compression at a frequency of 1Hz for 2 hours, three times per day for the total culture period following a sinusoidal loading profile. This equated to roughly 4 degrees of flexion at the knee joint as determined during calibration of knee flexion in Chapter 5.3.

6.2.3 Joint Shape Analysis

Cultured explants were either processed for 3D joint shape and size analysis or histology. Explants for 3D joint shape analysis were stained with Alcian Blue and imaged using OPT as described in Chapter 3.2 and 3.3. 3D reconstructions of each joint were virtually orientated into a resting flexed position from which their shape profile outlines were drawn and overlaid. Joint shape outlines were compared from the frontal, medial and lateral views of the joint. Characteristics of joint morphogenesis were highlighted in each group based on data presented in Chapter 4. Explants for histology were stained with Alcian Blue and Picro Sirius Red to assess joint cavitation following protocols outlined in Chapter 3.4.

6.2.4 Specimen Numbers

A total of twelve embryos were harvested after 7 days of incubation. Two dynamic cultures were performed in the bioreactor each with six right hindlimb explants. A static culture of twelve hindlimb explants was performed alongside the two dynamic cultures. For analysis, explants were pooled together for the dynamic and static cultures. Explants damaged during processing were discarded. A total of eight explants were used for 3D joint shape and size analysis for the dynamic group and six explants were used for the static group. Six uncultured day 7 joints were also included for comparison from data previously presented in Chapter 4. Two explants from the dynamic and static group were used for histological analysis.

6.2.5 Statistical Analysis

Joint region measurements were tested for normality using the Anderson-Darling test. All joint region measurements followed a normal distribution, hence a 1-way ANOVA was used to test for significant differences between each group. Where significant differences existed, the Tukey-Kramer pairwise comparison was made to identify which groups were significantly different from each other. p-values less than 0.05 were considered significantly different. Statistical tests were performed in MATLAB (The MathWorks Inc., USA).

6.3 RESULTS

The static cultures analysed here are the same as those that were used in Chapter 5.4 for comparison of 6 days to 3 days of culture, to examine the effect of culture duration on knee joint development *in vitro*. As already stated in Chapter 5.4, under static conditions, the anterior tibial crest, tibial plateau and posterior curl of the lateral condyle were present after 6 days of culture (Figure 6.1H & I).

Explants that experienced dynamic stimulation showed more features of normal joint shape development than those cultured under static conditions. The most striking difference in shape, was noticed in the frontal shape profile of the distal femur between static and dynamic groups. Following dynamic stimulation, both femoral condyles appeared similarly sized in the frontal view with clear separation between them and only a slight offset in condyle height (Figure 6.1K). In comparison, following static conditions, both femoral condyles appeared elongated and narrowed superiorly (Figure 6.1F). A large offset between the top of the medial and lateral condyle was also noticed in the static group (Figure 6.1F). The medial condyle was significantly larger in width, height and depth following dynamic stimulation compared to both uncultured day 7 and statically cultured explants (Figure 6.2A). The shape of the medial condyle was also more advanced following dynamic stimulation, with evidence of a posterior curl in the medial view which was not seen following static conditions (Figure 6.1L). The shape profile of the tibia in the dynamic group showed the same features of joint shape development as the static group with emergence of the anterior tibial crest and tibial plateau (Figure 6.1M). The upwards projection in the static group however, was missing in the dynamic group which appeared to have a flatter tibial surface (Figure 6.1H & M). No differences in joint shape were found on the lateral side of the joint between static and dynamic groups. The lateral condyle and fibula were similar in both shape and size in static and dynamic groups (Figure 6.1N & O) and significantly larger after culture compared to uncultured day 7 joints (Figure 6.2B & D).

Unfortunately, assessment of joint cavitation was inconclusive due to multiple unstained areas surrounding the rudiments in both static and dynamic groups. This made it difficult to comment on whether a lack of staining, normally identifying a joint cavity, was in fact a joint cavity or an experimentally introduced artefact (Figure 6.3).

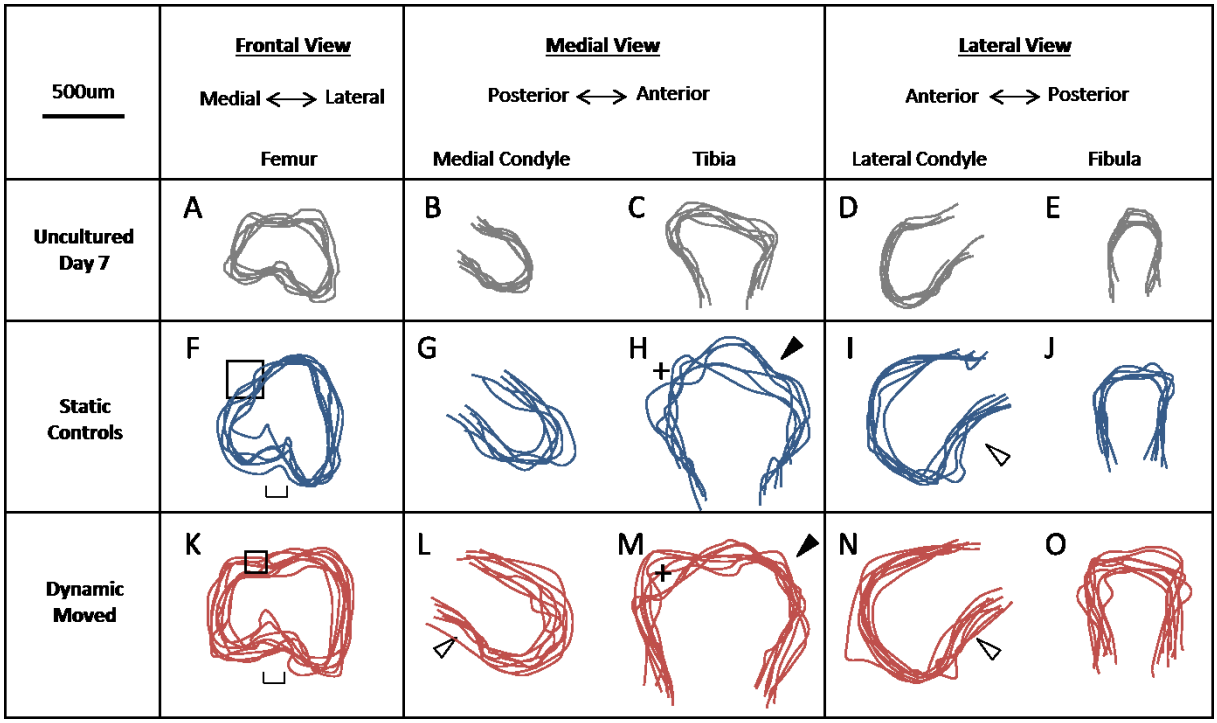


Figure 6.1: Shape profiles of uncultured (n=6), static (n=6) and dynamic (n=8) knee joints reveal differences in joint shape. Both cultured groups show signs of shape development compared to uncultured joints. Squares: dominance of the lateral condyle over the medial condyle; Hollow arrows: posterior curl of condyles; single edged bars: intercondylar fossa; + concave curve of the tibial plateau; filled arrows: anterior tibial crest.

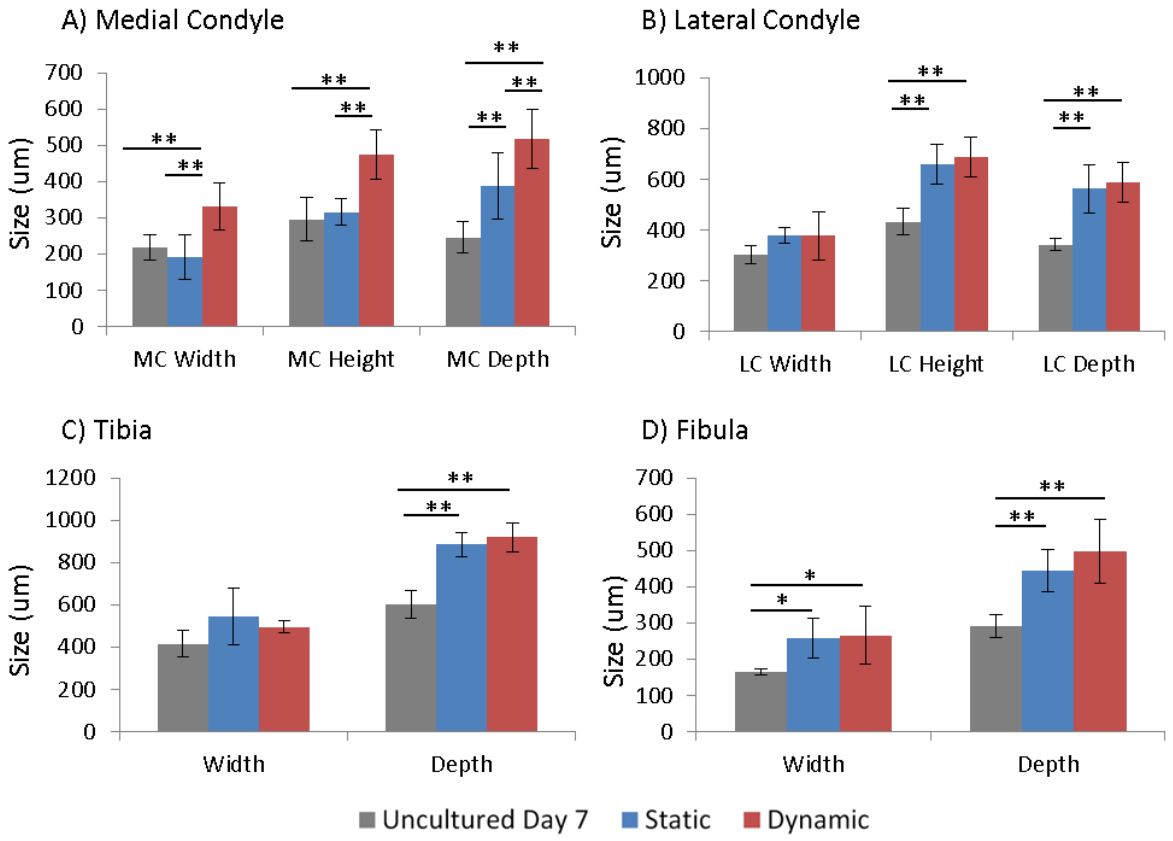


Figure 6.2: Dynamically stimulated joints were significantly larger in size compared to joints in the static group. Columns represent mean size of joint regions measured for uncultured (n=6), static (n=6) and dynamic (n=8) groups. Error bars represent standard deviation. *p-values < 0.05; **p-values < 0.01.

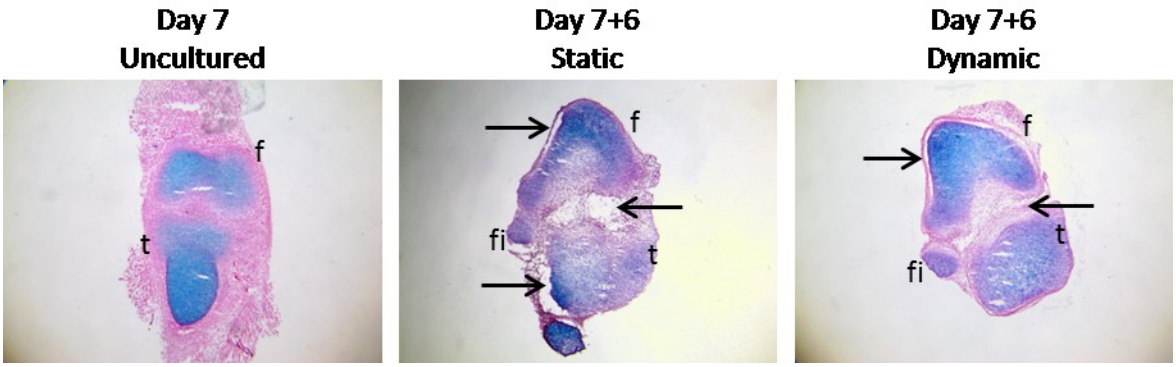


Figure 6.3: Both statically cultured and dynamically cultured showed potential joint cavities. Images are frontal sections of the knee joint. Arrows indicate areas of reduced staining which are present around the rudiments and between rudiments. f – femur; fi – fibula, t – tibia.

6.4 DISCUSSION

This chapter demonstrates the success of the new culture system in being able to culture the embryonic chick hindlimb for 6 days with applied dynamic movement. The comparison of statically cultured explants to dynamically stimulated explants showed clear evidence that the development of the knee joint was promoted by mechanical stimulation compared to static conditions. From Chapter 4, it was clear that the medial side of the joint undergoes rapid development between day 7 and 9. The application of dynamic movements to explants *in vitro* significantly increased the size of the medial condyle and generated more features of normal shape development compared to static cultures. This suggests that dynamic movements are needed to promote development of the medial side of the joint.

The movement regime used in this chapter is not representative of physiological movement patterns for the chick embryo but was considered appropriate as a first attempt at quantitative mechanical manipulation of explants during culture. Applying larger deformations to the explants increases the chance of overloading the tissue and causing trauma or necrotic behaviours. The displacement applied and timing of stimulation has previously been shown to support chondrocyte differentiation and proliferation *in vitro* (Elder et al., 2000) and hence was thought to be a tolerable regime for the hindlimb explants. Whilst dynamic movements are applied to the explants, the culture media in the bioreactor chambers is being moved. This could have potentially induced fluid flow over the explants and increased nutrient delivery by circulating the otherwise stagnant media. The differences found between dynamic and statically cultured explants, however, match those of immobilisation studies giving confidence that the response seen in joint development were due to joint movements and not the circulation of culture media. Joint regions, such as the medial condyle, which is reported to under-develop during immobilised conditions (Roddy et al., 2011b), was small and simple under static conditions, whilst, the application of dynamic movement saw this reversed in this study. Not being able to assess joint cavitation is a limitation of the new culture methodology, but does not impede the analysis of joint

morphogenesis. Since fusion between the femur and tibia had previously been reported in immobilised studies (Drachman and Sokoloff, 1966) and in static cultures of the chick knee joint (Lelkes, 1958) we assumed the process of soft tissue removal caused separation of tissues within the explants leading to unstained areas within the joint region.

Static conditions *in vitro* and *in ovo* have previously been shown to have detrimental effects on joint formation, whereas manipulation of explants during culture can counter act these effects and abnormalities (Lelkes, 1958). The results presented in this chapter support the hypothesis that the presence of mechanical stimulation during development leads to a more natural joint shape. This chapter also shows the culture system is a viable model to explore the effect of applied movement on morphogenesis of the chick knee joint. In the next chapter, the magnitude of movement is adjusted to represent more physiologically appropriate flexion magnitudes.

CHAPTER 7

7 THE EFFECTS OF MOVEMENT MAGNITUDE

Parts of this chapter have been published in the Journal of Biomechanics (Appendix III) (Chandaria et al., 2016).

7.1 INTRODUCTION

The quantitative relationship between mechanical stimulation and joint morphogenesis has not previously been investigated. It is already clear that the development of the chick knee joint is promoted by dynamic movement from previous immobilisation studies (Drachman and Sokoloff, 1966, Roddy et al., 2011b) and the experiments performed during this doctorate (Chapter 6). However, it remains unclear how variations in mode, magnitude and frequency of fetal movements affects joint shape development. Understanding how different magnitudes of movement contribute to joint morphogenesis could potentially help to identify optimal amounts of movement needed for normal joint formation.

It was theorised that the magnitude of movement experienced by a joint is a critical variable for the progression of joint shape development. High magnitudes of joint movement could potentially create more defined joint shapes compared to lower magnitudes due to an increase in mechanical stimuli. However, higher magnitudes of joint movement could also over stimulate and unbalance

biological activities and induce joint malformations compared to lower or less strenuous magnitudes.

To evaluate how variations of movement magnitude affects joint morphogenesis, three magnitudes of joint movement were applied to the developing chick knee joint using the newly created culture system designed during this doctorate. The aim was to characterise the relationship between the magnitude of applied movements and key aspects of fetal joint morphogenesis for the first time. It was hypothesised that joint shape development would be affected by movement magnitude in a dose-dependent manner, and that the most physiological movement regime would lead to a joint with the most normal progression of shape morphogenesis. An average-flexion movement regime mimicked normal flexion magnitudes of the chick embryo *in ovo*, and two additional dynamic regimes of lower and higher flexion magnitudes were studied.

7.2 METHODS

7.2.1 EXPLANT CULTURE

Hindlimb explants were prepared for culture after 7 days of incubation as described previously in Chapter 3.1. Immediately after dissection, the soft tissues surrounding the knee joint were removed as described in Chapter 5.4. Right hindlimbs of each embryo were subjected to dynamic movement whist the left hindlimbs were cultured under static conditions as controls. Explants were cultured in complete basal media (alpha – minimum essential media (α-MEM GlutaMAX, Gibco) supplemented with 1% antibiotic antimycotic solution and 100uM Ascorbic Acid (Sigma, UK)) which was replenished every 24 hours. Explants were mounted to foam supports and placed into the bioreactor for dynamic stimulation as described in Chapter 5.2.2.2. Explants were maintained at an air-liquid interface for a total period of 6 days.

7.2.2 Dynamic Movement Regimes

The three movement regimes were termed reduced-flexion, average-flexion and over-flexion where 2, 3 and 4mm of compressive displacement were applied respectively, resulting in knee flexion magnitudes of 9±3, 14±4.0 and 22±5.0 (mean±SD) degrees as determined during calibration in Chapter 5.3. Observations of chick motility *in ovo* report an approximate mean knee flexion of 12 degrees in 9–10 day old embryos (Watson and Bekoff, 1990). All dynamically stimulated explants were loaded with a sinusoidal waveform at an average rate of 4mm/s for 2 hours, three times per day as previously used in Chapter 6. The inclusion of a rest period between movement cycles replicated the activity-inactivity cycles observed in chick embryos *in ovo* (Chambers et al., 1995, Hamburger et al., 1965).

7.2.3 Specimen Numbers

A total of 72 chick embryos were harvested after 7 days of incubation. Explants selected for dynamic stimulation were split evenly across the three experimental groups. A total of four cultures were performed for each of the three dynamically moved groups, with static control cultures performed alongside each one. Explants were pooled together for the three experimental groups and static controls to give four groups for analysis.

This meant a total of 24 explants were cultured for each experimental group and a total of 72 explants were cultured under static control conditions. During media changes, each culture chamber was visually inspected for any signs of abnormal growth or infection. Contaminated or infected cultures were discarded and repeated. During the course of this study, two dynamic cultures and one static culture were repeated due to contaminations. Successfully cultured explants were used either for 3D joint analysis or for cellular level analysis. Explants damaged during processing were discarded. A total of 26, 7, 12 and 11 knee joints were analysed for shape and size in the static, reduced-flexion, average-flexion and over-flexion groups respectively. An additional two explants per group were used for cellular level activity assays, and within these

samples, two sections from each of the two explants were used to quantify proliferation rates and cell viability.

7.2.4 3D Joint Shape and Size Analysis

Explants chosen for 3D shape and size analysis were processed following protocols described in Chapter 3.2 and 3.3. To visualise the cartilaginous skeletal rudiments each explant was stained with Alcian Blue and imaged using OPT. Shape profiles were traced for each knee joint and overlaid within each group. Comparisons were made for each rudiment in the frontal, lateral and medial view. Eleven measurements were made of the distal femur, proximal tibia and fibula, as shown in Chapter 3.3.

7.2.5 Immunohistochemistry Analysis

Explants were prepared for cryopreservation and cryosectioning as described in Chapter 3.4. All explants were sectioned at 10μm. Proliferating cells were identified using the mitosis marker phospho-Histone H3 (pHH3), similarly to Roddy et al. (2011a). Background cells and proliferating cells were visualised under UV and red fluorescence channels respectively. Cell viability was assessed using a terminal deoxynucleotidyl transferase (TdT) dUTP nick-end labelling (TUNEL) detection kit (APO-BRDU-IHC, Bio-Rad Laboratories, USA) using the recommended protocols also described in Chapter 3.4 to identify cells undergoing apoptosis or necrosis. Dead cells were stained brown and live cells were counter stained green. All sections were imaged at 100x magnification (Brunel RX30F Microscope). The number of proliferating and total number of cells were counted using the particle analysis function in ImageJ (U.S. National Institutes of Health, USA). The number of dead cells was counted manually.

7.2.6 Statistical Analysis

All measurements were tested for normality using the Anderson-Darling test. Joint region size, cell proliferation and cell viability were tested for significance differences between static, reduced-flexion, average-flexion and over-flexion groups using 1-way ANOVA. Where significant differences existed, a Tukey-Kramer pairwise comparison was made to identify which groups

were significantly different from each other. For joint region sizes that were not considered normally distributed a Kruskal Wallis ANOVA was performed followed by a pairwise rank-rum test to identify significant differences between groups. p-values less than 0.05 were considered significantly different. Statistical tests were performed in MATLAB (The MathWorks Inc., USA).

7.3 RESULTS

7.3.1 3D JOINT REGION SHAPES AND SIZES

The characteristics of physiological shape development described in Chapter 4 were used as indicators to assess the normality of joints developed *in vitro*. The static controls in this study were used to test for consistency between cultures conducted at different times in the laboratory. The joint shapes of explants cultured under static conditions were similar to those previously seen (Figure 7.1A-E). Briefly, the medial condyle remained substantially smaller than the lateral condyle and was missing the posterior curl seen in normal shape development (Figure 7.1B). The tibia had produced the anterior tibial crest but was lacking a definitive concave tibial profile (Figure 7.1C). The lateral condyle and fibula showed a posterior curl (Figure 7.1D) and flattened epiphysis (Figure 7.1E) respectively, as seen in normal shape development.

Knee joints developed in the average-flexion group showed more features of normal shape development compared to the other dynamic stimulated groups. In the average-flexion group, both femoral condyles developed a posterior curl (Figure 7.1L & N) and appeared most similar in size with only a slight offset between the top of the femoral condyles (Figure 7.1K). While the lateral condyle was slightly bigger than the medial condyle, the medial condyle was only 20% less deep on average than its opposing lateral condyle, compared to 41% between condyles in static controls. No significant differences were found in femoral condyle height or lateral condyle depth between average-flexion and static controls (Figure 7.2A & B). Lateral condyle width was significantly larger following average-flexion compared to static controls (Figure 7.2B), as were the depth and width of the tibia (Figure 7.2C).

Joint shape profiles and joint region size differed between the three dynamically moved groups revealing an effect of movement magnitude on joint shape development. The relative size differences between the depths of the femoral condyles were more pronounced in the reduced-flexion group (40% on average) and the over-flexion group (34% on average) than in the average-flexion group (20%, as reported above). Evidence of a dorsal groove between the femoral condyles was observed in explants following average-flexion (Figure 7.1K), but not in any of the other groups (Figure 7.1A, F & P). The intercondylar fossa was also clearly distinguishable following average-flexion, but was distorted in both the reduced-flexion and over-flexion groups (Figure 7.1F, K & P). While no significant differences were found between the intercondylar fossa width between the different groups, there was greater variation in this joint region size in the reduced-flexion and over-flexion groups than in the average-flexion group (Figure 7.2E). On average, reduced-flexion joints were smaller than average-flexion joints, measuring significantly smaller in lateral condyle and fibula width and medial condyle and tibia depth. Measurements of joint regions in the over-flexion group were similar to those of the average-flexion group, except for medial condyle depth, which was significantly smaller with a difference of 21% in the over-flexion group compared with the average-flexion group (Figure 7.2A). Joint shape profiles in the over-flexion group were noticed to be less consistent when overlaid compared to other groups showing some variability in joint shape development following the larger movements (Figure 7.1P-T). In particular, measurements of the lateral condyle depth exhibited a large standard deviation of 22% compared to 12% in the average-flexion group (Figure 7.2B).

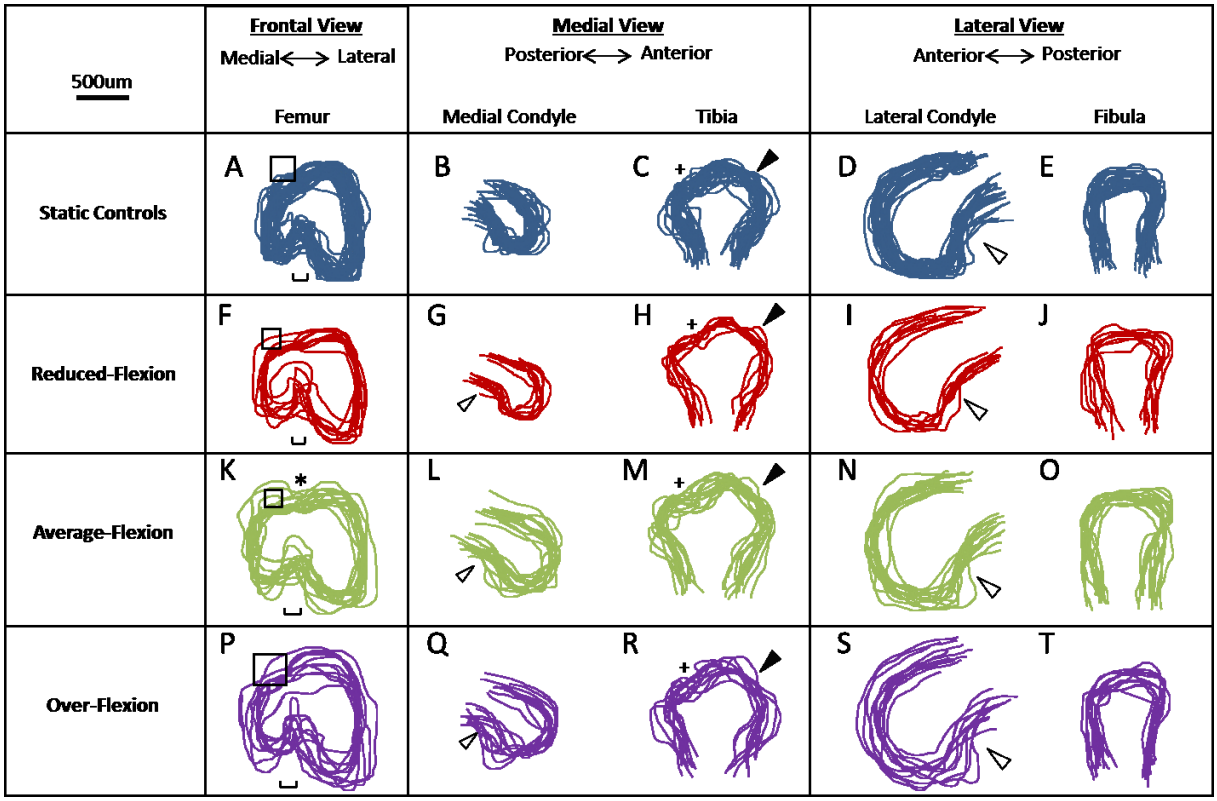


Figure 7.1: The average-flexion movement regime led to more normal progression of morphogenesis than other movement regimes or static culture. Shape profiles of the 3D reconstructed joint regions were outlined and overlaid for each cultured group. Static controls (n=26), reduced-flexion (n=7), average-flexion (n=12), over-flexion (n=11). Squares: dominance of the lateral condyle over the medial condyle; hollow arrows: posterior curl of condyles seen in moved explants; * dorsal groove between the two femoral condyles; single edged bars: intercondylar fossa; + concave curve of the tibial plateau; filled arrows: anterior tibial crest. Adapted and reproduced from Chandaria et al. (2016).

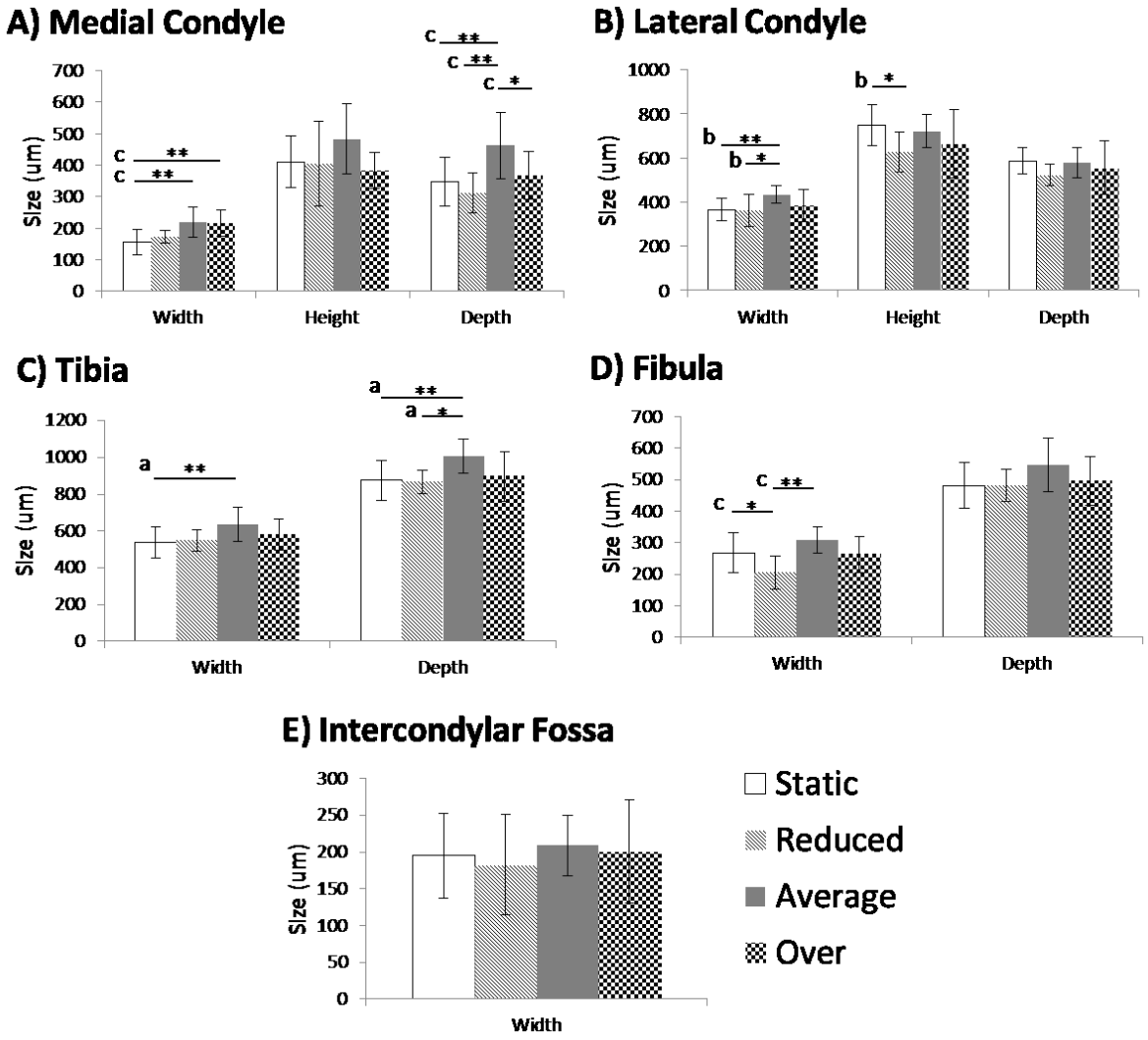


Figure 7.2: Significant differences in joint region measurements were most pronounced between the average-flexion regime and static culture. Mean size of joint regions measured for static (n=26), reduced-flexion (n=7), average-flexion (n=12) and over-flexion (n=11) explants. Error bars represent standard deviation. *p-values < 0.05; **p-values < 0.01. 'a' indicates a difference of 10-15%, 'b' indicates a difference of 16-20% and 'c' indicates a difference of 21-35%, where differences represent how much smaller the regions measured relative to the larger joint. Adapted and reproduced from Chandaria et al. (2016).

7.3.2 Cell Viability and Proliferation

Cell viability within the distal femur was greater than 95% in all groups, demonstrating that high cellular survival was maintained during the culture period. There were no significant differences between groups for cell viability (Figure 7.3A). However, average-flexion and over-flexion regimes led to significantly more proliferation than the static or reduced-flexion regimes (Figure 7.3B), with almost double the number of proliferating cells in the average-flexion regime compared to the static or reduced-flexion groups.

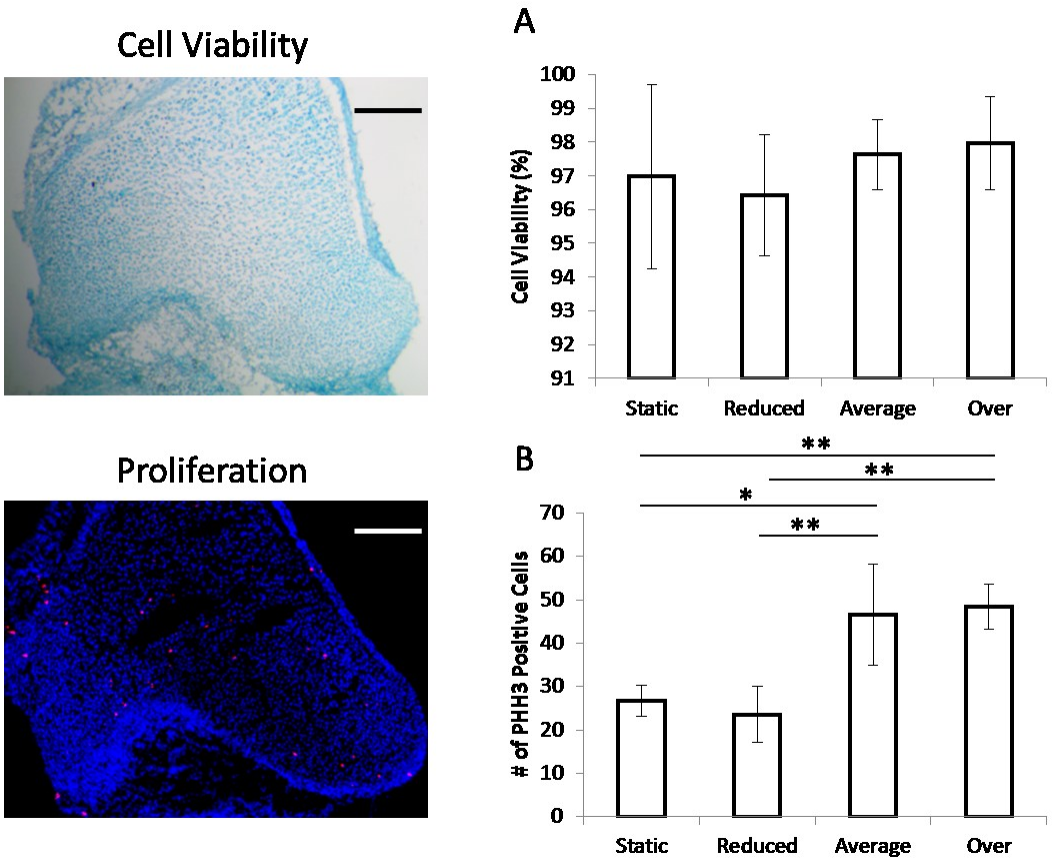


Figure 7.3: Average-flexion or over-flexion led to significant increases in cell proliferation, while movement regime did not affect cell viability. Stained sections are shown from the average-flexion group for live/dead and proliferating cells. Viability staining shows dead cells in brown and live cells in green. Proliferation staining shows background cells in blue and proliferating cells in red. Scales bars = 200um. A) shows live cell count as a percentage of total number of cells for each group. B) shows the total number of proliferating cells in the distal femur for each group (n=4). Error bars represent standard deviation. *p-values < 0.05; **p-values < 0.01. Adapted and reproduced from Chandaria et al. (2016).

7.4 DISCUSSION

This chapter explored the effects of movement magnitude on morphogenesis of developing joints. The effects of three dynamic movement regimes and one static regime on chick knee joint morphogenesis were compared and supported the hypothesis that joint shape development would be affected by movement magnitude in a dose-dependent manner. The average-flexion regime, which was most similar to physiological movement patterns *in ovo,* showed the most progression of normal joint shape development when compared to the sequence of physiological shape changes seen in normal embryos. Following average-flexion, the distal femur also contained significantly more proliferative cells than explants which experienced reduced-flexion or no movements, suggesting that the size and shape changes in this group were due to an upregulation in mechanically-mediated proliferation rates. The average-flexion regime also produced the largest joints with both femoral condyles significantly larger than statically-cultured explants. These results reveal that the magnitude of movement is a critical mechanical factor in driving joint morphogenesis. This study suggests that movements lower in extent than those seen physiologically can still advance joint morphogenesis but fail to promote proliferation and growth. The research also suggests that movement greater in extent than the physiological range can promote proliferation and growth but can cause irregularities and distortions in joint shape. Analysis of these three magnitudes supports the hypothesis that the most physiological movement regime would lead to a joint shape that more closely approximated normal development and further reveals a non-linear relationship between magnitude of movement and joint shape normality.

The aim of this study was to compare the effects of different movement magnitudes on joint morphogenesis, rather than to recreate physiological joint shapes *in vitro*. Joints developed *in vitro* and joints developed *in ovo* are not directly comparable due to the absence of systemic factors and differences in developmental environments. However, the relative comparisons made between the different groups of joints developed in this study, did provide an insight into the

quantitative relationship between mechanical stimulation and joint morphogenesis, which would not be possible with *in vivo* experiments. The forces experienced within the joint explant due to the applied movement regimes were not quantified due to the complexity of the culture system, but can be assumed to increase with increased movement magnitude. It was believed that movement, rather than load, was a better parameter to quantify the level of mechanical stimulation, as it is more directly comparable to physiological conditions *in vivo.* A computational model would be ideal to investigate the role of loading during joint morphogenesis and predict how the compressive load applied to the foam support is transferred to the developing explants. Conditioned medium can significantly increase chondrocyte differentiation, proliferation and ECM synthesis (Elder, 2002, Kanczler et al., 2012) and could potentially amplify the differences found in this study. However, variance in serum performance and biochemical activity would be a possible confounding factor, hence a serum-free medium was used in this study.

The only recent study that applied mechanical stimulation *in vitro* to developing limb explants did not report definitive findings on joint shape (Rodriguez and Munasinghe, 2016). The study presented in this chapter was the first to explore the effects of mechanical stimulation on chondrocyte viability and proliferation in embryonic joint explants cultured *in vitro*. Previous studies have explored the relationship between mechanical stimulation and proliferation using cellular micro-mass deformation culture models, but conflicting results have been reported. Evidence exists for both increases (Elder et al., 2000) and decreases (Juhász et al., 2014) in proliferating cells following mechanical loading, and some studies found no differences at all (Klumpers et al., 2015). The general consensus though is that mechanical loading of chondrocytes improves chondrogenesis and ECM synthesis (Bian et al., 2011, Elder et al., 2000, Sah et al., 1989, Cohen et al., 2005). The data from the current study suggests that mechanical stimulation does affect proliferation and that a threshold for the level of stimulation exists, above which proliferation was enhanced. This finding agrees with a recent meta-analysis of *in vitro* cultivation of chondrocytes, which found that a threshold of loading exists for mechanically-mediated enhanced cartilage proliferation and differentiation over a variety of animal species (Natenstedt

et al., 2015). For this experimental model, the threshold lies somewhere between the levels of stimulation applied in the reduced-flexion and average-flexion groups. The findings that proliferation is down-regulated in cases of static or reduced-stimulation agrees with Roddy et al. (2011b) who showed a significant decrease in cell proliferation in the distal femur of immobilised chick embryos.

In conclusion, the results of this study provide evidence that joint morphogenesis of the embryonic chick knee joint is affected by the magnitude of movement experienced *in vitro*. The most developed joint shapes were observed following a movement magnitude similar to those observed *in ovo*. Above this, the joint shapes were seen to vary and even deteriorate, whilst below this magnitude, joint shapes were similar to those of statically cultured explants. In the next chapter, the average-flexion regime was employed to explore the mechanotransductory pathways involved during joint morphogenesis.

CHAPTER 8

8 THE ROLE OF MECHANOSENSITIVE ION CHANNELS

8.1 INTRODUCTION

The previous chapters have shown that movement can promote joint shape development. However, the method of how mechanical stimuli is sensed and acted upon has never been tested in tissue explants. Mechanical cues are converted into biological processes and cellular responses through mechanotransduction. Physical deformation of chondrocytes *in vitro* has been shown to generate a flux of calcium, sodium and potassium ions across the cell membrane which then release intracellular messengers that activate cascades important for differentiation, growth and survival (reviewed in Mobasheri et al., 2002). In particular, stretch activated ion channels and L-type (long lasting activation) calcium ion channels have been shown to be involved in cartilage growth and maintenance following induced deformations (reviewed in Mobasheri et al., 2002). It was therefore thought that these mechanosensitive ion channels are potential candidates for the mechanotransduction and regulation of joint morphogenesis.

Cell membranes are directly manipulated by external mechanical stimuli (Martinac, 2004) and are heavily equipped with ion channels which are thought to be involved in the control of cell size through volume regulation or control of cell division (Sachs, 1991). Ion channels provide gated passageways for ions to cross the cell membrane and regulate intracellular and extracellular ion

concentrations (Alberts et al., 1998). Calcium ion concentrations have been shown to fluctuate during embryonic development and be involved in signalling sequential processes of skeletogenesis (reviewed in Webb and Miller, 2003). Stretch activated ion channels open and close based on physical tension in the cell membrane (Figure 8.1) and can be found in a variety of specific and nonspecific forms that together allow for the transfer of both cations and anions into and out of the cell (Alberts et al., 1998, Martinac, 2004). L-type calcium channels are voltage-gated channels, meaning they open and close based on the membrane potential (Alberts et al., 1998) (Figure 8.1).

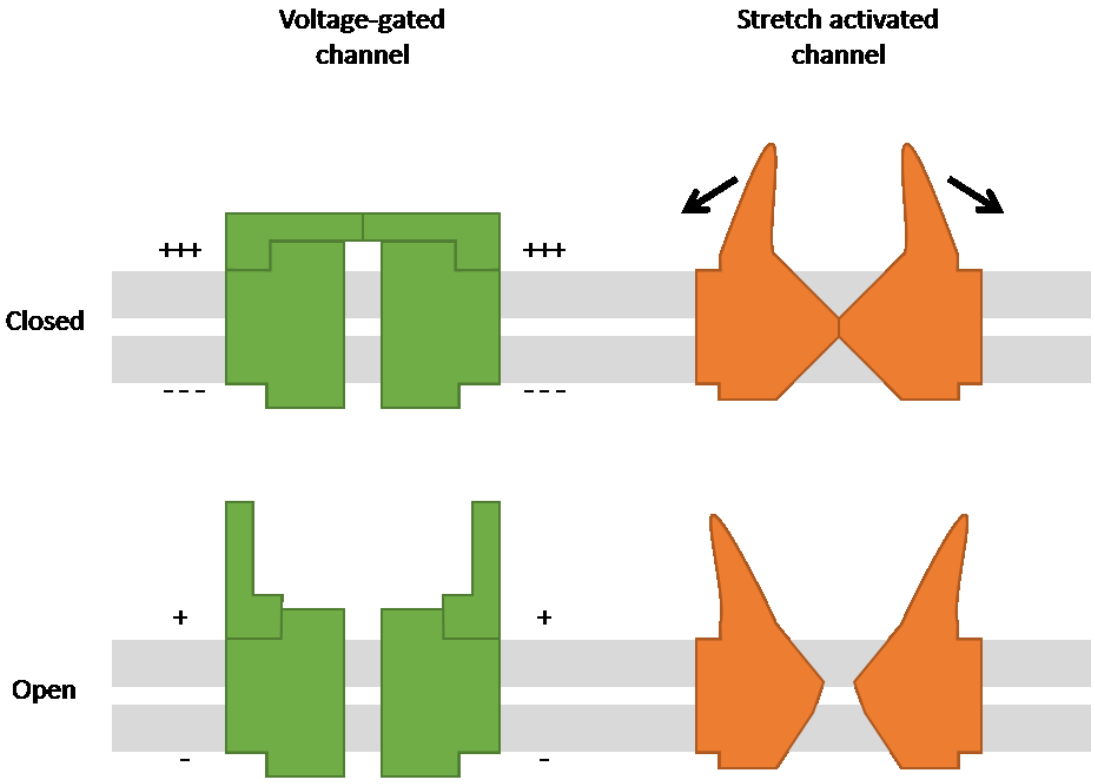


Figure 8.1: Voltage-gated channels and stretch activated ion channels open and close to regulate transmembrane ion concentrations. Voltage-gated ion channels respond to changes in the voltage difference across the membrane. Stretch activated ion channels respond to tension applied to the membrane.

The aim of the work described in this chapter was to test the involvement of stretch activated ion channels and L-type calcium ion channels in the mechanotransduction of joint shape development. It was hypothesised that mechanical stimuli that direct localised joint shape development are transduced through the function of mechanosensitive ion channels. Previously, it was shown that dynamic stimulation of developing chick hindlimbs promoted normal joint shape development *in vitro* compared to static conditions. The average-flexion movement regime from Chapter 7 was repeated in this chapter whilst the function of stretch activated ion channels and L-type calcium ion channels were blocked independently. The resultant joint shapes were then analysed and compared to assess if joint morphogenesis and the effects of dynamic movement had been affected.

8.2 METHODS

8.2.1 EXPLANT CULTURE

Fertilised DeKalb White eggs were incubated for seven days, after which the chick embryos were harvested and their hindlimbs dissected as described in Chapter 3.1. The surrounding tissues and digits of the foot were removed and explants were cultured at an air-liquid interface as described in Chapter 5.4. Explants were cultured on foam supports inside the bioreactor as described in Chapter 5.2.2.2 and kept in complete basal culture media (alpha – minimum essential media (α-MEM GlutaMAX, Gibco) supplemented with 1% antibiotic antimycotic solution and 100uM Ascorbic Acid (Sigma-Aldrich, UK)). Explants were cultured for six days and the culture media was changed every 24 hours.

8.2.2 DYNAMIC MOVEMENT REGIME

The average-flexion regime from Chapter 7 was applied to all explants as it had previously been shown to create the most developed joint shapes when compared to other magnitudes of movement. This included 3mm of compression applied by the bioreactor, which resulted in a knee flexion of 14±4.0 (mean+SD) degrees as determined during calibration in Chapter 5.3. Dynamic

stimulation was applied for two hours, three times per day in a sinusoidal waveform at an average rate of 4mm/s.

8.2.3 Administration of Ion Channel Inhibitors

The function of stretch activated ion channels was blocked using gadolinium chloride ($GdCl_3$) (Sigma-Aldrich, UK) dissolved in 1M hydrochloric acid (HCl) (Sigma-Aldrich, UK). L-type calcium ion channels were blocked using nifedipine (Nf) (Sigma-Aldrich, UK) dissolved in DMSO (Sigma-Aldrich, UK). Both agents have previously been used in 3D chondrocyte cultures to block the selected ion channels (Mouw et al., 2007). Two concentrations, one order of magnitude apart, were chosen for the blocking agents, based on previously used doses in cell cultures (Mouw et al., 2007). Low and high doses had a final concentration of 100μM and 1mM respectively for each ion channel blocker. Vehicle controls were also performed to assess the impact of the solvent agents used. Blocking agents were replaced every 24 hours along with the culture media.

A total of eight cultures were performed. Two cultures were treated as dynamic controls with no blocking agents administered during the experiments. Two cultures were treated individually with one of the blocking solvents only and termed vehicle controls. The remaining four cultures were treated with either a low or high dose of blocking agent, giving two blocked stretch activated ion channel cultures and two blocked calcium ion channel cultures.

8.2.4 Specimen Numbers

Each culture included six explants. Both left and right hindlimbs were split across the cultures to minimise the number of embryos needed for this study. During media changes, cultures were inspected for visual signs of contamination and infection. All eight cultures were successful with no incidence of infection recorded. Explants damaged during sample preparation or imaging were not included in the final analysis. The two dynamic control cultures were pooled together to make one group for analysis. A total of ten explants were included for analysis in the dynamic control group. All six explants were included from the two individual vehicle control groups. For blocked stretch activated ion channel cultures, all six explants from each dose were included in the final

analysis. For blocked calcium ion channel cultures, five explants from each dose were included in the final analysis. A summary of specimen numbers is presented in Table 8.1.

Group	Number of Cultures	Explants Cultured	Explants Analysed
Dynamic Controls	2	12	10
$GdCl_3$ Vehicle Controls	1	6	6
Nf Vehicle Controls	1	6	6
100um $GdCl_3$	1	6	6
1mM $GdCl_3$	1	6	6
100um Nf	1	6	5
1mM Nf	1	6	5

Table 8.1: Number of cultures performed, explants cultured and explants used for analysis.

8.2.5 3D Joint Shape and Size Analysis

All explants were processed for 3D joint shape and size analysis as described in Chapter 3.2 and 3.3. Shape profiles were drawn in the frontal, medial and lateral views for each culture group and overlaid for each rudiment. Joint shape profiles from right hindlimbs were mirrored to match the shape profiles of left hindlimbs. Comparisons were made between dynamic controls, HCl vehicle controls, 100μM $GdCl_3$ and 1mM $GdCl_3$ to identify the effects of blocking stretch activated ion channel function. Comparisons were made between dynamic controls, DMSO vehicle controls, 100μM nifedipine and 1mM nifedipine to identify the effects of blocking calcium ion channels. Comparisons were made between dynamic controls, 1mM $GdCl_3$ and 1mM nifedipine to identify differences between blocking stretch activated ion channels and calcium ion channels.

8.2.6 Statistical Analysis

All measurements were tested for normality using the Anderson-Darling test. For normally distributed data, joint region sizes were compared for significant differences between controls, vehicles and drugged groups using 1-way ANOVA for each study. If significant differences were identified, a Tukey-Kramer pairwise comparison was made to identify which groups were significantly different from each other. For joint region sizes that were not considered normally

distributed a Kruskal Wallis ANOVA was performed followed by a pairwise rank-rum test to identify significant differences between groups p-values less than 0.05 were considered significantly different. Statistical tests were performed in MATLAB (The MathWorks Inc., USA).

8.3 Results

8.3.1 Effects of Blocking Stretch Activated Ion Channels

Explants cultured with 1M HCl, the vehicle control for gadolinium chloride, showed the same characteristics of joint shape development seen in dynamic controls following an average-flexion regime (Figure 8.2F-J). A clear intercondylar fossa could be made out in the frontal view of the distal femur along with evidence of a dorsal groove between the condyles on the superior surface of the rudiment (Figure 8.2F). The offset between the top of the medial and lateral condyles appeared minimal and similar in both dynamic controls and vehicle controls (Figure 8.2A & F). Posterior curls were seen in both the medial and lateral condyles along with the development of the anterior tibial crest and concave tibial plateau (Figure 8.2G, H and I). An increasing trend in average lateral condyle height, depth, tibia width and depth was observed for vehicle controls compared to dynamic controls, however no statistically significant differences were found between the two groups (Figure 8.3).

Adding 100μM of $GdCl_3$ to the developing explants slightly altered the resultant joint shapes after six days of culture. In the frontal shape profile of the distal femur, an increased offset between the top of the femoral condyles was noticed along with the absence of the dorsal femoral groove (Figure 8.2K). The femoral condyles, the anterior tibial crest, and tibial plateau all appeared similar to controls, showing no difference in the medial and lateral shape profiles of the joint following a low dose of gadolinium chloride (Figure 8.2L, M, N & O). Joint region sizes measured in explants cultured with 100μM of gadolinium chloride were similar to both dynamic and vehicle controls with no significant differences (Figure 8.3).

The higher dose, 1mM of gadolinium chloride, noticeably changed the final shape of the distal femur in the frontal view (Figure 8.2P). Both femoral condyles appeared merged together with no clear sign of separation. The medial and lateral condyles showed a posterior curl similar to dynamic controls, however, for the lateral condyle this was not as defined as previously seen (Figure 8.2Q & S). The shape of the tibia was also noticeably different, with no clear sign of the anterior tibial crest or tibial plateau (Figure 8.2R). The average size of the joint regions following the high dose of blocking agent were similar to those measured in other groups, with only the average depth of the medial condyle and tibia significantly smaller than vehicle controls and the low dose group (Figure 8.3A &C).

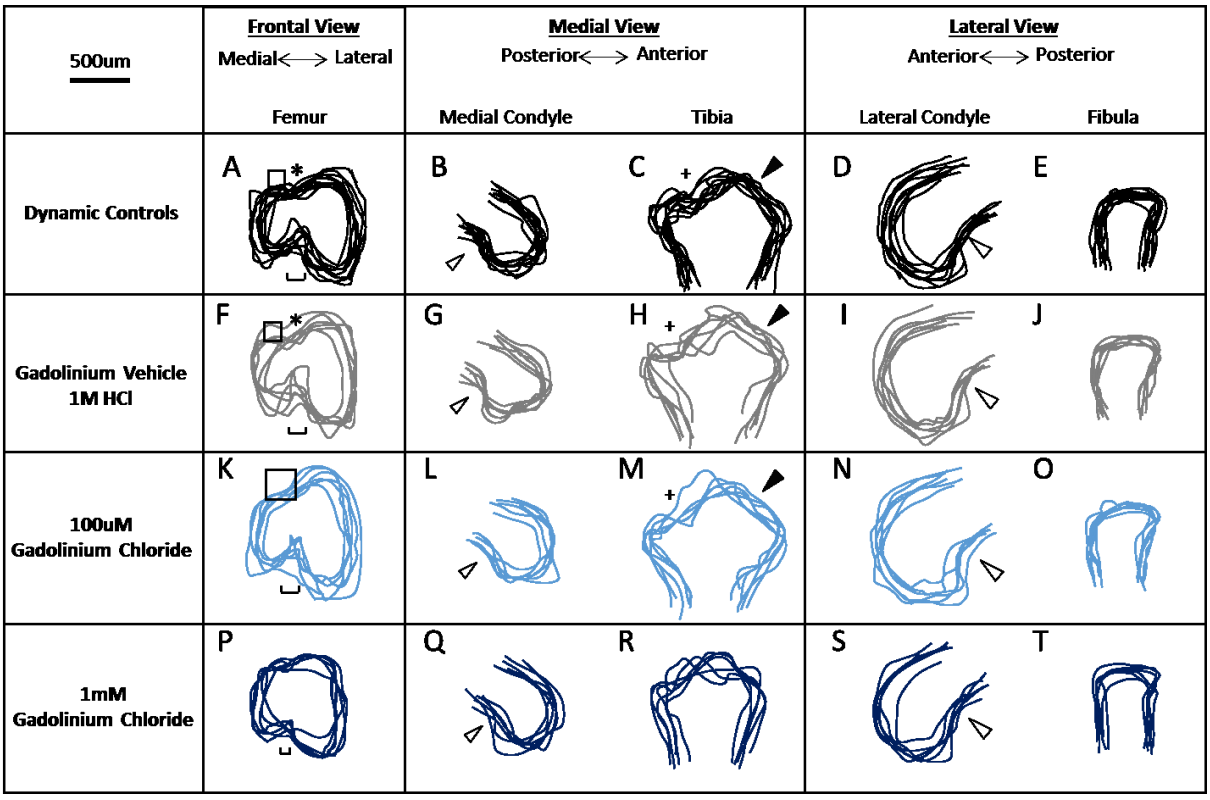


Figure 8.2: The shape profiles of the distal femur and tibia were most affected following the administration of gadolinium chloride. Shape profiles for each joint region were overlaid for each group and analysed for characteristics of joint shape development. Dynamic controls (n=10), gadolinium vehicle (n=6), 100uM gadolinium chloride (n=6), 1mM gadolinium chloride (n=6). Squares: dominance of the lateral condyle over the medial condyle; hollow arrows: posterior curl of condyles seen in moved explants; * dorsal groove between the two femoral condyles; single edged bars: intercondylar fossa; + concave curve of the tibial plateau; filled arrows: anterior tibial crest.

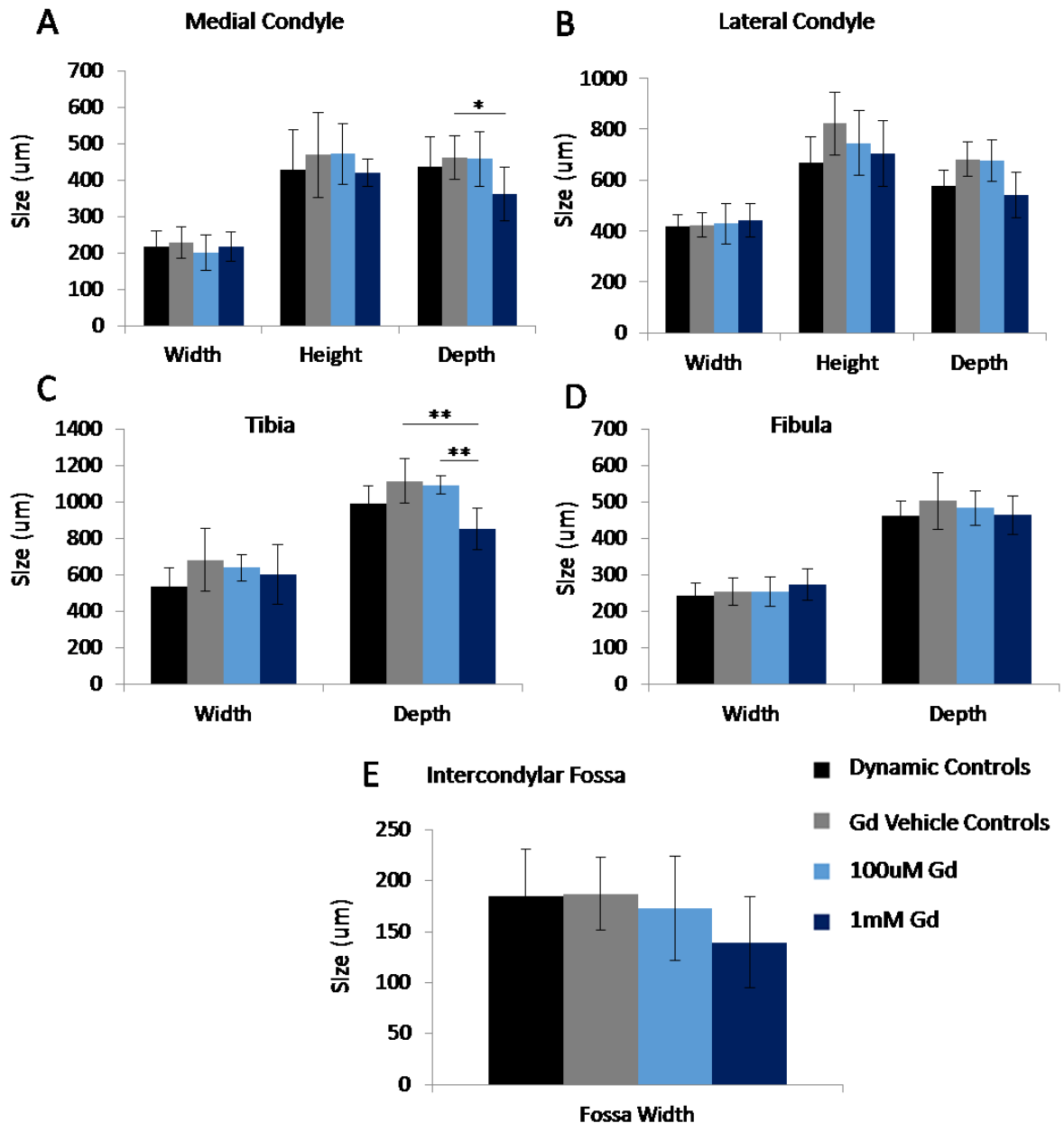


Figure 8.3: Blocking of stretch activated ion channels reduced the average size of joint regions following a high dose of 1mM gadolinium chloride. Bars represent the mean joint region size. Dynamic controls (n=10), gadolinium vehicle (n=6), 100uM gadolinium chloride (n=6), 1mM gadolinium chloride (n=6). Error bars represent the standard deviation. *p-values < 0.05, **p-values < 0.01.

8.3.2 Effect of Blocking Calcium Ion Channels

Using DMSO as a vehicle for nifedipine had little effect on joint shape in the medial and lateral views of the joint (Figure 8.4G-J). However, a difference was noticed in the frontal view of the distal femur. Separation of the femoral condyles was more varied and the shape of the intercondylar fossa was shallower in vehicle controls compared to dynamic controls suggesting some loss of shape definition on the ventral side (Figure 8.4F). The dorsal groove on the superior side appeared as in dynamic controls. Other characteristics of normal joint development including the posterior curl of the femoral condyles, the formation of the anterior tibial crest, tibial plateau and flattened profile of the fibula were all similar in vehicle controls and dynamic controls (Figure 8.4G, H, I & J). An increasing trend in average medial condyle, lateral condyle, tibia and fibula joint regions was seen in vehicle controls compared to dynamic controls, although these were not statistically significant (Figure 8.5) except for lateral condyle height which was significantly larger in vehicle controls compared to dynamic controls (Figure 8.5B).

Separation of the femoral condyles was further obscured following the administration of 100μM nifedipine, with both the intercondylar fossa and dorsal groove difficult to distinguish in the frontal femoral shape profiles compared to both control groups (Figure 8.4K). The shape of the medial condyle also appeared to be affected by blocking the calcium ion channels, with no posterior curl evident and a flattened articular end compared to controls (Figure 8.4L). The shape profile of the tibia was also different with no distinguishable tibial plateau in some explants (Figure 8.4M). The lateral side of the joint appeared unaffected with similar shaped lateral condyles and fibulas compared to control groups (Figure 8.4N & O). No differences in joint region size were found following a low dose of nifedipine compared to either vehicle controls or dynamic controls (Figure 8.5).

The high dose, 1mM nifedipine, considerably affected joint shape development. The distal femur appeared very simplified with no clear definition of each individual femoral condyle in the frontal view (Figure 8.4P). The width of the medial condyle was significantly smaller compared to vehicle

controls with a difference of 35% (Figure 8.5A). The medial view of the joint also revealed the posterior curl of the medial condyle was missing (Figure 8.4Q) and concave tibial plateau profile had reduced in definition (Figure 8.4R). The formation of the anterior tibial crest was present and appeared as seen in control groups. The lateral view of the joint did not reveal any major differences in joint shape (Figure 8.4S & T). Several joint regions were measured to be significantly smaller following a high dose of calcium ion channel blocker compared to vehicle controls. These included medial condyle width and height (Figure 8.5A), lateral condyle height and depth (Figure 8.5B), tibial width and depth (Figure 8.5C) and the width of the intercondylar fossa (Figure 8.5E).

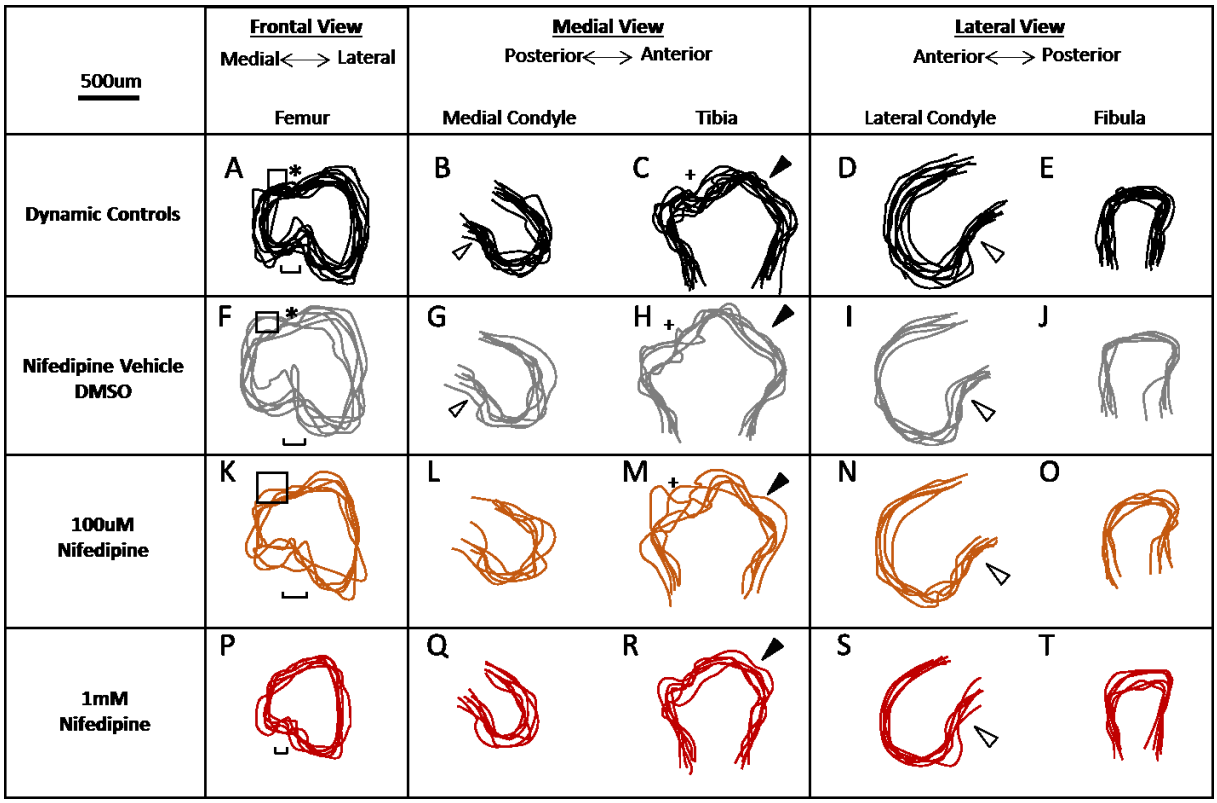


Figure 8.4: The shape profiles of the distal femur, medial condyle and tibia were most affected following the administration of nifedipine. Shape profiles for each joint region were overlaid for each group and analysed for characteristics of joint shape development. Dynamic controls (n=10), nifedipine vehicle (n=6), 100uM nifedipine (n=5), 1mM nifedipine (n=5). Squares: dominance of the lateral condyle over the medial condyle; hollow arrows: posterior curl of condyles seen in moved explants; * dorsal groove between the two femoral condyles; single edged bars: intercondylar fossa; + concave curve of the tibial plateau; filled arrows: anterior tibial crest.

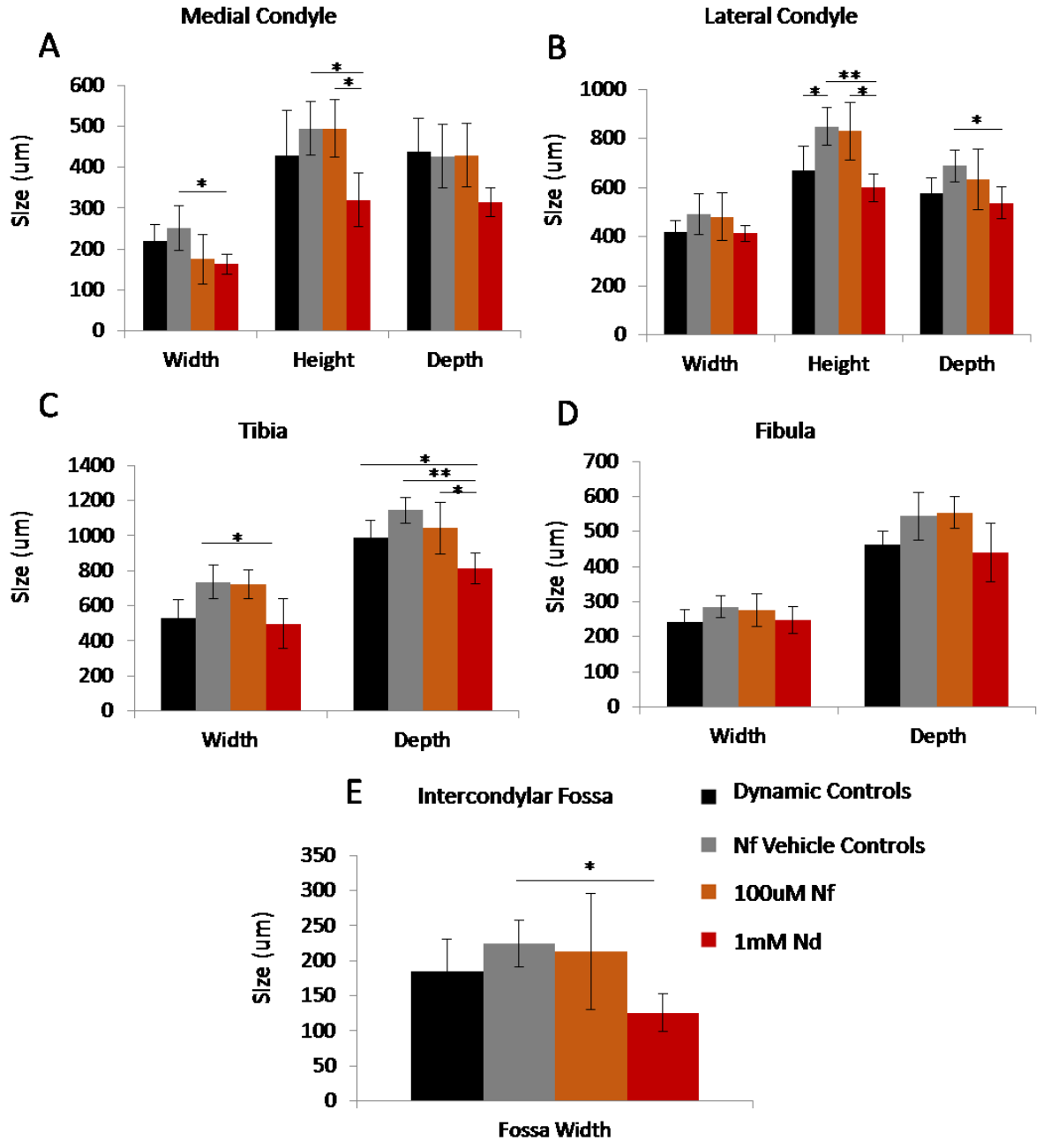


Figure 8.5: Blocking of L-type calcium ion channels reduced the average size of joint regions following a high dose of 1mM Nifedipine. Bars represent the mean joint region size. Dynamic controls (n=10), nifedipine vehicle (n=6), 100uM nifedipine (n=5), 1mM nifedipine (n=5). Error bars represent the standard deviation. *p-values < 0.05, **p-values < 0.01.

8.3.3 Comparison of Blocked Ion Channels

The joint shape profiles from both high dose group were compared to evaluate differences between the action of stretch activated ion channels and L- type calcium ion channels during joint shape development. The distal femur was similar in shape following the addition of gadolinium chloride and nifedipine (Figure 8.6F & K). Both femora showed a narrowed distal femur in the frontal view with a lack of separation on the superior surface and a reduced intercondylar fossa. In both cases, the tibial plateau was also missing (Figure 8.6H & M). The lateral side of the joint appeared unaffected in both groups, matching the shape profiles of dynamic controls and displaying all the normal features of joint shape development (Figure 8.6I, J, N & O). The only differences between the two high dose groups was that the posterior curl of the medial condyle was affected following 1mM nifedipine alone (Figure 8.6L), whereas the tibial plateau was only affected following 1mM gadolinium chloride (Figure 8.6H). The average joint region sizes between the two high dose groups were also similar to each other and to dynamic controls, with a single significant difference in average tibial depth between dynamic controls and 1mM nifedipine as previously reported (Figure 8.7C). No significant differences were found between the two high dose groups (Figure 8.7). Overall, it was determined that both high dose groups were affected equally by the blocking of stretch activated ion channels and L-type calcium ion channels.

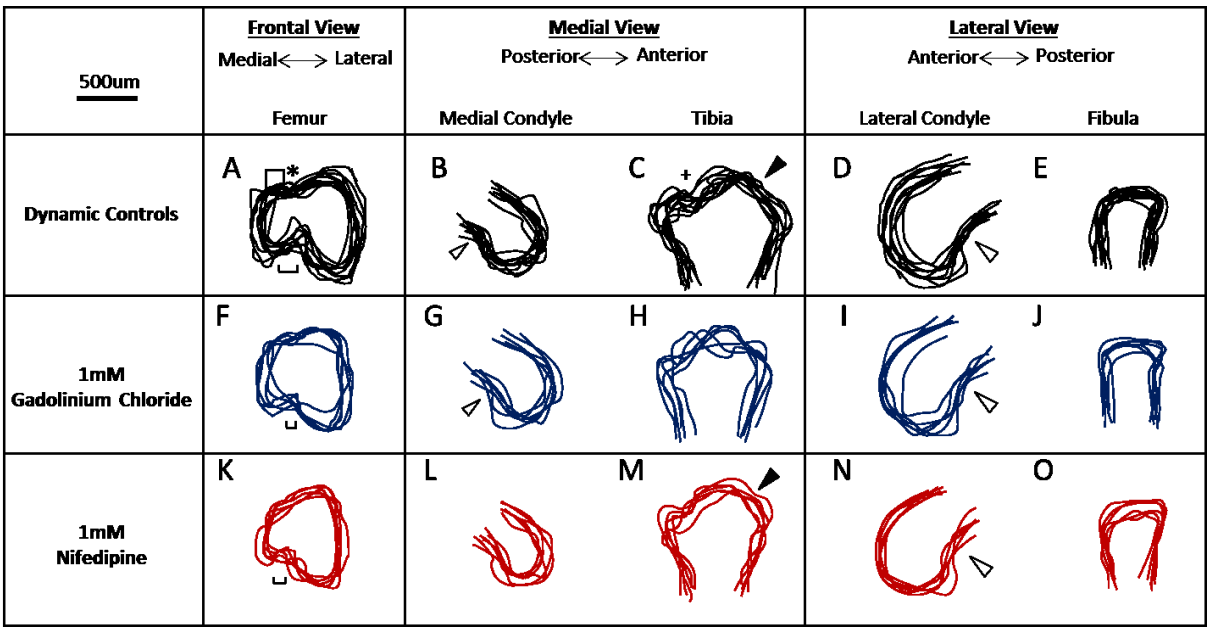


Figure 8.6: Joint shapes were equally affected when cultured with a high dose of nifedipine and a high dose of gadolinium chloride compared to dynamic controls. Shape profiles for each joint region were overlaid for each group and analysed for characteristics of joint shape development. Dynamic controls (n=10), 1mM gadolinium chloride (n=6), 1mM nifedipine (n=5). Squares: dominance of the lateral condyle over the medial condyle; hollow arrows: posterior curl of condyles seen in moved explants; * dorsal groove between the two femoral condyles; single edged bars: intercondylar fossa; + concave curve of the tibial plateau; filled arrows: anterior tibial crest.

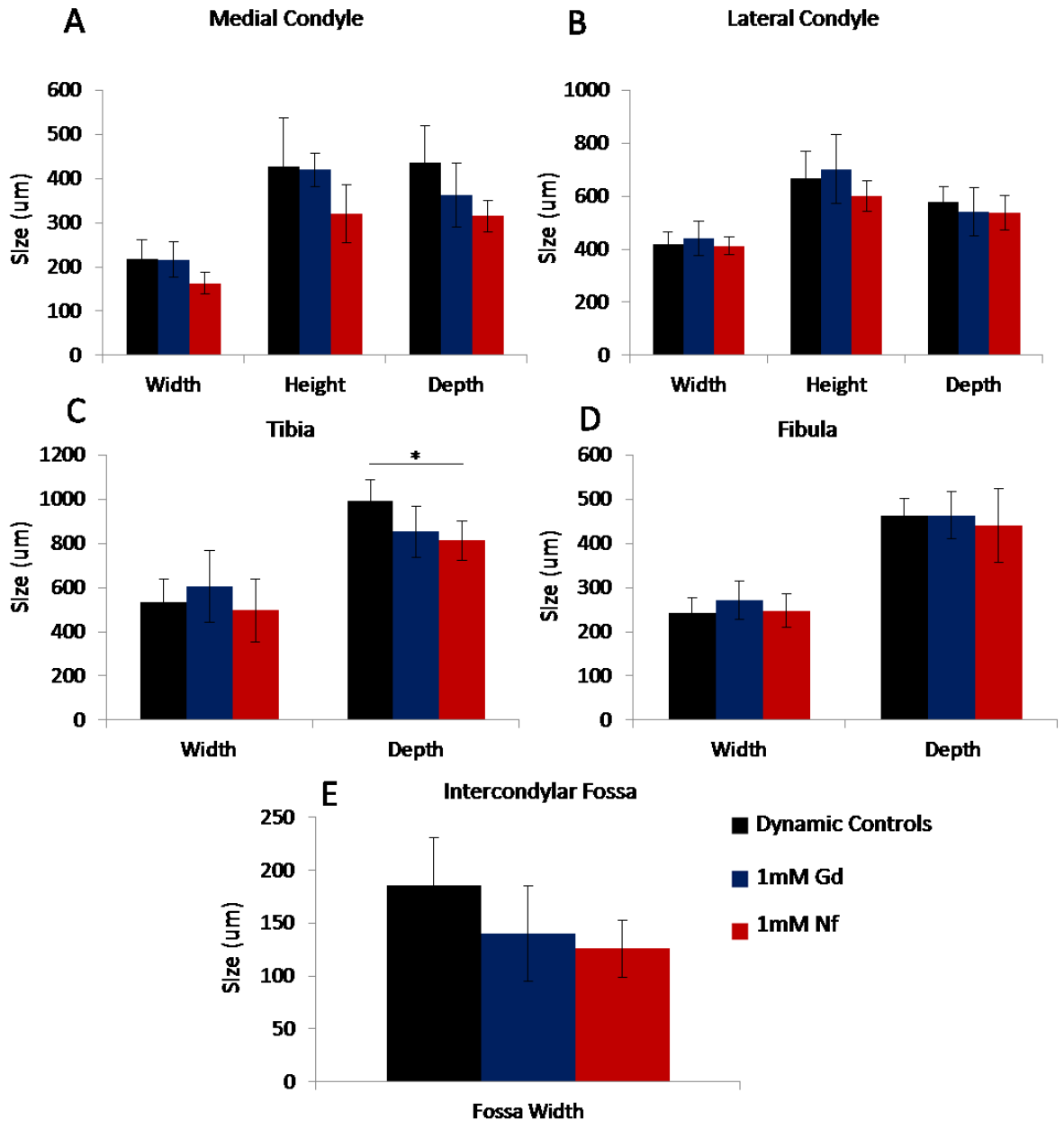


Figure 8.7: Joint region sizes were equally affected by a high dose of either gadolinium chloride (Gd) or nifedipine (Nf). Bars represent the mean joint region size. Dynamic controls (n=10), 1mM gadolinium chloride (n=6), 1mM nifedipine (n=5). Error bars represent the standard deviation. *p-values < 0.05, **p-values < 0.01.

8.4 DISCUSSION

In this chapter, it was attempted to block mechanosensitive ion channels that may be involved in mechanotransduction and regulation of joint morphogenesis. Blocking agents were added into dynamic cultures of the chick hindlimb to block the function of either stretch activated ion channels or L-type calcium ion channels for a period of six days. In both studies, the shape of the knee joint was altered compared to dynamic and vehicle controls where no blocking agents were added. A major difference was found in the frontal shape profile of the distal femur with no clear separation between the two femoral condyles, suggesting medial to lateral development was most affected when either stretch activated ion channels or calcium ion channels were blocked. The posterior curl and appearance of the medial condyle, emergence of the anterior tibial crest and shape of the tibial plateau were also affected when either ion channel was blocked. In both cases, joint shapes were considered under-developed compared to the control groups. Previously, it was shown that joints developed under static conditions were also under-developed compared to those cultured with dynamic stimulation (Chandaria et al., 2016). Explants cultured in the current study with a high dose of either gadolinium chloride or nifedipine showed similar joint shape characteristics to joints cultured under static conditions. Differences were consistently found on the development of the medial condyle and tibia when ion channels were blocked and in previous static cultures (Chandaria et al., 2016), suggesting that the inactivity of the selected ion channels removed the progressive effect of dynamic stimulation in developing explants. These studies therefore provide evidence for the involvement of both stretch activated ion channels and L-type calcium channels in mechanotransduction of joint morphogenesis.

The results of these studies have highlighted that the blocking agents administered during culture affect joint shape development in the presence of applied movement. However, since no analyses were performed to assess the performance of the ion channel blockers during these experiments, it was unknown whether the ion channels were completely or partially blocked. This means the differences observed in joint shape could not be directly linked to the inactivity of these ion

channels. However, since both blocking agents have repeatedly been used to block the activity of stretch activated ion channels and calcium ion channels in chondrocyte cultures (Guilak et al., 1999, Wu and Chen, 2000, Yellowley et al., 2002, Mouw et al., 2007), it was assumed that they were operating in the same way in these tissue explants. Methods to monitor ion movement, such as live calcium ion imaging (Yellowley et al., 2002), and measuring of membrane potentials, using patch-clamp techniques are challenging to reproduce in explant tissues making it extremely difficult to know if these concentrations were sufficient to block all ion channel activity. Another limitation of this study was that two different solvents were used to administer each block agent. This made it difficult to compare the effects of each blocking agent, especially since a slight increase in trend for some joint region measurements were observed for each vehicle solvent. The impact of these vehicle solvents was reversed in both studies when the blocking agent was included limiting this side effect, giving confidence that the results observed were indeed due to the action of the blocking agent rather than an amplified effect of the vehicle used. Finding a single vehicle solvent that can be used to administer either blocking agent would be a great improvement to this study. To fully complete the analysis, the blocking agents should also be tested on static cultures. If no differences are observed in static culture with and without the blocking agents, it would further strengthen the argument that mechanosensitive ion channels are involved in sensing and transducing mechanical stimuli for joint morphogenesis. A combined study where both blocking agents are administered together at the higher dose would also be of interest for future studies to investigate if there is a cumulative effect on joint shape development.

Since no literature was found in which mechanosensitive ion channels were blocked in whole tissue explants, it was difficult to evaluate the findings of this chapter against other research. The results do, however, compare with results of chondrocyte culture studies in which mechanosensitive ion channels were blocked whilst dynamic stimulation was applied. Mechanical stimulation of chondrocytes was shown to increase the intracellular calcium ion concentration (Guilak et al., 1999, Yellowley et al., 2002, Mouw et al., 2007), which normally triggers the secretion of growth factors (Wong and Carter, 2003). In the presence of gadolinium,

this increase was seen to vanish (Guilak et al., 1999, Yellowley et al., 2002), suggesting the influx of calcium ions through stretch activated ion channels was disrupted. This would also mean the release of growth factors would be affected. The reduction of medial-lateral growth seen in the distal femur in this study when stretch activated ion channels were blocked could possibly also be due to a decrease of calcium ion influx and release of growth factors. Mechanically induced proliferation, differentiation and ECM synthesis has also been reported to decrease in the presence of gadolinium (Wu and Chen, 2000, Chowdhury and Knight, 2006). A reduction in these cellular processes was also reported in the presence of nifedipine (Wu and Chen, 2000, Chowdhury and Knight, 2006, Mouw et al., 2007). This suggests a role for both stretch activated ion channels and L-type calcium ion channels in regulating these processes. A reduction in cell proliferation, differentiation and ECM synthesis are plausible scenarios for the reduced development of the knee joint presented in this study.

The aim of this work was to test whether the actions of stretch activated ion channels and voltage-gated calcium ion channels are involved in the mechanotransduction and regulation of joint shape development. Following a dynamic movement regime known to stimulate joint morphogenesis *in vitro*, the distal femur in the embryonic chick knee joint was found to be abnormally shaped when either candidate ion channels was blocked appearing similar to previously reported statically cultured joints. These results agree with previous findings that show both stretch activated ion channels and calcium ion channels are involved in transducing signals for cartilage growth, and furthermore provide new evidence to support the hypothesis that mechanical cues that direct localised joint shape development and organisation are transduced through the function of these channels. Further work can now be carried with confidence that these ion channels do play a function role in the mechanoregulation of joint morphogenesis.

CHAPTER 9

9 GENERAL DISCUSSION

9.1 INTRODUCTION

There is significant evidence to show that prenatal joint morphogenesis is sensitive to mechanical stimulation as reviewed in Chapter 2. Previous studies have managed to convincingly show that the reduction of spontaneous movement during development can severely impact the process of synovial joint formation with abnormalities appearing during both joint cavitation and morphogenesis. These studies highlight the sensitivity of synovial joint formation to the mechanical environment, but do not explore the relationship between mechanical stimulation and joint morphogenesis. This doctorate targeted this gap in scientific knowledge and explored how variations in quantified movements of a developing joint impacted its final shape and geometry. The research presented in this thesis investigated the quantitative relationship between joint morphogenesis and mechanical stimulation through three independent studies testing the following hypotheses:

- Dynamic stimulation leads to a more developed joint shape than static conditions.
- Joint shape development is affected by movement magnitude in a dose dependent manner.
- The most physiological movement regime leads to a joint with the most normal progression of shape morphogenesis.

- Mechanical stimuli that direct localised joint shape development are transduced through the function of mechanosensitive ion channels.

The results of these studies agreed with these original hypotheses and led to three major outcomes which are summarised and discussed below. These studies were not without limitations, which are also discussed along with potential avenues for further research to expand on the knowledge gained through the individual investigations.

Understanding how localised patterning of emerging joint structures is affected by changes in developmental conditions, such as movement, is important for a variety of research areas. Knowledge of how different levels of movement alter normal joint shape development could potentially lead to the development of diagnostic criteria to identify patients at risk of developing congenital joint malformations. This thesis has provided important understanding about the aetiology of congenital joint abnormalities showing that the relationship between prenatal movements and joint shape development is complex. Knowledge of how these critical anatomical structures are formed is also important for researchers trying to regenerate damaged and degraded tissues in patients with conditions such as OA. Tissue engineers are currently trying to develop functional cartilage tissue from stem cells or progenitor cell populations and it has been proposed that replicating the effects of mechanical stimulation during embryogenesis may be required to achieve this aim (Foster et al., 2015). This research provides useful cues to the cartilage tissue engineering field, in demonstrating that replicating the magnitude of physiological fetal movements leads to the most normal progression of cartilage growth.

9.2 Outcomes and Contributions

The research presented in this thesis focused on the role of movement in directing joint morphogenesis of the embryonic chick knee joint. The first major outcome of this doctorate was the creation of a novel culture system that allowed the embryonic chick hindlimb explant to develop *in vitro* whilst quantified physiological movement patterns could be applied to the knee joint. Previously, researchers explored the influence of mechanical stimulation in synovial joint

formation using both *in vitro* and *in vivo* animal models where natural embryonic movements were either reduced or inhibited. In these studies, it was repeatedly shown that the process of prenatal joint formation was abnormal with cases of fusion between opposing rudiments (Fell and Canti, 1934, Lelkes, 1958, Drachman and Sokoloff, 1966, Osborne et al., 2002), and the loss of articular joint morphology (Roddy et al., 2011b, Nowlan et al., 2014, Brunt et al., 2016). Whilst providing evidence to support the theory that mechanical stimulation is crucial to normal joint development, these studies could not characterise or quantify the relationship between the level of mechanical stimulation experienced and joint shape development. The newly created culture system addressed this limitation and was designed to apply controlled magnitudes of flexion to the embryonic chick knee joint following a predetermined regime, thus providing a novel methodology to explore how different movement patterns affect synovial joint formation.

The culture system was used to apply a passive physiological flexion movement to the developing chick knee joint which was considered more appropriate than applying a force or deformation to the tissue explant. Other bioreactor systems have applied hydrostatic pressure, compressive deformations and shear loading to tissue explants and 3D chondrocyte cultures to also explore the influence of mechanical stimuli on development (Pörtner et al., 2005, Henstock et al., 2013, Smith et al., 2013, Foster et al., 2015). However, when these stimuli are applied *in vitro,* they cannot be easily compared to natural developmental conditions. Movement of the joint *in vitro* and *in vivo* are more comparable making it a better variable to characterise with the progression of joint formation. Using joint movement also makes the studies performed during this doctorate relatable to real life scenarios where fetal movements can be monitored.

The ability to successfully culture developing joint explants using this system led to the second major outcome of this research. This was the characterisation of the effects of movement magnitude on joint morphogenesis. The differences in knee joint shapes from static and dynamic cultures were similar to those previously described for *in ovo* paralysis studies giving confidence in the performance of the culture system. The joint shapes produced were compared with the

sequence of normal morphological shape changes recorded for the chick knee joint, and supported the hypothesis that dynamic stimulation would lead to a more developed joint shape than static conditions with more anatomical features present after culture. The developing chick knee joint was subsequently cultured under a range of flexion magnitudes. This study provided the first understanding of the relationship between mechanical stimulation and joint morphogenesis and supported the hypothesis that joint shape development would be affected by movement magnitude in a dose dependent manner. The results of this study revealed that movements most similar to physiological magnitudes produced the most advanced joint shapes when compared to the sequence of normal morphological shape changes. Joint shapes developed under magnitudes of movement below the physiological range were similar to those cultured under static conditions. Joint shapes developed under magnitudes of movements greater than the physiological range were inconsistent and showed some irregularities, but still advanced joint shape development. These results suggest a bell-shaped relationship between movement magnitude and joint shape development supporting the hypothesis that the most physiological movement regime would lead to a joint with the most normal progression of shape morphogenesis (Figure 9.1). This new theorised relationship sits above a threshold of joint shape development that occurs naturally even in the absence of external joint movements and is skewed in the positive direction around an optimal magnitude of movement.

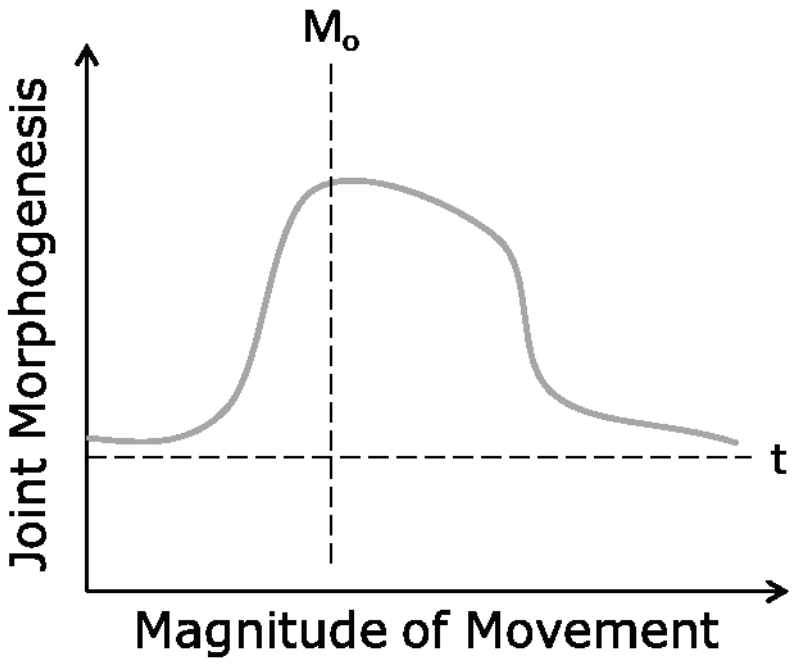


Figure 9.1: Following the studies of this thesis, a new theorised relationship between the magnitude of movement and joint morphogenesis during development is hypothesised. This includes a non-linear dose dependent bell-shaped curved which sits above a threshold, 't', and is skewed around an optimal magnitude of movement, 'M_o'.

In this study, the final joint shape after six days of culture was used as the primary means of measuring the progression of joint development. However, there are a range of other approaches which could also be used to measure the development of the tissue explants *in vitro*. Differences in joint shape occur due to changes in cellular activities such as proliferation, differentiation and migration. Cell proliferation has already been linked with localised areas of growth within the embryonic knee joint (Roddy et al., 2011a) and was seen to increase in the distal femur when flexion at and above the physiological range was applied during studies performed as part of this doctorate. Quantification of proliferation following different magnitudes of movement was performed during this doctorate, but further investigation into other cellular processes, such as differentiation or migration, could uncover potential changes responsible for the different joint shapes observed. Differentiation and the process of chondrogenesis can be used a measure of development by quantifying chondrogenic and hypertrophic markers as performed by Saha et al.

(2016). Quantifying the localised proliferation and differentiation patterns along with the ECM composition for different levels of mechanical stimulation could, together with the joint morphology data, reveal how the process of morphogenesis is changing in each scenario presented in this thesis. This research also opens new avenues to explore the signalling and mechanotransduction of these cellular activities. Previous research has shown that activity of the BMP, Wnt and Hedgehog signalling families are associated with processes of synovial joint formation such as interzone formation, differentiation, proliferation and ECM production, and are disturbed following changes in mechanical stimulation (Roddy et al., 2011b, Rolfe et al., 2014, Brunt et al., 2017, Salva and Merrill, 2017). The experiments performed during this doctorate can be repeated to explore the correlation between gene expression, matrix composition, cellular activity and joint morphology shedding light onto how morphogenesis is regulated and what signals are needed for normal joint development.

A range of joint shape changes following different movement regimes have been described in this thesis. Knowledge of how the geometry of the joint changes following different developmental conditions is important to understand how abnormal fetal movements lead to congenital joint malformation conditions, such as DDH, which impairs joint stability and affects the normal range of motion. Although each joint was developed *in vitro,* it is interesting to compare how the differences in joint features might impact the kinematics to predict how these shape changes may affect joint function. Description of the femoral articular surfaces from human cadaveric specimens have previously been used to describe the motion of the knee joint (Martelli and Pinskerova, 2002, Freeman and Pinskerova, 2005). However, the complicated 3D surfaces involved make this a difficult prediction. Flatter condyle surfaces have been suggested to increase translation capability, whereas increased condyle curvature suggests more freedom for rotation, either about the transverse axis representing flexion or rotation about the vertical axis representing internal and external rotation (Martelli and Pinskerova, 2002). In the human knee, the shapes of the femoral condyles are often described by a medial and lateral circle that fits the radius of the posterior portion of each condyle in the sagittal plane (Kurosawa et al., 1985,

Martelli and Pinskerova, 2002, Williams and Logan, 2004). In the results of this study, the posterior curls of the medial and lateral condyle were missing in joints cultured under reduced-flexion and static conditions, suggesting a smaller posterior condyle radius, and therefore a reduced capacity for flexion. This is not that surprising since these joints had experienced less flexion during development than those which developed large posterior curls. It is then interesting to ask, whether synovial joints are shaped for movements they have experienced during the developmental period and therefore, whether all joint motions are needed to create a fully functional joint. It is important to remember the differences in anatomy between the chick and human knee joint, and take caution when comparing joint function based on human kinematics and chick anatomy. However, by using the system developed for another animal model system (such as developing mouse limbs for example), it would be possible to further explore this hypothesis. Eventually, this research could form a bridge between the role of fetal movements and functional development of the knee joint.

The third major outcome of this doctorate was the identification that mechano-sensitive ion channels are involved in the regulation of joint morphogenesis. This was the first study to test the action of stretch activated and calcium ion channels during joint shape development in complete embryonic tissue explants. Following the administration of either ion channel blocker, both joint shape and size were affected giving evidence that the flux of ions through stretch activated and calcium channels are involved in signalling joint morphogenesis. This data supported the hypothesis that mechanical stimuli that direct localised joint shape development are transduced through the function of mechano-sensitive ion channels. The research contributes to the field of cartilage mechanobiology by demonstrating that ion channel function also affects cartilage organisation on the tissue scale as well as the cellular scale.

The cell membrane has long been identified as the site where mechanoreceptors form and function (Mobasheri et al., 2002). In cartilage, chondrocytes sense and respond to their mechanical environment through deformation of the ECM or changes in its molecular and ionic

composition. Chondrocytes are equipped with an array of mechanoreceptors including ion channels, primary cilia and integrins (Mobasheri et al., 2002, Millward-Sadler and Salter, 2004, McGlashan et al., 2006). Changes in intracellular and extracellular ion concentrations, integrin activation and bending of primary cilia have all been linked to various cellular activity including proliferation, differentiation and ECM production highlighting their involvement in chondrocyte mechanotransduction (Hirsch et al., 1997, Mobasheri et al., 2002, Shao et al., 2012). Primary cilia protrude from the cell membrane into the ECM and are equipped with integrins to interact with ECM molecules (McGlashan et al., 2006). The structure of primary cilium is mechanically sensitive with evidence of its length changing in response to mechanical deformation (McGlashan et al., 2010). Integrins connect the cell surface to ECM components, such as collagen and fibronectin, and mediate signals between the two through ligand and integrin binding (Millward-Sadler and Salter, 2004). Antibodies can be used to block the availability of either ligands or integrins to form new attachments (Millward-Sadler and Salter, 2004), however, this often causes apoptosis in cell culture (Hirsch et al., 1997, Mobasheri et al., 2002) which could lead to the destruction of tissue explants like those used in this doctorate. Stretch activated ion channels and L-type calcium ion channels were chosen to be investigated in this doctorate due to ease and established methodology of blocking their function in culture. As a pioneering study into mechanotransduction in embryonic explants this was the most sensible option. Further studies are still needed to fully understand the mechanobiology of cartilage and the associated pathways involved during skeletogenesis. It is very plausible that primary cilia, integrins and mechanosensitive ion channels all work in synergy to form a complex network of mechanoreceptors to regulate signalling events involved in embryonic joint formation. Further investigation into this exciting field will reveal important signalling relationships and lead to the identification of specific signalling pathways involved in joint development.

The results presented throughout this thesis are summarised in Figure 9.2 using the series of morphological events that were characterised for normal development of the chick knee joint as a reference. Morphological events that were disrupted are highlighted for the different

developmental conditions employed including static conditions, reduced-flexion, average-flexion, over-flexion and the blocking of both stretch activated ion channels and L-type calcium ion channels. The data gathered during this doctorate offers a unique insight into the anatomical shape development of the chick knee joint, which contributes to the field of developmental mechanobiology.

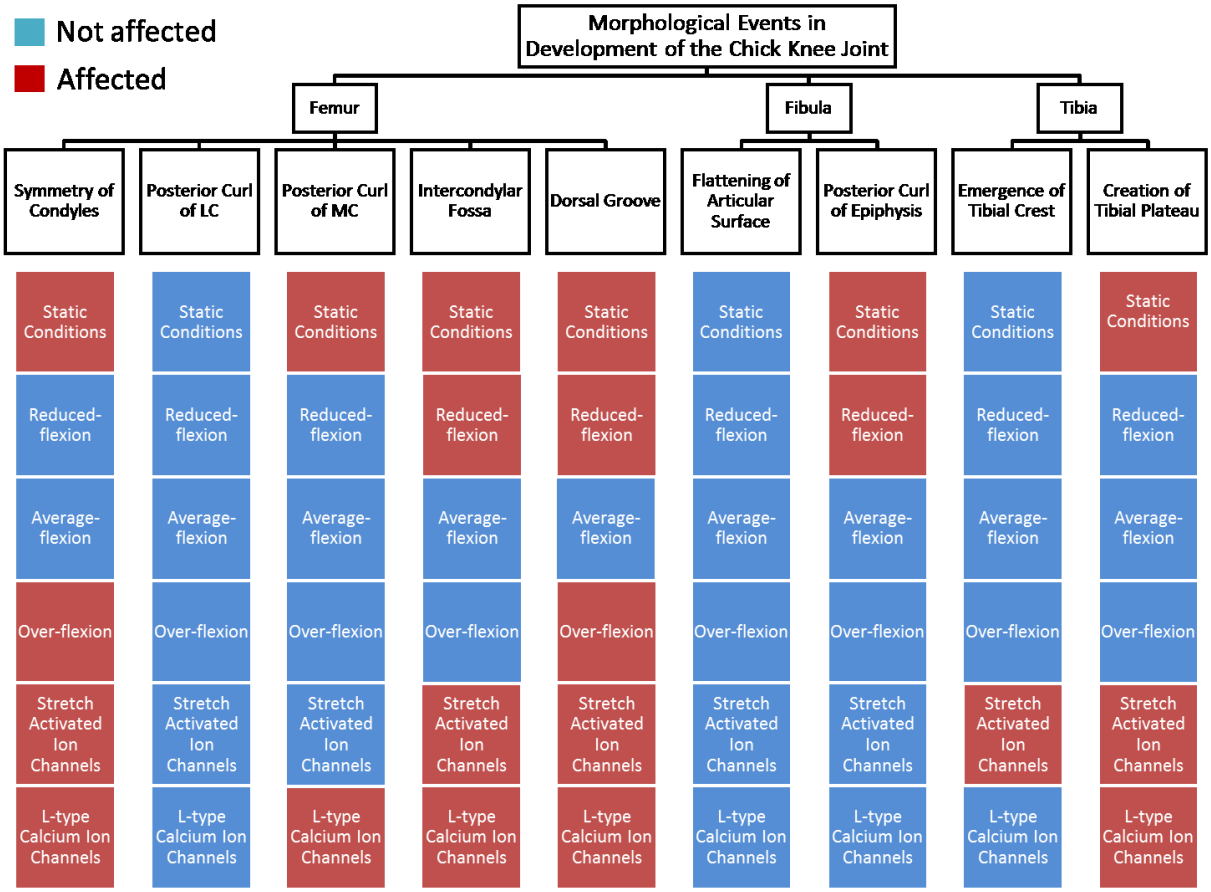


Figure 9.2: Several morphological events were affected during embryonic chick knee joint development when the mechanical conditions were altered except under average-flexion for which all events were unaffected. Morphological events that were unaffected are highlighted in blue and those that were affected are highlighted in red.

9.3 LIMITATIONS AND FURTHER WORK

A common theme throughout this thesis was the comparison of 2D shape profile outlines to qualitatively assess differences in joint shape from 3D reconstructed models. This meant the assessment of differences in joint shape were subjective. Quantitative analysis could be applied where each outline is converted into X-Y co-ordinates and compared using principal component analysis and a non-parametric MANOVA to reveal significant differences in joint shapes between groups as recently implemented by Brunt et al. (2016). However, this would only verify differences already observed when the 2D profiles are overlaid. A better approach would be to use 3D statistical shape analysis to compare anatomical landmarks between 3D models. In order to do this, all 3D models need to be aligned to remove the effect of location and rotation of each rudiment (Stegmann and Gomez, 2002). Using image registration techniques this is easily accomplished using dedicated software packages. During this doctorate, image registration was trialled, however, natural variations in each joint shape meant that once aligned and superimposed, the joints were extremely distorted which often resulted in a loss of resolution of fine shape characteristics. Due to these reasons, it was decided to continue with the 2D shape profiles which meant each joint region could be aligned individually in different views. Following the criteria set out in Chapter 3 to align each joint into the resting position, joint shape profiles were consistently grouped together in frontal, medial and lateral views showing this method was robust and repeatable.

Another theme of this work was that the evaluation of joint morphogenesis progression was based on the final joint shape for each explant at the end of the culture period. No data was collected to investigate the change in shape during the culture period itself. To do so, would provide even further knowledge about the process of joint shape development, but would require a considerably higher number of specimens to analyse after different time points of development. Analysis of the final joint shape did, however, identify differences in joint morphology for different mechanical conditions suggesting differences in the process of joint morphogenesis. The

mechanical conditions known to cause these differences can now be further explored at different time points and also at the cellular scale with confidence of identifying differences in both tissue structure and cellular activity during development. A proposed method to advance this would be to create a 4D imaging station similar to that created by Boot et al. (2008), in which explants can be removed from the bioreactor chambers each day and scanned using OPT without terminating development. This would allow for the capture of spatial and topographical information about the developing hindlimb over the whole culture period.

The effect of the timing regime used to apply dynamic movements was never investigated during the course of this doctorate which poses another drawback to this research. Explants were stimulated constantly for two hours, three times per day at the same displacement rate, with only the magnitude of movement being altered. This meant that the number of movements experienced within a two hour activity window differed for each magnitude of movement. To understand the implications of this, another study would be needed to characterise the effect of movement frequency and number of movements experienced. Repeating the average-flexion regime from Chapter 7, the frequency of movements could be adjusted to test if the number of movements experienced during an activity window affects joint morphogenesis. Changing the frequency of movements would mean explants would be moved at different rates and adjusting the number of movements would mean the activity and rest periods would differ. Further improvements can also be made to the culture system. As previously mentioned, the action of applying compression to the explants circulates the culture media improving nutrient delivery. Adding a perfusion system to the bioreactor would be an ideal way to ensure the culture media is fully mixed at all times in both static and dynamic cultures. The compressive plates used to push the foam supports could also be redesigned to grip the foam support and apply both a compressive and tensile displacement. This may potentially induce both a flexion and extension movement to the knee joint relative to the resting position.

Finally, to fully appreciate the role of mechanical stimuli during joint morphogenesis, a computational model of the experimental setup would be needed. Using geometric models of uncultured knee joints, a simulation of the explants during a flexion motion can be applied to predict the distribution of mechanical stress and strain across the joint region. This would add detailed quantitative data to the relationship between joint morphogenesis and mechanical stimuli. This would build on previous mechanobiological models of joint morphogenesis (Giorgi et al., 2014), which can be validated against the experimental results and lead to a more accurate picture of the mechanics involved during joint development.

9.4 CONCLUSIONS

This research has advanced the basic understanding of prenatal joint morphogenesis and highlighted how specific mechanical parameters can alter the progression of joint shape development. The consensus that mechanical stimuli influence joint morphogenesis has a growing amount of supportive evidence. However, until now, no investigations have been performed to characterise the relationship between joint morphogenesis and mechanical stimulation. This thesis provides, for the first time, details about how joint morphogenesis progression changes with joint movement, providing an innovative insight into the consequences of altered mechanical conditions during development. The results reveal a non-linear, dose dependent relationship which favours an optimal range of movement. Data has also been presented to support the role of mechanosensitive ion channels to transduce and regulate signals from mechanical stimuli needed for joint morphogenesis. These studies have provided a novel insight into joint morphogenesis furthering our understanding of this marvellous phenomenon.

BIBLIOGRAPHY

AbD Serotec. 2016. A Complete Kit for Measuring Apoptosis by Dual Color ImmunoHistoChemistry.

Ahrens, J., Geveci, B. & Law, C. 2005. ParaView: An End-User Tool for Large Data Visualization. *Visualization Handbook*.

Alberts, B., Bray, D., Johnson, A., Lewis, J., Raff, M., Roberts, K. & Walter, P. 1998. *Essential Cell Biology*, Garland Pub.

Archer, C. W., Dowthwaite, G. P. & Francis-West, P. 2003. Development of synovial joints. *Birth Defects Research Part C: Embryo Today: Reviews,* 69**,** 144-155.

ASTM D3574-11, S. 2011. Standard Test Methods for Flexible Cellular Materials - Slab, Bonded, and Molded Urethane Foams. *ASTM International, West Conshohocken, PA.*

Bader, D. L., Salter, D. & Chowdhury, T. 2011. Biomechanical influence of cartilage homeostasis in health and disease. *Arthritis,* 2011.

Bian, L., Zhai, D. Y., Zhang, E. C., Mauck, R. L. & Burdick, J. A. 2011. Dynamic compressive loading enhances cartilage matrix synthesis and distribution and suppresses hypertrophy in hMSC-laden hyaluronic acid hydrogels. *Tissue Engineering Part A,* 18**,** 715-724.

Blackburn, T. A. & Craig, E. 1980. Knee Anatomy: A Brief Review. *Physical Therapy,* 60**,** 1556-1560.

Boot, M. J., Westerberg, C. H., Sanz-Ezquerro, J., Cotterell, J., Schweitzer, R., Torres, M. & Sharpe, J. 2008. In vitro whole-organ imaging: 4D quantification of growing mouse limb buds. *Nature methods,* 5**,** 609-612.

Bronner-Fraser, M. 2008. *Avian Embryology*, Elsevier Science.

Brucker microCT 2011. SkyScan NRecon. Kontich, Belgium.

Brunt, L., Skinner, R., Roddy, K., Araujo, N., Rayfield, E. & Hammond, C. 2016. Differential effects of altered patterns of movement and strain on joint cell behaviour and skeletal morphogenesis. *Osteoarthritis and Cartilage*.

Brunt, L. H., Begg, K., Kague, E., Cross, S. & Hammond, C. L. 2017. Wnt Signalling Controls the Response to Mechanical Loading during Zebrafish Joint Development. *bioRxiv***,** 115105.

Brunt, L. H., Norton, J. L., Bright, J. A., Rayfield, E. J. & Hammond, C. L. 2015. Finite element modelling predicts changes in joint shape and cell behaviour due to loss of muscle strain in jaw development. *Journal of biomechanics,* 48**,** 3112-3122.

Carter, D. R. & Wong, M. 2003. Modelling cartilage mechanobiology. *Philosophical Transactions of the Royal Society B: Biological Sciences,* 358**,** 1461-1471.

Chambers, S., Bradley, N. & Orosz, M. 1995. Kinematic analysis of wing and leg movements for type I motility in E9 chick embryos. *Experimental Brain Research,* 103**,** 218-226.

Chandaria, V. 2013. *The Influence of Biophysical Stimuli on Joint Morphogenesis.* Master of Research, Imperial College London.

Chandaria, V. V., McGinty, J. & Nowlan, N. C. 2016. Characterising the effects of in vitro mechanical stimulation on morphogenesis of developing limb explants. *J Biomech,* 49**,** 3635-3642.

Chowdhury, T. T. & Knight, M. M. 2006. Purinergic pathway suppresses the release of .NO and stimulates proteoglycan synthesis in chondrocyte/agarose constructs subjected to dynamic compression. *Journal of Cellular Physiology,* 209**,** 845-853.

Cohen, I., Robinson, D., Melamed, E. & Nevo, Z. 2005. Use of a novel joint-simulating culture system to grow organized ex-vivo three-dimensional cartilage-like constructs from embryonic epiphyseal cells. *The Iowa orthopaedic journal,* 25**,** 102.

Corsello, G. & Giuffrè, M. 2012. Congenital malformations. *Journal of Maternal-Fetal and Neonatal Medicine,* 25**,** 25-29.

Decker, R. S., Koyama, E. & Pacifici, M. 2014. Genesis and morphogenesis of limb synovial joints and articular cartilage. *Matrix Biology,* 39**,** 5-10.

DiMarco, R. L., Su, J., Yan, K. S., Dewi, R., Kuo, C. J. & Heilshorn, S. C. 2014. Engineering of Three-Dimensional Microenvironments to Promote Contractile Behavior in Primary Intestinal Organoids. *Integrative biology : quantitative biosciences from nano to macro,* 6**,** 127-142.

Drachman, D. B. & Sokoloff, L. 1966. The role of movement in embryonic joint development. *Developmental Biology,* 14**,** 401-420.

Dumont, E. R. 2010. Bone density and the lightweight skeletons of birds. *Proceedings of the Royal Society B: Biological Sciences,* 277**,** 2193.

Ebers Med Tech SL. 2016. *Ebers TC-3 bioreactor* [Online]. Available: http://www.ebersmedical.com/tissue-engineering/bioreactors/load-culture/tc-3 [Accessed 29/09/2016 2016].

Elder, S. H. 2002. Conditioned medium of mechanically compressed chick limb bud cells promotes chondrocyte differentiation. *Journal of orthopaedic science,* 7**,** 538-543.

Elder, S. H., Kimura, J., Soslowsky, L. J., Lavagnino, M. & Goldstein, S. A. 2000. Effect of compressive loading on chondrocyte differentiation in agarose cultures of chick limb-bud cells. *Journal of Orthopaedic Research,* 18**,** 78-86.

Eyal, S., Blitz, E., Shwartz, Y., Akiyama, H., Schweitzer, R. & Zelzer, E. 2015. On the development of the patella. *Development,* 142**,** 1831-1839.

Faller, A., Schünke, M., Schünke, G. & Taub, E. 2004. *The human body: an introduction to structure and function*, Thieme.

Fell, H. B. 1925. The histogenesis of cartilage and bone in the long bones of the embryonic fowl. *Journal of Morphology,* 40**,** 417-459.

Fell, H. B. & Canti, R. G. 1934. Experiments on the Development in vitro of the Avian Knee-Joint. *Proceedings of the Royal Society of London. Series B, Biological Sciences,* 116**,** 316-351.

Fell, H. B. & Robison, R. 1929. The growth, development and phosphatase activity of embryonic avian femora and limb-buds cultivated in vitro. *Biochemical Journal,* 23**,** 767-784.5.

Fisher, J. P., Mikos, A. G. & Bronzino, J. D. 2007. *Tissue Engineering*, CRC Press.

Foster, N. C., Henstock, J. R., Reinwald, Y. & El Haj, A. J. 2015. Dynamic 3D culture: Models of chondrogenesis and endochondral ossification. *Birth Defects Research Part C: Embryo Today: Reviews,* 105**,** 19-33.

Freeman, M. & Pinskerova, V. 2005. The movement of the normal tibio-femoral joint. *Journal of biomechanics,* 38**,** 197-208.

Gilbert, S. F. 2000. Osteogenesis: the development of bones, Developmental Biology. 6th Edition ed. Sunderland (MA): Sinauer Associates.

Giorgi, M., Carriero, A., Shefelbine, S. J. & Nowlan, N. C. 2014. Mechanobiological simulations of prenatal joint morphogenesis. *Journal of Biomechanics,* 47**,** 989-95.

Giorgi, M., Carriero, A., Shefelbine, S. J. & Nowlan, N. C. 2015. Effects of normal and abnormal loading conditions on morphogenesis of the prenatal hip joint: application to hip dysplasia. *Journal of Biomechanics,* 48**,** 3390-3397.

Guilak, F., Zell, R. A., Erickson, G. R., Grande, D. A., Rubin, C. T., McLeod, K. J. & Donahue, H. J. 1999. Mechanically induced calcium waves in articular chondrocytes are inhibited by gadolinium and amiloride. *Journal of orthopaedic research,* 17**,** 421-429.

Haines, R. W. 1942. The tetrapod knee joint. *Journal of Anatomy,* 76**,** 270.

Hall, B. K. 2008. *Fins into limbs: evolution, development, and transformation*, University of Chicago Press.

Hall, B. K. & Herring, S. W. 1990. Paralysis and growth of the musculoskeletal system in the embryonic chick. *Journal of Morphology,* 206**,** 45-56.

Hall, B. K. & Miyake, T. 2000. All for one and one for all: condensations and the initiation of skeletal development. *Bioessays,* 22**,** 138-147.

Hamburger, V., Balaban, M., Oppenheim, R. & Wenger, E. 1965. Periodic motility of normal and spinal chick embryos between 8 and 17 days of incubation. *Journal of Experimental Zoology,* 159**,** 1-13.

Hamburger, V. & Hamilton, H. L. 1951. A series of normal stages in the development of the chick embryo. *Journal of morphology,* 88**,** 49-92.

Heegaard, J. H., Beaupré, G. S. & Carter, D. R. 1999. Mechanically modulated cartilage growth may regulate joint surface morphogenesis. *Journal of Orthopaedic Research,* 17**,** 509-517.

Henstock, J. R., Rotherham, M., Rose, J. B. & El Haj, A. J. 2013. Cyclic hydrostatic pressure stimulates enhanced bone development in the foetal chick femur in vitro. *Bone,* 53**,** 468-477.

Hirsch, M. S., Lunsford, L. E., Trinkaus-Randall, V. & Svoboda, K. K. 1997. Chondrocyte survival and differentiation in situ are integrin mediated. *Developmental dynamics,* 210**,** 249-263.

Hosseini, A. & Hogg, D. A. 1991. The effects of paralysis on skeletal development in the chick embryo. I. General effects. *Journal of Anatomy,* 177**,** 159-168.

Juhász, T., Matta, C., Somogyi, C., Katona, É., Takács, R., Soha, R. F., Szabó, I. A., Cserháti, C., Sződy, R. & Karácsonyi, Z. 2014. Mechanical loading stimulates chondrogenesis< i> via</i> the PKA/CREB-Sox9 and PP2A pathways in chicken micromass cultures. *Cellular signalling,* 26**,** 468-482.

Kahn, J., Shwartz, Y., Blitz, E., Krief, S., Sharir, A., Breitel, D. A., Rattenbach, R., Relaix, F., Maire, P., Rountree, R. B., Kingsley, D. M. & Zelzer, E. 2009. Muscle Contraction Is Necessary to Maintain Joint Progenitor Cell Fate. *Developmental Cell,* 16**,** 734-743.

Kanczler, J. M., Smith, E. L., Roberts, C. A. & Oreffo, R. O. C. 2012. A Novel Approach for Studying the Temporal Modulation of Embryonic Skeletal Development Using Organotypic Bone Cultures and Microcomputed Tomography. *Tissue Engineering Part C: Methods,* 18**,** 747-760.

Kelly, D. J. & Jacobs, C. R. 2010. The role of mechanical signals in regulating chondrogenesis and osteogenesis of mesenchymal stem cells. *Birth Defects Research Part C: Embryo Today: Reviews,* 90**,** 75-85.

Khan, I. M., Redman, S. N., Williams, R., Dowthwaite, G. P., Oldfield, S. F. & Archer, C. W. 2007. The Development of Synovial Joints. *In:* GERALD, P. S. (ed.) *Current Topics in Developmental Biology.* Academic Press.

Klumpers, D. D., Smit, T. H. & Mooney, D. J. 2015. The Effect of Growth-Mimicking Continuous Strain on the Early Stages of Skeletal Development in Micromass Culture.

Kurosawa, H., Walker, P., Abe, S., Garg, A. & Hunter, T. 1985. Geometry and motion of the knee for implant and orthotic design. *Journal of Biomechanics,* 18**,** 487493-491499.

Lefebvre, V. & Bhattaram, P. 2010. Vertebrate skeletogenesis. *Current topics in developmental biology,* 90**,** 291-317.

Lelkes, G. 1958. Experiments in vitro on the Role of Movement in the Development of Joints. *Journal of Embryology and Experimental Morphology,* 6**,** 183-186.

Martelli, S. & Pinskerova, V. 2002. The shapes of the tibial and femoral articular surfaces in relation to tibiofemoral movement. *Bone & Joint Journal,* 84**,** 607-613.

Martinac, B. 2004. Mechanosensitive ion channels: molecules of mechanotransduction. *Journal of Cell Science,* 117**,** 2449.

McGlashan, S. R., Jensen, C. G. & Poole, C. A. 2006. Localization of extracellular matrix receptors on the chondrocyte primary cilium. *Journal of Histochemistry & Cytochemistry,* 54**,** 1005-1014.

McGlashan, S. R., Knight, M. M., Chowdhury, T. T., Joshi, P., Jensen, C. G., Kennedy, S. & Poole, C. A. 2010. Mechanical loading modulates chondrocyte primary cilia incidence and length. *Cell biology international,* 34**,** 441-446.

Millward-Sadler, S. & Salter, D. M. 2004. Integrin-dependent signal cascades in chondrocyte mechanotransduction. *Annals of biomedical engineering,* 32**,** 435-446.

Mobasheri, A., Carter, S., Martın-Vasallo, P. & Shakibaei, M. 2002. Integrins and stretch activated ion channels; putative components of functional cell surface mechanoreceptors in articular chondrocytes. *Cell biology international,* 26**,** 1-18.

Mouw, J., Imler, S. & Levenston, M. 2007. Ion-channel regulation of chondrocyte matrix synthesis in 3D culture under static and dynamic compression. *Biomechanics and modeling in mechanobiology,* 6**,** 33-41.

Murray, P. D. F. & Selby, D. 1930. Intrinsic and extrinsic factors in the primary development of the skeleton. *Wilhelm Roux' Archiv für Entwicklungsmechanik der Organismen,* 122**,** 629-662.

Natenstedt, J., Kok, A. C., Dankelman, J. & Tuijthof, G. J. 2015. What quantitative mechanical loading stimulates in vitro cultivation best? *Journal of Experimental Orthopaedics,* 2**,** 1-15.

Nowlan, N. 2015. Biomechanics of foetal movement. *European cells & materials,* 29**,** 1.

Nowlan, N. C., Bourdon, C., Dumas, G., Tajbakhsh, S., Prendergast, P. J. & Murphy, P. 2010a. Developing bones are differentially affected by compromised skeletal muscle formation. *Bone,* 46**,** 1275-1285.

Nowlan, N. C., Chandaria, V. & Sharpe, J. 2014. Immobilized chicks as a model system for early-onset developmental dysplasia of the hip. *Journal of Orthopaedic Research,* 32**,** 777-785.

Nowlan, N. C., Murphy, P. & Prendergast, P. J. 2007. Mechanobiology of embryonic limb development. *Annals of the New York Academy of Sciences,* 1101**,** 389-411.

Nowlan, N. C. & Sharpe, J. 2013. Joint shape morphogenesis precedes cavitation of the developing hip joint. *Journal of Anatomy***,** n/a-n/a.

Nowlan, N. C., Sharpe, J., Roddy, K. A., Prendergast, P. J. & Murphy, P. 2010b. Mechanobiology of embryonic skeletal development: Insights from animal models. *Birth Defects Research Part C: Embryo Today: Reviews,* 90**,** 203-213.

O'Rahilly, R. & Gardner, E. 1956. The development of the knee joint of the chick and its corelation with embryonic staging. *Journal of Morphology,* 98**,** 49-87.

O'Conor, C. J., Case, N. & Guilak, F. 2013. Mechanical regulation of chondrogenesis. *Stem cell research & therapy,* 4**,** 1.

Osborne, A. C., Lamb, K. J., Lewthwaite, J. C., Dowthwaite, G. P. & Pitsillides, A. A. 2002. Short-term rigid and flaccid paralyses diminish growth of embryonic chick limbs and abrogate joint cavity formation but differentially preserve pre-cavitated joints. *Journal of Musculoskeletal and Neuronal Interactions,* 2**,** 448-456.

Oxford English Dictionary. *"skeleton, n."* [Online]. Oxford University Press. Available: http://www.oed.com/view/Entry/180700?rskey=dCALwc&result=1&isAdvanced=false.

Pacifici, M., Koyama, E. & Iwamoto, M. 2005. Mechanisms of synovial joint and articular cartilage formation: Recent advances, but many lingering mysteries. *Birth Defects Research Part C: Embryo Today: Reviews,* 75**,** 237-248.

Pörtner, R., Nagel-Heyer, S., Goepfert, C., Adamietz, P. & Meenen, N. M. 2005. Bioreactor design for tissue engineering. *Journal of bioscience and bioengineering,* 100**,** 235-245.

Quintana, L. & Sharpe, J. 2011. Optical Projection Tomography of Vertebrate Embryo Development. *Cold Spring Harbor Protocols,* 2011**,** pdb.top116.

Roach, H. I. 1990. Long-term organ culture of embryonic chick femora: A system for investigating bone and cartilage formation at an intermediate level of organization. *Journal of Bone and Mineral Research,* 5**,** 85-100.

Roddy, K. A., Kelly, G. M., van Es, M. H., Murphy, P. & Prendergast, P. J. 2011a. Dynamic patterns of mechanical stimulation co-localise with growth and cell proliferation during morphogenesis in the avian embryonic knee joint. *Journal of Biomechanics,* 44**,** 143-149.

Roddy, K. A., Nowlan, N. C., Prendergast, P. J. & Murphy, P. 2009. 3D representation of the developing chick knee joint: a novel approach integrating multiple components. *Journal of Anatomy,* 214**,** 374-387.

Roddy, K. A., Prendergast, P. J. & Murphy, P. 2011b. Mechanical Influences on Morphogenesis of the Knee Joint Revealed through Morphological, Molecular and Computational Analysis of Immobilised Embryos. *PLoS ONE,* 6.

Rodriguez, E. K. & Munasinghe, J. 2016. A Chick Embryo in-Vitro Model of Knee Morphogenesis. *Archives of Bone and Joint Surgery,* 4**,** 109-115.

Rodríguez, J., Palacios, J., García-Alix, A., Pastor, I. & Paniagua, R. 1988a. Effects of immobilization on fetal bone development. A morphometric study in newborns with congenital neuromuscular diseases with intrauterine onset. *Calcified Tissue International,* 43**,** 335-339.

Rodríguez, J. I., Garcia-Alix, A., Palacios, J. & Paniagua, R. 1988b. Changes in the long bones due to fetal immobility caused by neuromuscular disease. A radiographic and histological study. *J Bone Joint Surg Am,* 70**,** 1052-1060.

Rolfe, R., Roddy, K. & Murphy, P. 2013. Mechanical regulation of skeletal development. *Current osteoporosis reports,* 11**,** 107-116.

Rolfe, R. A., Nowlan, N. C., Kenny, E. M., Cormican, P., Morris, D. W., Prendergast, P. J., Kelly, D. & Murphy, P. 2014. Identification of mechanosensitive genes during skeletal development: alteration of genes associated with cytoskeletal rearrangement and cell signalling pathways. *BMC genomics,* 15**,** 48.

Sachs, F. 1991. Mechanical transduction by membrane ion channels: a mini review. *Molecular and Cellular Biochemistry,* 104**,** 57-60.

Sah, R. L. Y., Kim, Y. J., Doong, J. Y. H., Grodzinsky, A. J., Plass, A. H. & Sandy, J. D. 1989. Biosynthetic response of cartilage explants to dynamic compression. *Journal of Orthopaedic Research,* 7**,** 619-636.

Saha, A., Rolfe, R., Carroll, S., Kelly, D. J. & Murphy, P. 2016. Chondrogenesis of embryonic limb bud cells in micromass culture progresses rapidly to hypertrophy and is modulated by hydrostatic pressure. *Cell and Tissue Research***,** 1-13.

Salva, J. E. & Merrill, A. E. 2017. Signaling networks in joint development. *Developmental Dynamics,* 246**,** 262-274.

Sandell, L. J. 2012. Etiology of osteoarthritis: genetics and synovial joint development. *Nature Reviews Rheumatology,* 8**,** 77-89.

Scheuer, L. & Black, S. 2004. *The Juvenile Skeleton*, Elsevier Science.

Schneider, C. A., Rasband, W. S. & Eliceiri, K. W. 2012. NIH Image to ImageJ: 25 years of image analysis. *Nat Meth,* 9**,** 671-675.

Schwend, R. 2014. Developmental Dysplasia of the Hip. *In:* GOSSELIN, R. A., SPIEGEL, D. A. & FOLTZ, M. (eds.) *Global Orthopedics.* Springer New York.

Shao, Y. Y., Wang, L., Welter, J. F. & Ballock, R. T. 2012. Primary cilia modulate Ihh signal transduction in response to hydrostatic loading of growth plate chondrocytes. *Bone,* 50**,** 79-84.

Sharpe, J., Ahlgren, U., Perry, P., Hill, B., Ross, A., Hecksher-Sørensen, J., Baldock, R. & Davidson, D. 2002. Optical Projection Tomography as a Tool for 3D Microscopy and Gene Expression Studies. *Science,* 296**,** 541-545.

Shojaei, B., Talebhemat, M., Hashemnia, S. & Shojaeepour, S. 2015. Knee joint morphogenesis of the quail (Coturnix japonica) embryo. *Italian Journal of Anatomy and Embryology,* 120**,** 127-139.

Smith, E. L., Kanczler, J. M. & Oreffo, R. O. 2013. A new take on an old story: chick limb organ culture for skeletal niche development and regenerative medicine evaluation. *Eur Cell Mater,* 26**,** 91-106; discussion 106.

Smith, E. L., Locke, M., Waddington, R. J. & Sloan, A. J. 2010. An ex vivo rodent mandible culture model for bone repair. *Tissue Engineering Part C: Methods,* 16**,** 1287-1296.

Stegmann, M. B. & Gomez, D. D. 2002. A brief introduction to statistical shape analysis. *Informatics and mathematical modelling, Technical University of Denmark, DTU,* 15.

Storm, E. E. & Kingsley, D. M. 1996. Joint patterning defects caused by single and double mutations in members of the bone morphogenetic protein (BMP) family. *Development,* 122**,** 3969-3979.

Strangeways, T. & Fell, H. B. 1926. Experimental Studies on the Differentiation of Embryonic Tissues Growing in vivo and in vitro.--I. The Development of the Undifferentiated Limb-Bud (a) when Subcutaneously Grafted into the Post-Embryonic Chick and (b) when Cultivated in vitro. *Proceedings of the Royal Society of London. Series B, Containing Papers of a Biological Character,* 99**,** 340-366.

Watson, S. J. & Bekoff, A. 1990. A kinematic analysis of hindlimb motility in 9- and 10-day-old chick embryos. *Journal of Neurobiology,* 21**,** 651-660.

Webb, S. E. & Miller, A. L. 2003. Calcium signalling during embryonic development. *Nature reviews Molecular cell biology,* 4**,** 539-551.

Williams, A. & Logan, M. 2004. Understanding tibio-femoral motion. *The Knee,* 11**,** 81-88.

Wong, M. & Carter, D. 2003. Articular cartilage functional histomorphology and mechanobiology: a research perspective. *Bone,* 33**,** 1-13.

Wu, Q.-q. & Chen, Q. 2000. Mechanoregulation of Chondrocyte Proliferation, Maturation, and Hypertrophy: Ion-Channel Dependent Transduction of Matrix Deformation Signals. *Experimental Cell Research,* 256**,** 383-391.

Yang, Y. 2013. Skeletal Morphogenesis and Embryonic Development. *Primer on the Metabolic Bone Diseases and Disorders of Mineral Metabolism.* John Wiley & Sons, Inc.

Yellowley, C. E., Hancox, J. C. & Donahue, H. J. 2002. Effects of cell swelling on intracellular calcium and membrane currents in bovine articular chondrocytes. *Journal of cellular biochemistry,* 86**,** 290-301.

Zaman, G., Dallas, S. L. & Lanyon, L. E. 1992. Cultured embryonic bone shafts show osteogenic responses to mechanical loading. *Calcified tissue international,* 51**,** 132-136.

APPENDIX I – EXPERIMENTAL PROTOCOLS

Experimental protocols were created and optimised with the help of Ms. Samantha Martin.

Alcian Blue – Alizarin Red – Protocol – FOR CHICK HIND LIMBS

(Adapted from "Avian Embryology" Bronner-Fraser (2008) & "Manipulating the Mouse Embryo", Hogan et al., 1994)

Solutions:

- **0.055% Alcian Blue Stain (Make up at least 1 day before staining) in 95% Ethanol with 20% Glacial Acetic Acid**
- **0.01% Alizarin Red Stain in 1% KOH**
- **4% Paraformaldehyde**
- **0.01% Sodium Azide in PBS**

Methods:

Dehydrate and fix samples in Ethanol for 3-4 days before starting staining. Keep samples in sealed flat containers during protocol.

CONCENTRATIONS OF ALCIAN BLUE AND CLEARING TIMES MAY DIFFER FOR DIFFERENT TISSUE SAMPLES

Stage		T°	Duration	Time Started	Time Ended
1	Stain samples in Alcian Blue Stain and leave rocking gently	RT	5 hours		
2	Wash samples with 95% Ethanol	RT	10mins		
3	Submerge samples in fresh 95% Ethanol	4°C	24 hours		
4	Submerge samples in fresh 95% Ethanol	4°C	24 hours		
5	Clear samples in 1% KOH	RT	Until clear		
6	Stain samples older than HH32 in Alizarin Red Stain (if younger samples skip to stage8)	RT	1 hour		
7	Clear samples in 1% KOH	RT	1 hour		
8	Fix samples in 4% PFA	RT	2 hours		
9	Store samples in 0.01% Sodium Azide	4°C	-		

Results:

Blue – Cartilage

Red – Bone

Preparation of Samples for OPT Imaging

(Protocol adapted from Quintana and Sharpe (2011))

Solutions:

- Low melting point Agarose
- Sterile dH_2O
- 100% Methanol
- BABB (2:1 mix of benzyl alcohol and benzyl benzoate)

Methods: Samples should be fixed overnight in 4% PFA at 4°C before starting this protocol.

	Stage	To	Duration	Time Started	Time Ended
1	**Prepare 1% low melting Agarose solution in sterile water** Weigh out Agarose and add to bottle. Add volume of sterile dH20 and microwave till all dissolved. Weigh contents before and after heating to replace any water lost. Watch out for over boiling.	microwave			
2	**Filter Agarose Solution** Wait for Agarose to cool slightly and filter into clean 50ml tubes. Can store Agarose in tubes at 37°C for 1 day.	37 °C			
3	**Embed Samples in Agarose** Pour out Agarose solution in 6cm dishes. Wash samples in sterile dH20. Wash samples in Agarose dish moving around to remove bubbles. Place limbs in new dish with Agarose. Wait for gel to cool and orientate limbs with each other in centre of dish, floating at a medium depth. Once gel is solid, transfer to 4°C to set. If not going to trim immediately after setting, add water to agarose and cover with parafilm and foil. Store at 4°C.	RT			
4	**Trimming** Using a blade cut square block around each sample and remove into 9cm plates. Align samples along axis of rotation and cut parallel either side of sample using razor blade. Cut top and bottom of sample also leaving 5mm on one end for attachment to rotation stage. Stand the sample up with 5mm end at the bottom. Trim corners off to make octagonal shape.	RT			
5	**Dehydrate samples** Place samples in glass vials with 100% methanol. Replace methanol 2/3 times to ensure full dehydration.	RT	24 hours		
6	**Clear samples** Replace methanol with BABB solution, place in fume hood with foil lid. Make holes in foil for methanol to evaporate.	RT	24 hours		
7	**Mount and Image Samples**	RT			

	Remove specimen from sample into GLASS dish. Dry bottom surface of block on paper towel. Place glue on mount and block on top. Wait for glue to set and then place in OPT scanner.				

Cryo Sample Prep

Samples should be fixed before embedding. 4% PFA 2 hour at RT. Store in PBS and embed within couple of days.

	Stage	Duration	Temp	Time Started
1	**Clearing** Place samples in 15% Sucrose	O/N	4°C	
2	**Clearing** Place Samples in 30% Sucrose	O/N	4°C	
3	**Infiltration I** Place samples in 50:50 mix of 30% sucrose and OCT	Until sinks (1-2hours)	RT	
4	**Embedding** Set up level platform in dry ice. Label moulds for samples and half fill with 50:50 30% sucrose and OCT mix Place samples into blocks and orientate Mark position of samples on moulds Leave to set on dry ice		Dry ice -20°C	
5	**Section** Stick samples to chuck using OCT and leave to cool Trim block until can see sample Set blade angle to 5° and cut section thickness Label slides and keep ready to mount sections. Keep slides at RT so sections melt onto glass Use brush to pull sample over blade as cutting to stop from rolling		-20°C	

Notes:

- OCT sucrose mix will melt at RT. Keep frozen as much as possible.

CRYOSECTION MORPHOLOGY STAINING

Alcian Blue:

Alcian Blue pH 2.5 0.025% Alcian blue in 3% aq acetic acid

Alcian blue 8GX ------ 0.025 g

distilled water ---------- 97.0 ml
glacial acetic acid ---------- 3.0 ml

Dissolve the dye in the distilled water, add acid, mix well. Filter before use.

Picro Sirius Red Solution:

250 ml Picric Acid

0.25 g direct red

Acidified Water:

0.5% solution using acetic acid in water (tap or distilled)

Methods:

Incubate slides at RT for 1-2hrs to ensure sections stick to slides.

Stage		To	Duration	Time Started	Time Ended
1	Wash in PBS	RT	5mins		
2	Wash in fresh PBS	RT	5mins		
3	Stain with Alcian Blue (0.025% Alcian blue in 3% acetic acid)	RT	30mins		
4	Rinse gently with tap water	RT	10mins		
5	Stain with Picro Sirius Red Solution	RT	30mins		
6	Wash 0.5% acidified water	RT	10mins		
18	Was in PBS	RT	5mins		

PHH3 Immuno-fluorescent protocol CryoSections

Solutions:

- **Wash Buffer: PBTD – 1x PBS, 0.1% Tween 20, 1% DMSO**
- **Blocking: 5% Normal Goat Serum (NGS) in Wash Buffer**
- **Primary AntiBody: Anti-phospho-Histone H3 from rabbit (PHH3) ser10**
- **Secondary AntiBody: Cy3 anti-rabbit**

Methods:

Allow sections to adhere to slides for 2 hours at RT before starting. If sample has not been fixed, fix with cold acetone for 10mins and let dry for at least 20mins.

	Stage	To	Duration	Time Started	Time Ended
1	**Hydrate Slides** Submerge slides in PBTD	RT	5mins		
2	**Blocking** Cover slides in blocking solution (200uL per slide) in humid chamber. Parafilm on sides	RT	2Hr		
3	**Blot slides**	RT	-		
4	**Incubate with primary antibody** Dilute antibody 1:50 in wash buffer. Cover slides in primary antibody (200uL per slide) in humid chamber. Parafilm on sides	4oC	O/N		
5	**Wash in Wash Buffer**	RT	30 mins		
6	**Incubate with secondary antibody in dark** Dilute antibody 1:200 in wash buffer Cover slides in secondary antibody (200uL per slide) in humid chamber. Parafilm on sides	RT	1Hr		
7	**Wash in Wash Buffer**	RT	25 mins		
8	**Mount sections of slides with DAPI mounting media**	RT	-		

APO-BrdUTP Apoptosis Immuno protocol

(Taken from AbD Serotec (2016))

Methods: (fixed tissue)

Stage		To	Duration	Time Started	Time Ended
1	**Rehydration** Immerse slides in: • 1x PBS Blot slides	RT	15’		
2	**Permeabilisation of specimen** Dilute Proteinase K (pink cap) 1:100 in 10mM Tris pH 8 Cover slides in 100uL proteinase K working solution Rinse slides with 1x PBS	RT	10’ **Don’t overincubate**		
3	**Inactivation of endogenous peroxidases** Dilute 30% H_20_2 1:10 in Methanol Cover slides in 100uL of 3% H_20_2 Rinse with 1x PBS	RT	5’		
4	**Equilibration and end labelling reaction** Dilute 5x reaction buffer 1:5 with dH_20 Cover slides with 100uL reaction buffer Prepare labelling solution (for 1 slide) • 10uL 5x Reaction Buffer (green cap) • 0.75uL TdT Enzyme (yellow cap) • 8uL Br—dUTP (violet cap) • 32.25uL Distilled H_20 Carefully blot reaction buffer from samples Immediately apply 50uL of labelling solution to slides Cover with parafilm and put in humid chamber Remove parafilm and rinse with 1x PBS	RT 37 oC	10-30’ 1-1.5hours		
5	**Detection** Cover slides in 100uL blocking buffer (white cap) Carefully blot blocking buffer from samples Immediately cover slides with 100uL Antibody Solution prepared as (1slide): • 5uL Biotin anti BrdU (orange cap) • 95uL Blocking Buffer (white cap) Incubate with Antibody solution in the dark Rinse in 1x PBS Cover slide in 100uL Blocking Buffer (white cap)	RT RT	10’ 1-1.5hours		

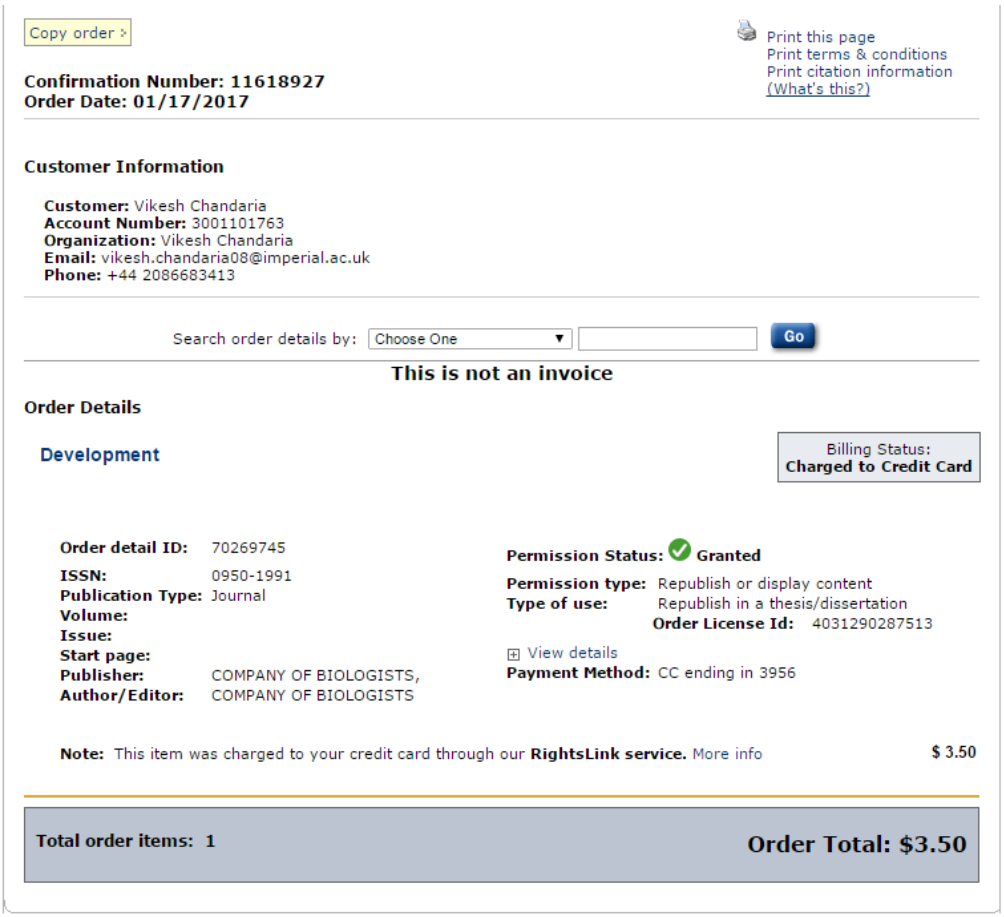
	Dilute 200x Conjugate (black cap) 1:200 in blocking buffer (white cap) (for 1 slide 0.5uL conjugate, 100uL blocking) Blot blocking buffer from samples Immediately apply 100uL of Conjugate to specimen Five minutes before time dissolve one DAB (amber vial) tablet and one H_20_2/Urea (amber vial) in 1mL TAP H_20 Rinse slides 1x PBS Cover slides with 100uL DAB solution Rinse with H_20 and blot	RT RT	30’ 15’		
6	**Counterstain** Immediately cover slides in 100uL of Methyl Green Counterstain (natural cap) Press edge of slide against towel to draw off stain Submerge slides in 100% ethanol briefly Blot with towel Wash in 100% ethanol Blot with towel Wash in Histoclear	RT	3’		

APPENDIX II – COPYRIGHT PERMISSIONS

Figure Number	Type of Work	Source Work	Copyright Holder	Permission Requested	Permission Received	Permission Note
2.4	Figure	(Lelkes, 1958)	© 1958 by Company of Biologists	Jan 17, 2017	Yes	Written permission
2.5	Figure	(Drachman and Sokoloff, 1966)	© 1966 Published by Elsevier Inc.	Jan 17, 2017	Yes	Written permission
2.6	Figure	(Roddy et al., 2011b)	© 2011 Roddy et al.	Jan 17, 2017	N/A	Licensed with a Creative Commons Attribution License (CC BY)
2.7	Figure	(Brunt et al., 2016)	© 2016 The Author(s). Published by Elsevier Ltd.	Jan 17, 2017	N/A	Licensed with a Creative Commons Attribution License (CC BY)
2.8	Figure	(Nowlan et al., 2010a)	© 2009 Elsevier Inc.	Jan 17, 2017	N/A	Licensed with a Creative Commons Attribution License (CC BY)
2.9	Figure	(Giorgi et al., 2014)	& 2014 The Authors. Published by Elsevier Ltd.	Jan 17, 2017	N/A	Licensed with a Creative Commons Attribution License (CC BY)
2.10	Figure	(Giorgi et al., 2015)	& 2015 The Authors. Published by Elsevier Ltd.	Jan 17, 2017	N/A	Licensed with a Creative Commons Attribution License (CC BY)
2.11	Figure	(Roddy et al., 2011b)	© 2011 Roddy et al.	Jan 17, 2017	N/A	Licensed with a Creative Commons Attribution License (CC BY)

3.6	Figure	(Chandaria et al., 2016)	© 2016 The Authors. Published by Elsevier Ltd.	Jan 17, 2017	N/A	Licensed with a Creative Commons Attribution-NonCommercial-No Derivatives License (CC BY NC ND)
4.2	Figure	(Chandaria et al., 2016)	© 2016 The Authors. Published by Elsevier Ltd.	Jan 17, 2017	N/A	Licensed with a Creative Commons Attribution-NonCommercial-No Derivatives License (CC BY NC ND)
5.4	Figure	(Chandaria et al., 2016)	© 2016 The Authors. Published by Elsevier Ltd.	Jan 17, 2017	N/A	Licensed with a Creative Commons Attribution-NonCommercial-No Derivatives License (CC BY NC ND)
7.1	Figure	(Chandaria et al., 2016)	© 2016 The Authors. Published by Elsevier Ltd.	Jan 17, 2017	N/A	Licensed with a Creative Commons Attribution-NonCommercial-No Derivatives License (CC BY NC ND)
7.2	Figure	(Chandaria et al., 2016)	© 2016 The Authors. Published by Elsevier Ltd.	Jan 17, 2017	N/A	Licensed with a Creative Commons Attribution-NonCommercial-No Derivatives License (CC BY NC ND)
7.3	Figure	(Chandaria et al., 2016)	© 2016 The Authors. Published by Elsevier Ltd.	Jan 17, 2017	N/A	Licensed with a Creative Commons Attribution-NonCommercial-No Derivatives License (CC BY NC ND)

Permission order for Figure 2.4:



Copy order

Print this page
Print terms & conditions
Print citation information
(What's this?)

Confirmation Number: 11618927
Order Date: 01/17/2017

Customer Information

Customer: Vikesh Chandaria
Account Number: 3001101763
Organization: Vikesh Chandaria
Email: vikesh.chandaria08@imperial.ac.uk
Phone: +44 2086683413

Search order details by: Choose One Go

This is not an invoice

Order Details

Development

Billing Status:
Charged to Credit Card

Order detail ID: 70269745
ISSN: 0950-1991
Publication Type: Journal
Volume:
Issue:
Start page:
Publisher: COMPANY OF BIOLOGISTS,
Author/Editor: COMPANY OF BIOLOGISTS

Permission Status: Granted
Permission type: Republish or display content
Type of use: Republish in a thesis/dissertation
Order License Id: 4031290287513
View details
Payment Method: CC ending in 3956

Note: This item was charged to your credit card through our **RightsLink service.** More info $ 3.50

Total order items: 1 **Order Total: $3.50**

Permission order for Figure 2.5:

ELSEVIER LICENSE
TERMS AND CONDITIONS

Feb 01, 2017

This Agreement between Vikesh V Chandaria ("You") and Elsevier ("Elsevier") consists of your license details and the terms and conditions provided by Elsevier and Copyright Clearance Center.

License Number	4031270238469
License date	Jan 17, 2017
Licensed Content Publisher	Elsevier
Licensed Content Publication	Developmental Biology
Licensed Content Title	The role of movement in embryonic joint development
Licensed Content Author	Daniel B. Drachman,Leon Sokoloff
Licensed Content Date	December 1966
Licensed Content Volume Number	14
Licensed Content Issue Number	3
Licensed Content Pages	20
Start Page	401
End Page	420
Type of Use	reuse in a thesis/dissertation
Portion	figures/tables/illustrations
Number of figures/tables/illustrations	1
Format	both print and electronic
Are you the author of this Elsevier article?	No
Will you be translating?	No
Order reference number	
Original figure numbers	Figure 2
Title of your thesis/dissertation	Mechanical Stimulation and Morphogenesis of the Embryonic Chick Knee Joint
Expected completion date	Feb 2017
Estimated size (number of pages)	150
Elsevier VAT number	GB 494 6272 12
Requestor Location	Vikesh V Chandaria 58 Old Lodge Lane Purley, Surrey CR8 4DF United Kingdom Attn: Vikesh V Chandaria
Total	0.00 GBP
Terms and Conditions	

APPENDIX III – PUBLISHED WORK

Journal of Biomechanics 49 (2016) 3635–3642

Contents lists available at ScienceDirect

Journal of Biomechanics

journal homepage: www.elsevier.com/locate/jbiomech
www.JBiomech.com

Characterising the effects of *in vitro* mechanical stimulation on morphogenesis of developing limb explants

Vikesh V. Chandaria [a], James McGinty [b], Niamh C. Nowlan [a,*]

[a] Department of Bioengineering, Imperial College London, London SW7 2AZ, UK
[b] Department of Physics, Imperial College London, London, UK

ARTICLE INFO

Article history:
Accepted 19 September 2016

Keywords:
Joint morphogenesis
Joint shape
Explant culture
Chick knee (Stifle) joint
Mechanobiology

ABSTRACT

Mechanical forces due to fetal movements play an important role in joint shape morphogenesis, and abnormalities of the joints relating to abnormal fetal movements can have long-term health implications. While mechanical stimulation during development has been shown to be important for joint shape, the relationship between the quantity of mechanical stimulation and the growth and shape change of developing cartilage has not been quantified. In this study, we culture embryonic chick limb explants *in vitro* in order to reveal how the magnitude of applied movement affects key aspects of the developing joint shape. We hypothesise that joint shape is affected by movement magnitude in a dose-dependent manner, and that a movement regime most representative of physiological fetal movements will promote characteristics of normal shape development. Chick hindlimbs harvested at seven days of incubation were cultured for six days, under either static conditions or one of three different dynamic movement regimes, then assessed for joint shape, cell survival and proliferation. We demonstrate that a physiological magnitude of movement *in vitro* promotes the most normal progression of joint morphogenesis, and that either under-stimulation or over-stimulation has detrimental effects. Providing insight into the optimal level of mechanical stimulation for cartilage growth and morphogenesis is pertinent to gaining a greater understanding of the etiology of conditions such as developmental dysplasia of the hip, and is also valuable for cartilage tissue engineering.

© 2016 The Authors. Published by Elsevier Ltd. This is an open access article under the CC BY-NC-ND license (http://creativecommons.org/licenses/by-nc-nd/4.0/).

1. Introduction

Each type of synovial joint has a highly specialised shape, and alterations or abnormalities in the development of these shapes can compromise their functionality. Reduced fetal movements are implicated in musculoskeletal conditions of impaired joint shape development, such as development dysplasia of the hip and arthrogryposis (reviewed in Nowlan (2015)). However, it is unclear how the quantity, timing and type of mechanical stimulation due to fetal movements influence joint shape morphogenesis. This question is relevant to lifelong musculoskeletal health, as developmental joint abnormalities can affect the joint's range of motion and the transmission of mechanical loads, increasing the risk of degenerative joint diseases such as osteoarthritis later in life (Sandell, 2012). Furthermore, a better understanding of how mechanical stimulation directs or determines cartilage growth during prenatal development is highly relevant to cartilage tissue engineering, in which the aim is to recapitulate the developmental processes occurring in fetal rudiments.

Previous studies have explored the influence of mechanical stimuli on skeletal development using animal models of reduced, absent or abnormal fetal movements (reviewed in Nowlan et al. (2010b)). While many of these studies focused on cavitation or ossification rather than joint morphogenesis, we do have some understanding of the effects of immobility on joint shape development. In immobilised chicks embryos, articular joints are often fused across the joint site, and normal interlocking joint shapes are lost (Drachman and Sokoloff, 1966; Hall and Herring, 1990; Hosseini and Hogg, 1991; Nowlan et al., 2014; Osborne et al., 2002; Roddy et al., 2011b). Paralysis of zebrafish embryos leads to alterations in jaw joint shape and inhibition of normal joint function (Brunt et al., 2015). Failure to produce joint cavities and abnormal joint shapes have also been observed in 'muscle-less' mice embryos (Kahn et al., 2009; Nowlan et al., 2010a) along with signs of irregular joint shape development in 'reduced muscle' mice embryos (Kahn et al., 2009). Early studies used *in vitro* culture methods to investigate the role of movement on joint development. Explants from four day old embryos failed to form a complete knee (stifle) joint after six days of static culture *in vitro*, using the "watch glass" technique (Fell and Canti, 1934). However, when six or seven day old embryonic chick knee explants were

* Corresponding author.
E-mail address: n.nowlan@imperial.ac.uk (N.C. Nowlan).

http://dx.doi.org/10.1016/j.jbiomech.2016.09.029
0021-9290/© 2016 The Authors. Published by Elsevier Ltd. This is an open access article under the CC BY-NC-ND license (http://creativecommons.org/licenses/by-nc-nd/4.0/).

cultured for six days by Lelkes (1958), manual manipulation of the explants led to cavitation and development of articular surfaces between the femur and tibia (or tibiotarsus). Since these pioneering papers were published, *in vitro* culture methods have improved dramatically. Modern bioreactors enable repeatable cultivation of tissue and application of controlled mechanical stimulation in ways that are not possible *in vivo* (Cohen et al., 2005; Pörtner et al., 2005). *In vitro* culture of embryonic chick hindlimb elements has been shown to be a versatile model for studying skeletal development (Smith et al., 2013), and a bioreactor system has been used to apply cyclic hydrostatic pressure to promote bone growth and mineralisation in embryonic chick femurs (Henstock et al., 2013). A recent feasibility study showed the whole chick hindlimb could be cultured whilst applying flexion and extension movements to the knee joint (Rodriguez and Munasinghe, 2016). However, the quantitative relationship between mechanical stimulation and joint morphogenesis has not been described, a deficit that is addressed in this current study.

In this study, a novel 3D explant culture system is used to investigate the development of the embryonic chick knee joint under a range of flexion movement regimes, with the aim of characterising the relationship between the magnitude of applied movements and key aspects of fetal joint morphogenesis. It was hypothesised that joint shape development would be affected by movement magnitude in a dose-dependent manner, and that the most physiological movement regime would lead to a joint with the most normal progression of shape morphogenesis.

2. Methods

2.1. Characterisation of physiological knee morphology

To evaluate the progression of joint shape development in cultured explants, we first analysed the morphology of the knee joint over 7 to 9 days of incubation, a period of dramatic shape change for the joint. Limbs were processed for 3D shape and size analysis as described below.

2.2. Preparation of explants for culture

Fertilised white DeKalb eggs (Henry Stewart & Co, UK) were incubated at 37 °C under humidified conditions for seven days. Hindlimbs were harvested, the digits removed, and the soft tissues surrounding the rudiments removed as described by Henstock et al. (2013). Preliminary experiments demonstrated that this step of soft tissue removal increased the duration of time that the explant could be viably maintained *in vitro* (data not shown).

2.3. Explant culture setup

Rectangular pieces ($35 \times 20 \times 15$ mm^3) of polyurethane foam (Sydney Heath & Son, UK) were used to support the hindlimb explants during culture. The foam support was cut to create a step running horizontally along the top surface (Fig. 1A). Each hindlimb was positioned, medial side down, onto the lower level and oriented with the distal end nearest the step (Fig. 1B). Six specimens were placed on each support (Fig. 1B). Once positioned, each explant was pinned to the support using a 27G needle through the superior part of the pelvis to secure the limb. The foam supports were transferred into a uniaxial compression bioreactor (Ebers TC-3, Spain) and filled with basal culture media (alpha – minimum essential media (α-MEM GlutaMAX, Gibco) supplemented with 1% pen/strep, 1% Amphotericin B and 100 μM Ascorbic Acid (Sigma, UK)). The explants were maintained at an air–liquid interface, and the culture medium was replenished every 24 h.

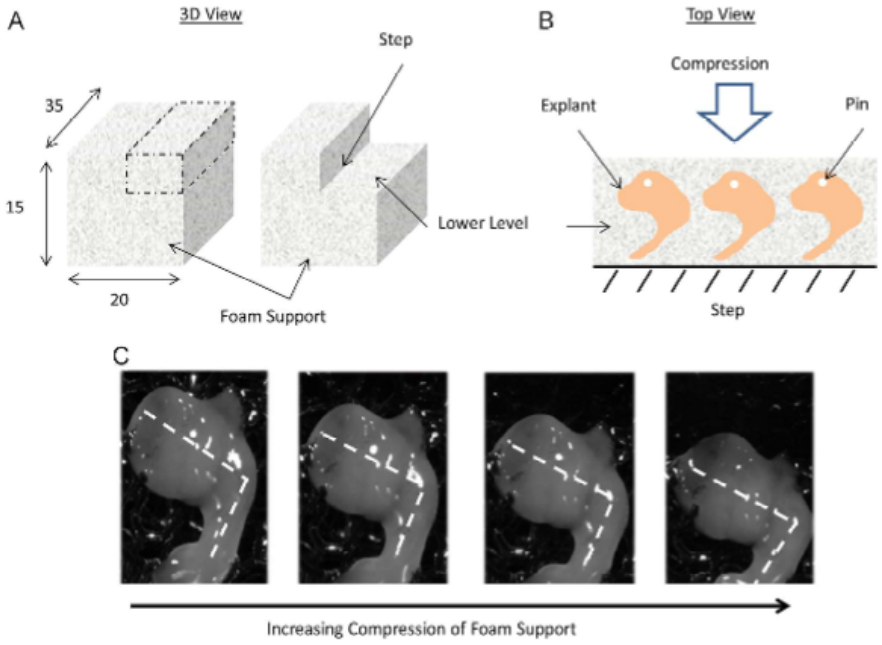


Fig. 1. Dynamic explant culture setup. A) A polyurethane foam support was used to support the hindlimb explants during culture. The rectangular piece of foam was cut to create a step along the horizontal axis. Measurements are in mm. B) Explants were positioned onto the lower level of the foam and pinned into place. Explants were orientated medial side down with the hip joint furthest away from the step. C) Uniaxial compression of the foam support caused the hindlimb to bend at the knee joint mimicking a flexion motion of the knee joint.

2.4. Application of in vitro movement regime

The bioreactor was programmed to apply compressive displacement regimes to the foam supports which caused the angle between the thigh and shank to decrease, mimicking a flexion motion of the knee joint (Fig. 1C). A range of compressive displacements were applied during calibration to quantify the amount of flexion experienced at the knee joint. Six explants were subjected to 1–4 mm of compression and their movement patterns recorded using a high-definition camera (HV-5080, HAVIT, China). The change in the joint angle was calculated using ImageJ (Schneider et al., 2012) to give the flexion magnitudes for each applied displacement. An average-flexion movement regime was designed in order to mimic normal flexion of the chick embryo, and two additional dynamic regimes of lower and higher magnitudes were also included. The three movement regimes were termed reduced-flexion, average-flexion and over-flexion where 2, 3 and 4 mm of compressive displacement were applied respectively, resulting in flexion magnitudes of 9 ± 3, 14 ± 4.0 and 22 ± 5.0 (mean $\pm$ SD) degrees. Observations of chick motility *in ovo* report an approximate mean knee flexion of 12 degrees in 9–10 day old embryos (Watson and Bekoff, 1990). All dynamically stimulated explants were loaded with a sinusoidal waveform at an average rate of 4 mm/s for 2 h, three times per day, replicating aspects of activity-inactivity cycles observed *in ovo* (Chambers et al., 1995; Hamburger et al., 1965), and similar to stimulation patterns used in *in vitro* micromass cultures (Bian et al., 2011; Elder et al., 2000). Limbs cultured under the same conditions but without dynamic stimulation were used as controls. Six days was chosen as the duration of the culture, as this allowed for sustained viability of the explants and enabled sufficient time for shape morphogenesis to progress *in vitro*. (Supplementary Video 1 shows the culture system in action).

Supplementary material related to this article can be found online at http://dx.doi.org/10.1016/j.jbiomech.2016.09.029.

2.5. Analysis

2.5.1. Specimen numbers

Three knee joints from 7, 8 and 9 day non-experimental control embryos were analysed for physiological joint shape and size. For the *in vitro* culture study, a total of 72 chicks were harvested at day 7. For each embryo, the right hindlimb was subjected to movement and the left hindlimb was kept under static conditions. Explants selected for dynamic stimulation were split evenly across the three experimental groups. A total of four cultures were performed for each group, with static controls performed alongside each culture. Explants were pooled together for the three experimental groups and static controls to give four groups for analysis. This yielded a total of 24 explants cultured for each experimental group and a total of 72 static control explants. During media changes, each culture chamber was visually inspected for any signs of abnormal growth or infection. Contaminated or infected cultures were discarded and repeated. Successfully cultured explants were used either for 3D joint analysis or for cellular level analysis. Explants damaged during processing were discarded. A total of 26, 7, 12 and 11 knee joints were analysed for shape and size in the static, reduced-flexion, average-flexion and over-flexion groups respectively. An additional two explants per group were used for cellular level activity assays, and within these samples, two sections from each of the two explants were used to quantify proliferation rates and cell viability.

2.5.2. 3D shape and size analysis

To visualise the cartilaginous skeletal rudiments each explant was stained with 0.055% Alcian blue for 5 h and cleared in 1% KOH for 2 h at room temperature. Samples were prepared for Optical Projection Tomography (OPT) (Sharpe et al., 2002) using protocols outlined in Quintana and Sharpe (2011). 3D models of the limbs were rendered using Mimics (Materialise, Belgium). Models were virtually orientated into a flexed resting position, where the tibia and fibula were aligned vertically and the femur was flexed to align the ventral tip of the lateral condyle with the dorsal surface of the fibula. Frontal, lateral and medial views of the joint were traced to produce shape profiles for each specimen. Shape profiles for each rudiment (femur, tibia and fibula) were grouped and analysed independently. Eleven measurements were made of the distal femur, proximal tibia and fibula, as listed in Fig. 2.

2.5.3. Immunohistochemistry analysis

Limbs were fixed in 4% PFA immediately after culture for 2 h at room temperature. Explants were prepared for cryopreservation by incubating in 15% and 30% sucrose overnight at 4 °C and then embedded and frozen in an OCT-30% Sucrose (50:50) medium over dry ice. All explants were sectioned at 10 μm at −18 °C. Proliferating cells were identified using the mitosis marker phospho-Histone H3 (pHH3), similarly to Roddy et al. (2011a). Cryosections were blocked (5% normal goat serum, 1% DMSO) for 2 h at room temperature before being incubated with anti-phospho-Histone H3 from rabbit ser10 (Merck Millipore, Germany) diluted 1:50 overnight at 4 °C. Cryosections were then incubated with goat anti-rabbit secondary antibody, Cy3 conjugate (Invitrogen, USA) diluted 1:200 at room temperature for 1 h. Sections were counter stained and mounted using a DAPI fluoroshield medium (Sigma, UK). Cell viability was assessed using a terminal deoxynucleotidyl transferase (TdT) dUTP nick-end labelling (TUNEL) detection kit (APO-BRDU-IHC, Bio-Rad Laboratories, USA) using the recommended protocols (AbD Serotec, 2016) to identify cells undergoing apoptosis or necrosis. Dead cells were stained brown and live cells were counter stained green. All sections were imaged at 100x magnification. The number of proliferating and total number of cells were counted using the particle analysis function in ImageJ (U.S. National Institutes of Health, USA). The number of dead cells was counted manually.

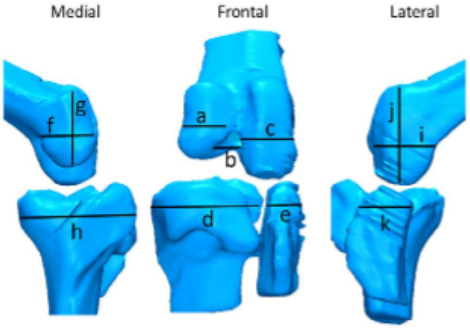
2.6. Statistical analysis

For all measured variables and quantities, 1-way ANOVA tests were performed to investigate if significant differences existed between the four groups. If significant differences existed, a post-hoc Tukey-Kramer pairwise comparison was performed to identify specifically which groups were significantly different from each other. p-values less than 0.05 were considered statistically significant.

3. Results

3.1. Physiological chick knee shape development

In the distal femur at 7 days, both condyles can be identified as simple outgrowths, with the size of the lateral condyle exceeding that of the medial condyle by 60% in anterior–posterior depth (Fig. 3A, B, D). At this timepoint, the proximal fibula and tibia shapes resemble a simple rounded rod and in the case of the tibia the rounded end appears to protrude posteriorly since the anterior tibial crest is yet to develop (Fig. 3C and E). At 8 days, the lateral condyle remains bigger than the medial condyle (Fig. 3F), but has



Measurement	Region
a	Medial Condyle Width
b	Intercondylar Fossa Width
c	Lateral Condyle Width
d	Tibia Width
e	Fibula Width
f	Medial Condyle Depth
g	Medial Condyle Height
h	Tibia Depth
i	Lateral Condyle Depth
j	Lateral Condyle Height
k	Fibula Depth

Fig. 2. Joint regions measured. Eleven joint regions were defined and analysed. Medial, frontal and lateral views of the knee joint were used to visualise the anatomical locations of each joint region.

developed a posterior curl which can be seen in the sagittal plane (Fig. 3I) which also leads to the intercondylar fossa between the femoral condyles becoming more distinct (Fig. 3F). The fibula remains rounded in shape but is 40% larger than at day 7 (Fig. 3J). At this point, the anterior tibial crest first becomes obvious, creating a concave tibial plateau in the sagittal plane (Fig. 3H). At 9 days, the femoral medial condyle appears similar to the lateral condyle, both exhibiting posterior curls seen in the sagittal profiles (Fig. 3K, L and N), with the lateral condyle remaining slightly larger (16%) in anterior–posterior depth than the medial condyle. At this stage, the condyles are clearly separated by the intercondylar fossa on the ventral side, and a channel like groove on the dorsal surface

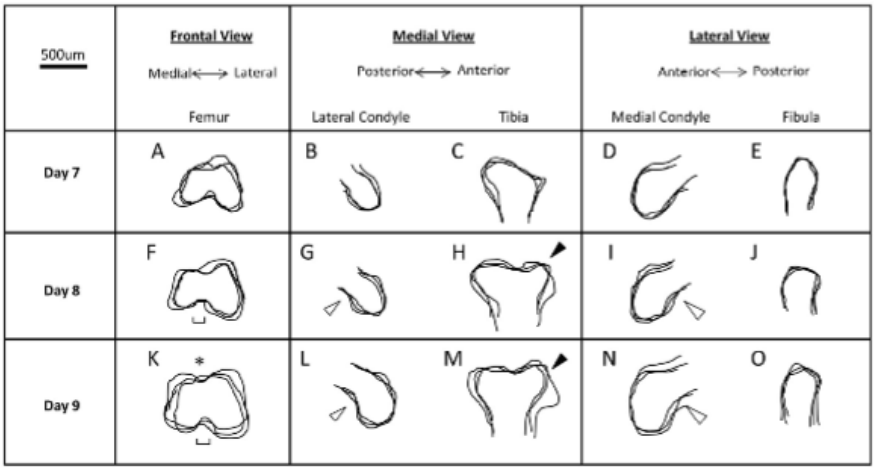


Fig. 3. Distinct shape changes occur in the knee joint shape of normal controls between 7 and 9 days of incubation. Shape profiles of 7 (A–E), 8 (F–J) and 9 (K–O) day old chick embryo knee joints were outlined and overlaid ($n=3$). Hollow arrows: posterior curl of the condyles; * dorsal groove between the two femoral condyles; single edged bars: intercondylar fossa; filled arrows: emergence of anterior tibial crest.

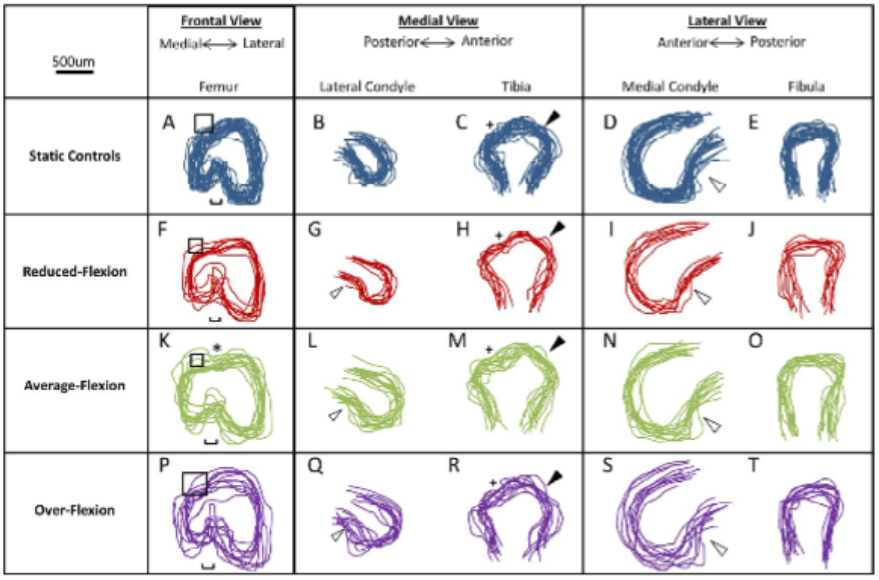


Fig. 4. The average-flexion movement regime led to more normal progression of morphogenesis than other movement regimes or static culture. Shape profiles of the 3D reconstructed joint regions were outlined and overlaid for each cultured group. Squares: dominance of the lateral condyle over the medial condyle; hollow arrows: posterior curl of condyles seen in moved explants; * dorsal groove between the two femoral condyles; single edged bars: intercondylar fossa; + concave curve of the tibial plateau; filled arrows: anterior tibial crest.

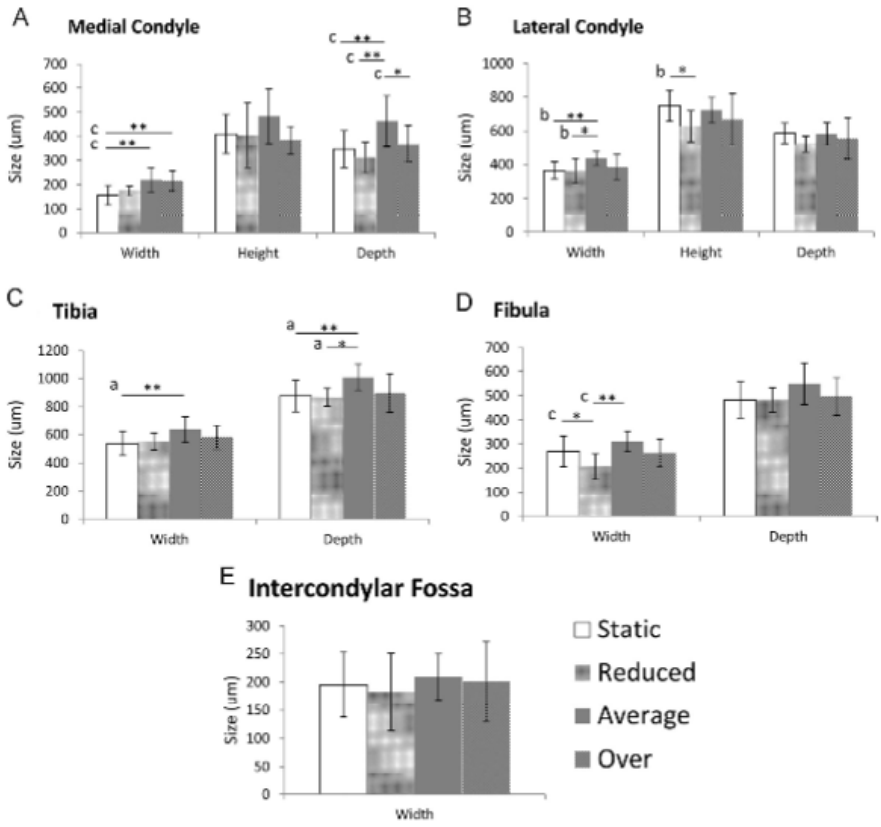


Fig. 5. Significant differences in joint region measurements were most pronounced between the average-flexion regime and static culture. Mean size of joint regions measured for static, reduced-flexion, average-flexion and over-flexion explants. Error bars represent standard deviation. *p-values < 0.05; **p-values < 0.01. 'a' indicates a difference of 10–15%, 'b' indicates a difference of 16–20% and 'c' indicates a difference of 21–35%, where differences represent how much smaller the regions measured relative to the larger joint.

(Fig. 3K). The articular end of the fibula has flattened and curled slightly in the posterior direction (Fig. 3O). The anterior tibial crest has further matured to lengthen the concave shape of the tibial plateau.

3.2. 3D joint region shapes and sizes

The characteristics of physiological shape development described above were used as indicators to assess the normality of joints developed *in vitro*. Under this classification system, the joint shapes of explants cultured under static conditions were less developed than any of the dynamically moved explants. In the distal femur of statically cultured limbs, the medial condyle remained substantially smaller than the lateral condyle, measuring 41% smaller on average in condyle depth (Fig. 4A, B and D). The shape of the medial condyle was abnormal, appearing rounded and missing the posterior curl seen in normal shape development (Fig. 4B). In contrast, the lateral side of the statically cultured knee joints exhibited features of normal development, in particular a posterior curl of the lateral condyle (Fig. 4D) and flattening of the proximal fibula (Fig. 4E). While emergence of the anterior tibial crest was detectable in static controls, the tibial plateau exhibited only a slight concave profile in the medial view (Fig. 4C).

Joints cultured under dynamic movement regimes displayed more features of physiological shape development than seen in the static controls. Of the three dynamic stimulation groups, the average-flexion regime led to joint shapes which most closely approximated normal shape development. In the average-flexion group, both femoral condyles developed a posterior curl (Fig. 4L and N) and were most comparable in size. While the lateral condyle was still bigger than the medial condyle (as seen in the frontal view of the distal femur) (Fig. 4K), the medial condyle was only 20% less deep on average than its opposing lateral condyle, compared to the 41% difference between the condyles reported above for the static controls. The medial condyle was significantly larger in width and depth following average-flexion compared to static controls (Fig. 5A). No significant differences were found in femoral condyle height or lateral condyle depth (Fig. 5A and B) between average-flexion and static groups. The lateral condyle width was significantly wider following average-flexion compared to static controls (Fig. 5B), as were the depth and width of the tibia (Fig. 5C).

Differences in joint shape profiles and joint region measurements were also observed between moved groups. The average-flexion regime promoted the most normal progression of shape morphogenesis when compared to reduced-flexion or over-flexion groups. The relative size differences between the depths of the femoral condyles were more pronounced in the reduced-flexion (40% on average) and the over-flexion groups (34% on average) than in the average-flexion group (20%, as reported above). Evidence of a dorsal groove between the femoral condyles was only observable in explants following average-flexion (Fig. 4K), but not in any of the other groups (Fig. 4A, F and P). The intercondylar fossa was clearly distinguishable following average-flexion, but was distorted in both the reduced-flexion and over-flexion groups (Fig. 4F, K and P). While no significant differences were found between the intercondylar fossa widths between the different groups (Fig. 5E), there was greater variation in this joint region size in the reduced-flexion and over-flexion groups than in the average-flexion group (Fig. 5E). On average, reduced-flexion joints were smaller than average-flexion joints, measuring significantly smaller lateral femoral condyle and fibula width and medial femoral condyle and tibia depth. Measurements of joint regions in the over-flexion group were not significantly different to those of the average-flexion group, except for the medial condyle depth, which was significantly smaller by 21% in over-flexion joints compared with average-flexion (Fig. 5A). However, joint shape profiles in the over-flexion group were less consistent when overlaid showing some variability in joint shape development following the larger movements (Fig. 4P–T). In particular, measurements of the lateral condyle depth exhibited a large standard deviation of 22% compared to 12% in the average-flexion group (Fig. 5B). A 3D representation of each experimental group is included in Supplementary materials (Supplementary Videos 2–5).

3.3. Cell viability and proliferation

Cell viability within the distal femur was greater than 95% in all groups, demonstrating that high cellular survival was maintained during the culture period, and there were no significant differences between groups for cell viability (Fig. 6A). However, average-flexion and over-flexion regimes led to significantly more proliferation than the static or reduced-flexion regimes (Fig. 6B), with almost double the number of proliferating cells in the average-flexion regime compared to the static or reduced-flexion groups.

4. Discussion

This research used *in vitro* culture of embryonic limb explants to quantify, for the first time, the effects of movement magnitude on morphogenesis of developing joints. The effects of three dynamic movement regimes and one static regime on chick knee joint morphogenesis were compared and supported our hypothesis that joint shape development would be affected by movement magnitude in a dose-dependent manner. The average-flexion regime, which was most similar to physiological movement patterns *in ovo*, showed the most progression of normal joint shape development when compared to the sequence of physiological shape changes seen in normal embryos. Following average-flexion, the distal femur also contained significantly more proliferative cells than explants which experienced reduced-flexion or no movements, suggesting that the size and shape changes in this group were due to an upregulation in mechanically-mediated proliferation rates. The average-flexion regime also produced the largest joints with both femoral condyles significantly larger than statically-cultured explants. The medial femoral condyle was the

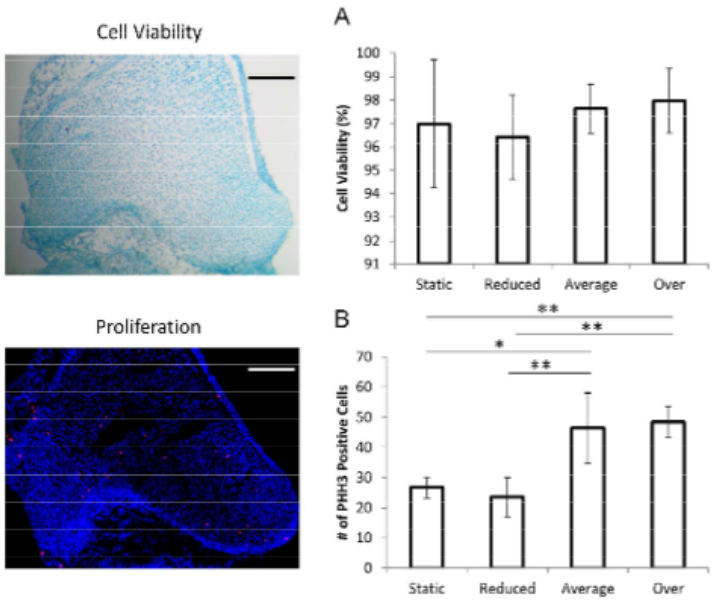


Fig. 6. Average-flexion or over-flexion led to significant increases in cell proliferation, while movement regime did not affect cell viability. Stained sections are shown from the average-flexion group for live/dead and proliferating cells. Viability staining shows dead cells in brown and live cells in green. Proliferation staining shows background cells in blue and proliferating cells in red. Scales bars – 200 m. A) shows live cell count as a percentage of total number of cells for each group. B) shows the total number of proliferating cells in the distal femur for each group. Error bars represent standard deviation. *p-values < 0.05; **p-values < 0.01. (For interpretation of the references to color in this figure legend, the reader is referred to the web version of this article.)

most consistently affected region by mechanical stimulation, with differences found in both shape and size between moved and unmoved explants. In the chick, the medial condyle articulates with the tibia and the lateral condyle with the fibula (Roddy et al., 2009). Since the majority of the significant differences between the static and average-flexion regimes were on the medial condyle and tibia, this suggests that average-flexion conditions preferentially promoted development of the medial side of the joint as compared to statically cultured explants. These results highlight the importance of movement during joint development and reveal that the magnitude of movement is a critical mechanical factor in driving joint morphogenesis. This study suggests that movements lower in extent than those seen physiologically can still advance joint morphogenesis but fail to promote proliferation and growth. The research also suggests that movement greater in extent than the physiological range can promote proliferation and growth but can cause irregularities and distortions in joint shape. Analysis of these three magnitudes supports our hypothesis that the most physiological movement regime would lead to a joint shape that more closely approximated normal development and further reveals a non-linear relationship between magnitude of movement and joint shape normality.

The aim of this study was to compare the effects of different movement magnitudes on joint morphogenesis, rather than to recreate physiological joint shapes *in vitro*. Whilst joints developed *in vitro* and joints developed *in ovo* are not directly comparable, the relative comparisons made between the different groups of joints developed in this study do provide an insight into the quantitative relationship between mechanical stimulation and joint morphogenesis, which would not be possible with *in vivo* experiments. The forces experienced within the joint explant due to the applied movement regimes were not quantified due to the complexity of the culture system, but can be assumed to increase with increased movement magnitudes. We believe that movement, rather than load, is a better parameter to quantify the level of mechanical stimulation, as it is more directly comparable to physiological conditions *in vivo*. A computational model would be ideal to investigate the role of loading during joint morphogenesis and predict how the compressive load applied to the foam support is transferred to the developing explants. Conditioned medium can significantly increase chondrocyte differentiation, proliferation and ECM synthesis (Elder, 2002; Kanczler et al., 2012) and could potentially amplify the differences found in this study. However, variance in serum performance and biochemical activity would be a possible confounding factor, hence a serum-free medium was used in this study.

While there are limited studies with which to directly compare our findings to, aspects of the shape changes found for *in vitro* cultured explants correlate with results found in *in vivo* models. In pharmacologically immobilised chicks, similar abnormal shape features found in statically cultured limbs were reported in the knee joint, including a smaller medial condyle and a flatter, more simplified distal femur (Roddy et al., 2011b). The only recent description of the effects of applying mechanical stimulation *in vitro* to developing limb explants did not report definitive findings on joint shape (Rodriguez and Munasinghe, 2016). This current study is the first to explore the effects of mechanical stimulation on chondrocyte viability and proliferation in embryonic joint explants cultured *in vitro*. Previous studies have explored the relationship between mechanical stimulation and proliferation using cellular micro-mass deformation culture models, but conflicting results have been reported (Elder et al., 2000; Juhász et al., 2014; Klumpers et al., 2015). The data from the current study suggests that mechanical stimulation affects proliferation and that a threshold for the level of stimulation exists, above which proliferation is enhanced. This finding agrees with a recent meta-analysis of *in vitro* cultivation of chondrocytes, which found that a threshold of loading exists for mechanically-mediated enhanced cartilage proliferation and differentiation (Natenstedt et al., 2015). For our experimental model, this threshold lies somewhere between the levels of stimulation applied in the reduced-flexion and average-flexion groups. Our findings that proliferation is down-regulated in cases of static or reduced-stimulation agrees with Roddy et al. (2011b) who showed a significant decrease in cell proliferation in the distal femur of immobilised chick embryos. Tissue engineers are currently trying to develop functional cartilage from stem cells or progenitor cell populations and it has been proposed that replicating the effects of mechanical stimulation during embryogenesis may be required to achieve this aim (Foster et al., 2015). This study provides evidence to support this theory, and shows that physiological magnitudes of mechanical stimulation *in vitro* are most beneficial.

In conclusion, we have shown that joint morphogenesis of the embryonic chick knee joint is affected by the magnitude of movement experienced *in vitro*. The most developed joint shapes were observed under a movement regime similar to those observed *in ovo*. Above this, the joint shape was seen to vary and even deteriorate, whilst reduced-flexion produced shapes more similar to those of statically cultured explants. This study reveals for the first time, how the magnitudes of fetal movements direct and determine aspects of prenatal joint morphogenesis, with important implications for understanding the etiology of congenital joint abnormalities related to abnormal fetal movements. Furthermore, this research provides useful cues to the cartilage tissue engineering field, in demonstrating that replicating the magnitude of physiological fetal movements leads to the most normal progression of cartilage growth.

Conflict of interest statement

The authors have no conflicts of interest relating to this research.

Acknowledgements

This research was funded by the European Research Council under the European Union's Seventh Framework Programme (ERC Grant agreement no. [336306]), and in part by the Medical Engineering Solutions in Osteoarthritis Centre of Excellence funded by the Wellcome Trust and the EPSRC (088844/Z/09/Z). The funders had no role in study design, data collection and analysis, decision to publish, or preparation of the manuscript.

We thank Dr Mariea Brady for her consultation with the design and optimisation of the novel explant culture system, and Ms Samantha Martin for assistance with optimisation of the histology and immunohistochemistry analyses and technical advice.

References

AbD Serotec. 2016. A Complete Kit for Measuring Apoptosis by Dual Color ImmunoHistoChemistry.

Bian, L., Zhai, D.Y., Zhang, E.C., Mauck, R.L., Burdick, J.A., 2011. Dynamic compressive loading enhances cartilage matrix synthesis and distribution and suppresses hypertrophy in hMSC-laden hyaluronic acid hydrogels. Tissue Eng. Part A 18, 715–724.

Brunt, L.H., Norton, J.L., Bright, J.A., Rayfield, E.J., Hammond, C.L., 2015. Finite element modelling predicts changes in joint shape and cell behaviour due to loss of muscle strain in jaw development. J. Biomech. 48, 3112–3122.

Chambers, S., Bradley, N., Orosz, M., 1995. Kinematic analysis of wing and leg movements for type I motility in E9 chick embryos. Exp. Brain Res. 103, 218–226.

Cohen, I., Robinson, D., Melamed, E., Nevo, Z., 2005. Use of a novel joint-simulating culture system to grow organized ex-vivo three-dimensional cartilage-like constructs from embryonic epiphyseal cells. Iowa Orthop. J. 25, 102.
Drachman, D.B., Sokoloff, L., 1966. The role of movement in embryonic joint development. Dev. Biol. 14, 401–420.
Elder, S.H., 2002. Conditioned medium of mechanically compressed chick limb bud cells promotes chondrocyte differentiation. J. Orthop. Sci. 7, 538–543.
Elder, S.H., Kimura, J., Soslowsky, L.J., Lavagnino, M., Goldstein, S.A., 2000. Effect of compressive loading on chondrocyte differentiation in agarose cultures of chick limb-bud cells. J. Orthop. Res. 18, 78–86.
Fell, H.B., Canti, R.G., 1934. Experiments on the Development in vitro of the avian knee-joint. Proc. R. Soc. Lond. Ser. B, Biol. Sci. 116, 316–351.
Foster, N.C., Henstock, J.R., Reinwald, Y., El Haj, A.J., 2015. Dynamic 3D culture: models of chondrogenesis and endochondral ossification. Birth Defects Res. Part C: Embryo Today: Rev. 105, 19–33.
Hall, B.K., Herring, S.W., 1990. Paralysis and growth of the musculoskeletal system in the embryonic chick. J. Morphol. 206, 45–56.
Hamburger, V., Balaban, M., Oppenheim, R., Wenger, E., 1965. Periodic motility of normal and spinal chick embryos between 8 and 17 days of incubation. J. Exp. Zool. 159, 1–13.
Henstock, J.R., Rotherham, M., Rose, J.B., El Haj, A.J., 2013. Cyclic hydrostatic pressure stimulates enhanced bone development in the foetal chick femur in vitro. Bone 53, 468–477.
Hosseini, A., Hogg, D.A., 1991. The effects of paralysis on skeletal development in the chick embryo. I. General effects. J. Anat. 177, 159–168.
Juhász, T., Matta, C., Somogyi, C., Katona, É., Takács, R., Soha, R.F., Szabó, I.A., Cserháti, C., Szódy, R., Karácsonyi, Z., 2014. Mechanical loading stimulates chondrogenesis via the PKA/CREB-Sox9 and PP2A pathways in chicken micromass cultures. Cell. Signal. 26, 468–482.
Kahn, J., Shwartz, Y., Blitz, E., Krief, S., Sharir, A., Breitel, D.A., Rattenbach, R., Relaix, F., Maire, P., Rountree, R.B., Kingsley, D.M., Zelzer, E., 2009. Muscle contraction is necessary to maintain joint progenitor cell fate. Dev. Cell 16, 734–743.
Kanczler, J.M., Smith, E.L., Roberts, C.A., Oreffo, R.O.C., 2012. A novel approach for studying the temporal modulation of embryonic skeletal development using organotypic bone cultures and microcomputed tomography. Tissue Eng. Part C: Methods 18, 747–760.
Klumpers, D.D., Smit, T.H. & Mooney, D.J. 2015. The Effect of Growth-Mimicking Continuous Strain on the Early Stages of Skeletal Development in Micromass Culture.
Lelkes, G., 1958. Experiments in vitro on the role of movement in the development of joints. J. Embryol. Exp. Morphol. 6, 183–186.
Natenstedt, J., Kok, A.C., Dankelman, J., Tuijthof, G.J., 2015. What quantitative mechanical loading stimulates in vitro cultivation best? J. Exp. Orthop. 2, 1–15.
Nowlan, N., 2015. Biomechanics of foetal movement. Eur. Cells Mater. 29, 1.
Nowlan, N.C., Bourdon, C., Dumas, G., Tajbakhsh, S., Prendergast, P.J., Murphy, P., 2010a. Developing bones are differentially affected by compromised skeletal muscle formation. Bone 46, 1275–1285.
Nowlan, N.C., Chandaria, V., Sharpe, J., 2014. Immobilized chicks as a model system for early-onset developmental dysplasia of the hip. J. Orthop. Res. 32, 777–785.
Nowlan, N.C., Sharpe, J., Roddy, K.A., Prendergast, P.J., Murphy, P., 2010b. Mechanobiology of embryonic skeletal development: Insights from animal models. Birth Defects Res. Part C: Embryo Today: Rev. 90, 203–213.
Osborne, A.C., Lamb, K.J., Lewthwaite, J.C., Dowthwaite, G.P., Pitsillides, A.A., 2002. Short-term rigid and flaccid paralyses diminish growth of embryonic chick limbs and abrogate joint cavity formation but differentially preserve pre-cavitated joints. J. Musculoskelet. Neuronal Interact. 2, 448–456.
Pörtner, R., Nagel-Heyer, S., Goepfert, C., Adamietz, P., Meenen, N.M., 2005. Bioreactor design for tissue engineering. J. Biosci. Bioeng. 100, 235–245.
Quintana, L., Sharpe, J., 2011. Optical projection tomography of vertebrate embryo development. Cold Spring Harb. Protoc. 2011, 586–594, pdb.top116.
Roddy, K.A., Kelly, G.M., van Es, M.H., Murphy, P., Prendergast, P.J., 2011a. Dynamic patterns of mechanical stimulation co-localise with growth and cell proliferation during morphogenesis in the avian embryonic knee joint. J. Biomech. 44, 143–149.
Roddy, K.A., Nowlan, N.C., Prendergast, P.J., Murphy, P., 2009. 3D representation of the developing chick knee joint: a novel approach integrating multiple components. J. Anat. 214, 374–387.
Roddy, K.A., Prendergast, P.J., Murphy, P., 2011b. Mechanical influences on morphogenesis of the knee joint revealed through morphological, molecular and computational analysis of immobilised embryos. PLoS One, 6.
Rodriguez, E.K., Munasinghe, J., 2016. A chick embryo in-vitro model of knee morphogenesis. Arch. Bone Jt. Surg. 4, 109–115.
Sandell, L.J., 2012. Etiology of osteoarthritis: genetics and synovial joint development. Nat. Rev. Rheumatol. 8, 77–89.
Schneider, C.A., Rasband, W.S., Eliceiri, K.W., 2012. NIH image to ImageJ: 25 years of image analysis. Nat. Methods 9, 671–675.
Sharpe, J., Ahlgren, U., Perry, P., Hill, B., Ross, A., Hecksher-Sørensen, J., Baldock, R., Davidson, D., 2002. Optical projection tomography as a tool for 3D microscopy and gene expression studies. Science 296, 541–545.
Smith, E.L., Kanczler, J.M., Oreffo, R.O., 2013. A new take on an old story: chick limb organ culture for skeletal niche development and regenerative medicine evaluation. Eur. Cell Mater. 26, 91–106, discussion 106.
Watson, S.J., Bekoff, A., 1990. A kinematic analysis of hindlimb motility in 9- and 10-day-old chick embryos. J. Neurobiol. 21, 651–660.